Fatigue Damage Characterization and Life Prediction in Carbon Fiber Reinforced Plastic Composites

by

Johar Khurshid Farooqui

A Thesis Presented to the

FACULTY OF THE COLLEGE OF GRADUATE STUDIES

KING FAHD UNIVERSITY OF PETROLEUM & MINERALS

DHAHRAN, SAUDI ARABIA

In Partial Fulfillment of the
Requirements for the Degree of

MASTER OF SCIENCE

In

MECHANICAL ENGINEERING

December, 1996

INFORMATION TO USERS

This manuscript has been reproduced from the microfilm master. UMI films the text directly from the original or copy submitted. Thus, some thesis and dissertation copies are in typewriter face, while others may be from any type of computer printer.

The quality of this reproduction is dependent upon the quality of the copy submitted. Broken or indistinct print, colored or poor quality illustrations and photographs, print bleedthrough, substandard margins, and improper alignment can adversely affect reproduction.

In the unlikely event that the author did not send UMI a complete manuscript and there are missing pages, these will be noted. Also, if unauthorized copyright material had to be removed, a note will indicate the deletion.

Oversize materials (e.g., maps, drawings, charts) are reproduced by sectioning the original, beginning at the upper left-hand corner and continuing from left to right in equal sections with small overlaps. Each original is also photographed in one exposure and is included in reduced form at the back of the book.

Photographs included in the original manuscript have been reproduced xerographically in this copy. Higher quality 6" x 9" black and white photographic prints are available for any photographs or illustrations appearing in this copy for an additional charge. Contact UMI directly to order.

UMI

A Bell & Howell Information Company
300 North Zeeb Road, Ann Arbor MI 48106-1346 USA
313/761-4700 800/521-0600

Fatigue Damage Characterization and Life Prediction in Carbon Fiber Reinforced Plastic Composites

BY

Johar Khurshid Farooqi

A Thesis Presented to the

FACULTY OF THE COLLEGE OF GRADUATE STUDIES

KING FAHD UNIVERSITY OF PETROLEUM & MINERALS

DHAHRAN, SAUDI ARABIA

In Partial Fulfillment of the
Requirements for the Degree of

MASTER OF SCIENCE

In

MECHANICAL ENGINEERING

December, 1996

UMI Number: 1384114

UMI Microform 1384114
Copyright 1997, by UMI Company. All rights reserved.

This microform edition is protected against unauthorized copying under Title 17, United States Code.

UMI
300 North Zeeb Road
Ann Arbor, MI 48103

بسم الله الرحمن الرحيم

KING FAHD UNIVERSITY OF PETROLEUM AND MINERALS

DHAHRAN, SAUDI ARABIA

COLLEGE OF GRADUATE STUDIES

This thesis, written by

Johar Khurshid Farooqi

under the direction of his Thesis Advisor, and approved by his Thesis committee, has been presented to and accepted by the Dean, College of Graduate Studies, in partial fulfillment of the requirement for the degree of

MASTER OF SCIENCE IN MECHANICAL ENGINEERING

Thesis Committee:

Dr. Zafarullah Khan (Chairman)

Dr. F. A. Al-Sulaiman (Co-Chairman)

Anwar Khalil Sheikh

Dr. Anwar K. Sheikh (Member)

Department Chairman (Mech. Engg.)

Dr. Ibrahim M. Allam (Member)

Dean, College of Graduate Studies

Date: 7-1-97

كلية الدراسات العليا
COLLEGE OF GRADUATE STUDIES

Dedicated to

my dear departed father

whose unending prayers and love went a long way to shape his dream into this successful reality

and

my mother and sisters

whose love, encouragement and inspiration made this effort possible

Acknowledgments

In the name of Allah, Most Gracious, Most Merciful. Read in the name of thy Lord and Cherisher, Who Created man from a {leech-like} *clot. Read and thy Lord is most Bountiful. He who taught* { the use of } *the pen. Taught man that which he knew not. Nay, but man doth transgress all bounds. In that he looketh upon himself as self-sufficient. Verily, to thy Lord is the return* {of all}.

(The Holy Quran, Surrah Al-A'alaq, No. 96)

First and foremost, all praise to Allah, *subhanahu-wa-tala*, the Almighty, Who provided me with the opportunity, patience and perseverance to carry out this work. I, forever, seek His mercy, forgiveness and blessings. I feel honored as well as privileged to glorify His name and give due reverence to Allah and only Allah Almighty that this small objective is accomplished.

Acknowledgement is due to King Fahd University of Petroleum & Minerals for providing support to this research work.

I am indebted to my thesis advisor. Dr. Zafarullah Khan for his timely guidance, support and supervision with valuable advice throughout the course of this research. I am also thankful for his immense moral support and understanding during adverse

and difficult times along the way. I am grateful to my thesis co-advisor, Dr. Faleh A. Al-Sulaiman, for his practical interest and due contribution in the experimental work involved. His valuable criticism was productive in shaping this work conclusively. I am also really thankful to my thesis committee member, Dr. Anwar K. Sheikh, for his expert opinion, constructive criticism and thorough understanding. Thanks are also in order to my thesis committee member, Dr. Ibrahim M. Allam, for his useful comments on the research work conducted and a thorough review of the thesis. I am also thankful to the department chairman, Dr. M. O. Budair, for his spirited research support and also other faculty members especially Mr. M. Younas for their help and guidance during research. I would like to pay a special tribute to Dr. Esmail M. A. Mokheimer who really inspired me positively in my research and thesis. Dr. Syed M. Zubair and Dr. M. Antar also deserve similar gratitude for their collaboration in indirect building of my research approach and understanding.

I would like to thank Dr. Qutub Ali Khan for his guidance and supervision for conducting the X-Ray Radiography at the university medical center. Special thanks for Mr. Latif Hashmi for his unending input as experimental expertise in material sciences and metallurgy. Thanks are also in order for Mr. Zainulabideen for his laboratory collaboration and companionship during experimental work.

Notable mentions go to all my friends on campus especially Sultan whose positive attitude towards the Masters program made it all the more fruitful. Friends and

colleagues in and outside my department like Asim, Asif, Ikram, Khurram, Arshad, Salman, *Late* Aamir, Fayyaz, Shahid, Rashid, Rashad, Imtiaz, AbdurRahim, Saqib, Rehan, Shoaib, Quddus, Raza, Yousaf, Kamran, Khaqan, Aijaz are the ones that made my stay here memorable and it is their comradeship that I will always cherish in my professional career ahead.

Last but not the least, thanks and gratitude is due for all my family members for their love and affection along with their patience and emotional support. Without a doubt no accomplishment of mine would have been possible without the proper guidance and best upbringing of my parents.

This work has been specially dedicated to my dearest father who passed away during my study at KFUPM. May Allah Almighty bless his soul in Paradise. My heart goes out to him for he prayed for my success and bright future day and night for all his life. His teachings and education have really shaped the best in me. Also I thank my dear mother for her patience which I have tried all my academic life out of my home. May this completion mark the long awaited reunion of this family. I also deeply acknowledge, with much gratitude, the affection, love and moral support of my dear sisters.

Contents

List of Tables

List of Figures

Nomenclature

β	angle of undulations in the woven fabric
c	empirical constant obtained from mechanical properties
D	damage parameter
dD/dN	damage rate
dE/dN	modulus reduction rate
D_f	damage at failure
D_i	initial damage
$\Delta\sigma$	stress range
E	stiffness, (Young's Modulus)
ε	strain
E_A	modulus in the longitudinal direction
ε_c	critical strain
E_f	modulus of the fibers
E_m	modulus of the matrix
E_o	Stiffness of the nascent specimen
E_T	modulus in the transverse direction
f	frequency of loading
G	strain energy release rate
$g'(D)$	first derivative of g(D) with respect to D

$g(D)$	function of D
G_A	shear modulus in the longitudinal direction
G_c	interlaminar fracture energy
G_f	shear modulus of the fibers
G_m	shear modulus of the matrix
N	number of fatigue cycles
ν_A	Poisson's ratio in the longitudinal direction
N_f	cycles to failure
ν_f	Poisson's ratio of the fibers
ν_m	Poisson's ratio of the matrix
P_a	load amplitude applied
P_{max}	maximum applied load
P_{min}	minimum applied load
θ	orientation angle of the plies
R	stress ratio
σ	stress applied
σ_{max}	maximum applied stress
$\sigma_{TS.A}$	tensile strength in the longitudinal direction
$\sigma_{TS.T}$	tensile strength in the transverse direction
V_f	fiber volume fraction
V_m	matrix volume fraction

Abstract

Name: Johar Khurshid Farooqi

Title : Fatigue Damage Characterization and Life Prediction in Carbon Fiber Reinforced Plastic Composites

Major Field: Mechanical Engineering

Date of Degree: December, 1996

Fatigue damage is one of the most unwelcome failure categories encountered in modern engineering components. Recent advent of Carbon fiber reinforced plastic composites in advanced engineering components and structures such as the present-day advanced aircrafts, marine, and other high performance structures has made it essential for properly characterizing fatigue damage process and developing reliable fatigue life prediction methodologies for these materials. In the present study fatigue damage mechanisms have been investigated in three classes of Carbon-Carbon Fabric Reinforced Plastic Composites. Both destructive and nondestructive techniques such as X-Ray Radiography, Optical Microscopy, Edge Replication and Scanning Electron Fractography have been used to characterize the fatigue damage in these composites. It is shown that the fatigue damage in carbon fabric reinforced composites is a complex, combined and interactive damage process between several damage mechanisms such as delamination, fiber fracture, matrix cracking, fiber-matrix debonding etc.

An analytical model used for carbon fiber composite life prediction based on stiffness degradation during cyclic loading has been employed to the Plain-Weave Carbon-Carbon Fabric composites. A reasonably good correlation has been obtained between the analytically determined fatigue lives and the observed fatigue lives of the Carbon-Carbon Fabric Reinforced Plastic Composites.

Master of Science Degree
Department of Mechanical Engineering
King Fahd University of Petroleum And Minerals
Dhahran, Saudi Arabia

December, 1996

خلاصة الرسالة

الاسم : جوهر خورشيد فاروقي

العنوان : تحديد الانهيار الناتج عن التعب والتنبؤ بالعمر الافتراضي للمركبات البلاستيكية المقواة بالالياف الكربونية

التخصص : الهندسة الميكانيكية

تاريخ الدرجة : ديسمبر ١٩٩٦ م

يعتبر الانهيار الناتج عن التعب أحد أهم أصناف الأنهيار غير المرغوب فيها في المركبات الهندسية الحديثة . وقد أصبحت المركبات البلاستيكية المقواه بالألياف الكربونية مستخدمة في المكونات والهياكل مثل الطائرات الحديثة ، السفن والمركبات ذات الأداء العالي، وقد برزت أهمية تحديد الانهيار الناتج عن التعب وكذلك تطوير طرق ذات اعتمادية عالية للتنبؤ بالعمر الافتراضي لهذه المواد . وقد تم في الدراسة الحالية بحث الانهيار الناتج عن التعب لثلاثة انواع من المركبات البلاستيكية المقواة بنسيج مصنوع كلية من الكربون وقد تم تطبيق الاختبار الاتلافي والاختبار غير الاتلافي مثل اشعة اكس ، الميكروسكوب الضوئي ، طريق النسخة المطابقة للطرف بالاضافة الى المسح الالكتروني المجهري للسطح . وقد أظهرت الدراسة أن الانهيار الناتج عن التعب في المركبات المقواه بالنسيج الكربوني يعد عملية معقدة ، مركبة وتبادلية اذ تشترك فيها عدة آليات مثل فصل السطح الى رقائق ، التصدع النسيجي ، كسر القالب ، انفصال النسيج عن القالب .. الخ

وقد استخدم نموذج تحليلي للتنبؤ بالعمر الافتراضي للنسيج الكربوني المركب بحيث يعتمد على تقليل الصلابة اثناء التحميل الدوري ويطبق على المركبات النسيجية الكربونية ذات النسيج البسيط . وقد تم استنباط علاقة جيدة بين القيم التحليلية للعمر الكلالي والقيم المرصودة عمليا له بالنسبة للمركبات البلاستيكية المقواه بالنسيج الكربوني .

درجة الماجستير في العلوم
قسم الهندسة الميكانيكية
جامعة الملك فهد للبترول والمعادن
الظهران - المملكة العربية السعودية
ديسمبر - ١٩٩٦

Chapter 1

Introduction

1.1 General Background

The present day increasingly complex design of engineering components and structures, demand of superior performance and weight savings have propelled materials scientists, engineers, and designers into a continued search of new materials which can meet the above requirements. Development of composite materials and their introduction into the engineering industry to obtain light weight, high performance, and increasingly complex geometries was a result of a significant amount of research during the last few decades. Since the 1960s when the first carbon fiber reinforced epoxy plastics were developed, the extent of their application has

been continuously increasing and now it ranges from a simple sports gear industry to a modern advanced aviation to space technology.

As the application of the composite materials increased so did the occurances of failure and fracture of these composites. The failure and fracture of these materials under a variety of severe conditions became common place as was the case with their metallic counterparts. Consequently more and more attention is now being directed toward understanding the mechanics and mechanism of failure and to develop the service life prediction methodolgy. As is there with the metallic components, fatigue failure is also one of the main causes of failure in the composite materials. The present study aims at investigating the fatigue behavior in carbon fibre reinforced composite materials.

1.2 Composites in the Modern Era

These days composite materials have found their way in all trades of society. Scientist and engineers are constantly engaged in a substantial volume of research directed toward performance enhancement and widening application of the composites in increasingly challenging engineering components. The main areas of industrial applications of composites can be summarized here.

In the aerospace industry, a wide range of load-bearing and non-load-bearing components are already being used in both fixed wing and rotary wing aircrafts. Many

military and civil aircrafts now contain substantial quantities of light weight, high-strength carbon, Kevlar™ and glass fiber reinforced composites, as laminated panels and moldings, and as composite honeycomb structures with metallic or resin impregnated paper honeycomb core materials. They are used in air frames, wing spars, spoilers, tail-plane structures, fuel tanks, drop tanks, bulkheads, flooring, helicopter rotor blades and structural components, pressured gas containers, radomes, nose and landing gear doors, fairings, engine nacelles, air distribution ducts, seat components, access panels, and so forth. For elevated temperature applications carbon-fiber reinforced-carbon is under consideration. Concorde's disk brakes use this material. Similarly rocket nozzles and re-entry shields have also been fashioned from this material.

In automotive engineering there is increasing interest in weight reduction in order to permit both energy conservation and increased motoring economy. Reduction in the weight of an automobile structure achieves primary weight saving and if carried to sufficiently great lengths, enables the designer to use smaller and more efficient engines, thus achieving substantial improvements in fuel economy. A wide range of car and truck body moldings, fascias, bumper moldings, and various kinds of trim have experienced a change from conventional metals to composite materials. Leaf and coil springs and truck drive shafts made of composites are also in service. Graphite Reinforced Plastic (GRP) wheel rims and inlet manifolds are now becoming common place.

In chemical engineering applications GRP composite is currently being used for containers, pressure vessels, pipe work, valves, centrifuges etc. Whereas in civil and structural engineering the bulk of composite being used is of glass-reinforced plastic type. Glass reinforced cement (GRC) products using Cemfil are gradually being introduced as structural cement-based composite. A good deal of GRP is used in this industry for folded-plate structures, cladding panels, decorated "sculptured" panels, service moldings, ducting, racking, pipework, rainwater moldings, domestic and industrial water tanks, form-work for concrete, and complete small structures like foot-bridges. Also in electrical engineering applications there are radomes, structural components for switch gear, power generator coolant containment, large-diameter butterfly valves, high-strength insulators and printed circuit boards. The majority of these applications use GRP as they are thermally stable and moisture-resistant.

In marine engineering a vast range of pleasure craft has long been produced GRP. A much serious use is also made of the same material for hull and superstructure construction of mine-countermeasures and many kinds of submarines, including castings for towed transducer arrays for sea-bed sonar mapping.

One of the interesting mix of technologies is bioengineering where carbon fiber reinforced plastics and carbon components are coming into use for prosthetic purposes. Components such as orthopedic fracture fixation plates, mandibular and maxillary prosthesis (e.g. jaw remodeling), and external orthotic supports in case of limb deformity etc., are now being manufactured from composite materials. Pyrolytic

carbon is used to manufacture heart valve components, and the substitution of this material with a carbon/carbon composite is not unlikely.

Engineers and scientists are constantly probing into the response and behavior of all the composites being used all around us in order to better understand and optimize the use of design capabilities of these exotic materials. It has been established that the composites are the inevitable replacement for the conventional materials all over and the next century is going to practically change the look of the global infrastructure.

1.3 Carbon Fiber Reinforced Composites

Among all the different types of composites such as filled, particulate, fiber reinforced composites which are being used in the present day industry, fiber reinforced composites have gained the greatest popularity. Due to the ability to tailor different strength characteristics in different directions, long continuous fibers have been used extensively. Since the fibrous form of most materials is many times stronger than its bulk form because of less surface volume and hence less surface flaws, engineers have long sought ways of making practical use of fibers as engineering materials. The most efficient method yet found is to combine a fibrous material of high tensile strength and high elastic modulus with a light-weight bulk material of lower strength and lower modulus of elasticity, yet good ductility. Hence

the fiber type (specifically the inclusion of the fiber in a matrix) has gained the most interest among designers and manufacturers of advanced engineering components and structures.

Carbon fibers have been classified as really good candidate for this reinforcement because of its high stiffness and axial strength as compared to others available fiber materials. Hence light-weight, high strength and high stiffness properties of these fibers have proved very useful for designers and engineers. The Carbon Fiber Reinforced Composites (CFRC) comprise of strong, stiff carbon fibers of solid, circular cross-section embedded in a much weaker, more flexible matrix e.g. synthetic resins. The uses of these reinforced materials range from the low performance cafeteria tray to the high-performance rocket-motor case. The most interesting and favorite facility provided generally by the fiber reinforced composites is the prospect of "tailoring" the composite to exhibit high resistance to fatigue and flexural loading in the desired orientation as the optimal design necessitates. But along with the fiber direction many other factors in the manufacturing of carbon fiber composites influence the performance.

1.4 Factors of Performance

1.4.1 Fiber Factor

Factors contributing towards the performance of Carbon Fiber Reinforced Plastic (CFRP) composites related to fibers are *orientation*, *composition*, *length* and *shape* [1]. These are briefly described below.

Orientation is considered the most influential factor among all the others. There are three types of fiber orientation: one dimensional reinforcement, planar (two-dimensional) reinforcement, and three-dimensional reinforcement. The one-dimensional type has maximum composite strength and modulus in the direction of the fiber axis. The planar type exhibits different strengths in each direction of fiber orientation. The three-dimensional type is anisotropic but has greatly decreased reinforcing values (all three dimensions are reinforced but only to about one-third of the one-dimensional reinforced value). The mechanical properties in any one direction are proportional to the ratio of fiber by volume oriented in that direction.

Length of the fibers vary from short to continuous type. Although continuous fibers are more efficiently oriented than short fibers they are not necessarily better. Besides mechanical properties such as strength, load carrying capacity etc., fiber length has a bearing on the processability of the fiber composites.

Practically all fibers presently being used have a circular cross section whether they are continuous or short; however, hexagonal, rectangular, polygonal, annular (hollow circle), and irregular **shapes** appear to promise improved mechanical properties. Usually solid circular fibers are easy to produce and handle. Steel reinforcing rods for concrete are examples of thick fibers; some glass fibers have diameters as small as 0.01 mm (0.0004 in). In general, the smaller the diameter of a fiber the greater is its strength. Single-crystal whiskers with hexagonal fibers make the strongest fibers, but handling them and incorporating them into a fiber composite is difficult.

Fiber of Both organic and inorganic **composition** are available for FRC materials. The organics, such as cellulose, polypropylene, and graphite fiber can be characterized in general as lightweight, flexible, elastic, and heat sensitive. Inorganic fibers such as glass, tungsten, and ceramic can be generally described as very high in strength, heat-resistant, rigid, low in energy absorption and fatigue resistance. While many organic fibers satisfy both the strength and elasticity requirements for structural composites, graphite in recent years has become the most popular. The inorganics, notably glass, dominate the field. Most of the other inorganic fibers, e.g., metallic whiskers and ceramic fibers, have recently (within the past 5-7 years) received the financial backing required for development into an accepted material.

1.4.2 Matrix Factor

The **matrix** serves two very important functions. Firstly it holds the fibrous phase in place, and secondly under an applied force it deforms and distributes the stress to the high-modulus fibrous constituent (load is borne longitudinally by the reinforcements). Many reinforcements tend to be brittle and the matrix protects their surface against abrasion or environmental effects, both of which can initiate fracture. In order to accomplish the transfer of loads, and also reduce the chance of failure in the matrix, adhesion to fibers or other reinforcements is ensured to be coupled with sufficient matrix shear strength to sustain these loads. In the event of fiber breakage, the matrix redistributes the load among neighboring reinforcements, as well as to both halves of the broken reinforcement. While strong and stiff (but brittle) reinforcements provide high tensile and flexural properties, plastic flow at crack tips in the matrix absorbs energy and reduces stress concentration, thus promoting fracture toughness. Matrix which plastically deforms also serves to deflect cracks parallel to fibers, preventing the failure of fibers all in one plane. Thus, for a crack to extend through ductile matrix materials, it is also necessary for the fibers to pull out the matrix as they break, which absorbs a significant amount of energy [1].

1.4.3 Stacking Sequence

Another important parameter in laminated fiber reinforced composites is the stacking sequence of the different layers (laminae). Pagano and Pipes [2] regarded it as one of

the key tools in designing the structure to sustain any specific type of loading (fatigue or flexural). They presented an optimization of the orientation and stacking sequence in order to design delamination-free structures. Although it was concluded that for design purpose rigorous confirmation of the results was required through a boundary value problem in theory of elasticity for n-ply laminates, but still the influence of the stacking sequence on laminate strength was marked. The authors also emphasized the use of tubular specimens for strength characterization in which the interlaminar shear stresses vanish in the gage section.

1.5 Fatigue in Composites

Composite materials have offered substantial improvements over metals for application to structures subjected to fatigue loads. Their characteristic response to fatigue, however, has been quite different from that of metals. While the metals exhibit simple failure mode which can be described as cracking caused by a single dominant fatigue crack, composites can exhibit one or a combination of failure modes, including fiber breakage, delamination, matrix cracking, interface debonding, and void growth under fatigue loading.

During cyclic loading different regions inside a composite material have different micro-responses. The weaker matrix can act temporarily as a homogenous material like the conventional metal but only till some other constituent of the

composite takes over in the deformation process. This matrix exploits the inherent defects of manufacturing like voids and impurities and produces a crack. The serrated teeth-like countenance emerging from the matrix cracks is called "Hackle". After sufficient matrix cracking the crack encounters the fiber/matrix interface. Here the circumferential stiffness of the fibers does not allow it to be broken by the crack and hence the crack moves along the interface. This type of process eventually leads to damage called delamination, where the laminae are separated from each other or the fiber is debonded from matrix material which is called fiber-matrix debonding. From here onward the large alteration in the internal structure of the composite dictates reduction in strength and stiffness of the composite as a whole. The load bearing fibers are always the ones in the direction of the loading and at this stage the failure and fracture of the composite member is directly linked to the resistance of those fiber to fracture. When they break, the composite fails completely.

In low cycle fatigue all types of individual damages caused by fatigue are intricately amalgamated. Just as the matrix starts cracking, somewhere nearby a fiber breaks and that fiber pulls out of the matrix (conveniently termed as "fiber pull-out"). With a little displacement from that broken fiber the neighboring fibers start debonding and simultaneously other localities experience similar damage. Fiber pull-outs force voids to grow larger, but again the growth process is slow and under high cycle fatigue such degradations are overpowered by the dominating fiber fracture and delamination after little matrix cracks initiate. The delamination process is very much

dependent on the stacking sequence of the plies. If there are angle-plies involved, the damage by delamination will start from the interface joining different direction laminates. For example, in a $(0,0,\pm45)_s$ fiber composite, the interface of the 0° and the 45° will be most prone to delamination as compared to other interfaces having same direction laminates. Also the fiber fracture in different angled-plies is different. For example, in a composite with 0° and 90° plies, the 90° plies will not bear any load and will not hinder damage. They will straight away split in the transverse direction and the remaining load will be transferred to the 0° fibers. Again the fracture will take place according to the load bearing capacity of the 0° fibers. Still it is not easy to monitor and separate the different events as they are closely interconnected in high cycle fatigue.

The cumulative fatigue damage is usually characterized using different destructive and non-destructive techniques. These techniques such as X-Ray Radiography, C-Scan, Acoustic Energy Discrimination method, Fractography, Edge Replication, Deplying technique, Optical Microscopy etc., have been used over the last three decades in order to examine the fatigue damage process in fiber reinforced composites. Different damage modes under fatigue loading are observed with different techniques. For example, the delamination has been examined by X-Ray radiography and Edge Replication along with the proceeding fatigue life successfully and hence growth of delamination is captured in-situ for the fiber reinforced composites under fatigue loading. These techniques eventually help in characterizing

the damage and which in turn guide designers for predicting that behavior, qualitatively and even quantitatively. This in the end can become the basis for the design of components with fiber reinforced composites such as CFRP.

1.6 Fatigue Damage and Damage Characterization in Composites

Composite materials as a whole, unlike metals, are inhomogeneous and anisotropic. They accumulate damage in a general rather than a localized fashion, and failure does not always occur by propagation of a single macroscopic crack. The microstructural mechanism of damage accumulation, including fiber and matrix cracking, debonding, transverse ply cracking, and delamination, occur sometimes independently and sometimes interactively, and the predominance of one or the other may be strongly affected by both material variables and testing conditions.

At low monotonic stress levels, or early in the life of a composite undergoing cyclic loading, most types of composite sustain damage of a very general kind, distributed throughout the stressed region. The damage does not always immediately reduce the strength of the composite although it frequently reduces the stiffness. Such strength reduction is sometimes offset in the early stage of life by slight increase in the strength. This increase could be attributed to improvement in fiber alignment resulting from small stress-induced viscoelastic or creep deformations in the matrix. At a later stage in life, the amount of damage may accumulate in some region of the

composite causing the residual load-bearing capacity of the composite in that region to fall to the level of the maximum applied stress in the fatigue cycle, when failure ensues. This process may occur gradually, when it is simply referred to as degradation, or catastrophically, when it is sometimes termed as "sudden death". Changes of this kind do not necessarily relate to the propagation of a single crack, and this is to be recognized when attempting to interpret composite fatigue data obtained by methods developed for metallic materials.

When a pre-existing crack is present in the composite it may or may not propagate under cyclic loading conditions, depending upon the nature of the composite. In a metal-fiber/metal-matrix composite the fiber itself will be subject to conventional fatigue processes. Planar crack propagation can occur with both fibers and matrix exhibiting normal signs of fatigue and the material behaves simply like a homogeneous metal of higher strength than the unreinforced matrix. In higher anisotropic composites of high V_f (fiber volume fraction) the crack will often refuse to propagate normal to the fibers but will be diverted into a splitting mode. In such composites as unidirectional CFRP this may result in a brittle, end-to-end splitting failure which simply eliminates the crack. While in the metal matrix composites the splitting will be preceded by a localized but elongated region of intense plastic deformation [3].

1.7 Analytical Methodologies for Life Prediction

The performance and response of composite materials in different components is far different from the conventional structural materials such as carbon steels, alloy steels, Aluminum and other non-ferrous alloys. In the case of metals there is only the presence of a dominating flaw or crack and the whole fracture mechanics is there to quantitatively predict the time of failure. In the fiber reinforced composites it is quite complex to analyze and relate the failure to its precursors. Various damage phenomena as described above are operative when a composite material is subjected to fatigue loading. There is always the possibility of any one of these taking control and dictate the eventual failure of the composite component. The problem of predicting fatigue life is further complicated due to the uncertainty arising from the poor knowledge on how interactions between different failure modes at different stress levels and loading cycles combine to produce the final failure.

Engineers started understanding the mechanics of the composite laminates at a novice level. Their initial approach was of the qualitative. Then there were attempts to relate the fatigue damage, for example, to the degradation of the mechanical properties of the composite material such as strength, stiffness etc. of the composite materials. The other approach was the statistical evaluation of the data pooled from the experiments run on composite materials with simulated service conditions. Many statistical distributions were assumed to govern certain properties such as the strength

which was in one case considered to be governed by a two-parameter Weibull distribution. Later on, assumptions like these became the basis for developing empirical models for predicting life and to validate experimental results.

Since the late sixties and the early seventies modeling fatigue damage in the composite materials was an attractive topic for research as it was becoming really necessary to establish an extremely reliable infrastructure with these materials as the backbone of the aviation industry. A substantial volume of investigative work was carried out on carbon, graphite, glass reinforced plastics as these were considered to be useful for infinite number of applications.

1.8 Scope and Objective of the Present Study

The preceding discussion must certainly have highlighted that composites such as CFRPs have emerged as one of the most promising and most challenging classes of materials to meet the present and future material requirements to produce complex, light weight yet high performance engineering components and structures. The heterogenic property characteristic of this material has made it a popular candidate for use where such "dexterity and smartness" of the material is desired. A manufacturer could well dictate optimal properties in a composite from its same constituents by only varying some factors such as lay-up sequence or orientation etc. as explained earlier.

Any attempt to develop a model of the fatigue damage response of such composite materials has to incorporate a clear understanding of the fatigue damage mechanisms and their complex interactions in producing the overall damage. With the increase in the comprehension of fatigue damage mechanisms the predictive capabilities of the models developed will certainly be enhanced. A thorough understanding of the damage mechanism can be accomplished through non-destructive and destructive examination during and after the fatigue loading of a specimen.

An effort is to be made not only to identify the various damage mechanisms operative during the fatigue life but also to characterize the interaction between these damage mechanisms which is considered as the prime factor dictating fatigue life and the eventual failure in the fiber reinforced composite material. A fatigue life prediction model which considers the real damage mechanisms can then be employed to provide reliable and sound predictions that can be used with a reasonable confidence in design, service and maintenance of engineering components and structures made of carbon fiber reinforced plastic composites. The fact that this material is of popular use for many high performance engineering components and structures, extensive research is demanded to understand the behavior of Carbon-Carbon Fabric Reinforced Plastic Composite along with the understanding of its characteristic behavior in its service life. A motivation has developed due to the fact that such investigation for this fabric composite type material has been reported by

only a few researchers but the use of this material has increased by many times in numerous applications due to the dexterous tailorability, high strength and stiffness characteristics and low weight quality of this material. So experiments are carried out in order to generate valuable fatigue data to understand the fatigue behavior qualitatively and also to incorporate the obtained data in a suitable analytical model to bring about the fatigue life predictions for future designers, researchers and engineers. Therefore destructive and nondestructive experimentation are carried out for characterization of fatigue damage in plain-weave woven carbon-carbon fabric reinforced plastic composites.

Chapter 2

Literature Review

2.1 History of Composites

Research on fatigue behavior of Carbon Fiber Reinforced Composites (CFRC) started in the 60s in the Department of Defense in United States with limited field applications. During the last twenty years composites have become a material of intense research due to its increasing use in the engineering industry. The main driving force in this research is the significant increase in the application of these material due to high strength, high stiffness, tailorability into producing complex structures, and substantial weight savings offered by composites such as the carbon fiber reinforced plastic composites.

Salkind [4] has reviewed the available literature on fatigue behavior of composites. He has suggested that the fatigue test data should be reported in terms of cycles to a given change in the stiffness rather than cycles to fracture. He reiterated the need of multiple damage detection schemes to be used for both material and structural testing. He also pointed out one great advantage for using composite materials as the ability to tailor the stiffness and strength in different directions.

2.2 Fatigue of Carbon Fiber Reinforced Plastics

A definition relating to fatigue in composites was presented by Fong [5] to help in the selection of measuring techniques and parameters for relating fatigue life with damage. For this he presented an example of Small Angle Neutron Scattering (SANS) method. He gave a review of typical damage factors for composite materials. He also forwarded a summary of an ASTM E9.01 panel study on fatigue damage and research opportunities in the 1980s. Constant and variable amplitude fatigue strengths and tensile and compressive strengths of CFRP were also determined [6]. Flight-by-flight loading sequences typical for the wing root area of the fighter aircrafts were experimentally studied. It was shown that several different interactive failure modes such as fiber fracture, matrix cracking, delamination, and debonding cause excessive loss in stiffness, and strength and lead to the final fracture. More experiments were conducted by Sturgeon [7] on (0), (0±45) and (90±45) oriented CFRP coupons. He

emphasized the presence of holes as initiation sites. One of the main finding was that the notch sensitivity of (0±45) CFRP was much more pronounced under monotonic loading than under fatigue loading. He also showed that the fatigue strength of 0° laminates is greater than the (0±45) and (90±45) oriented laminates. A study of strength distribution of 90° plies in the laminates $(\pm\theta/90_n)_s$ with $\theta = 0°$ and 45° and n = 2, 3 and 6 was forwarded by Peters [8] in the form of two parameter Weibull distribution. A common feature for both orientations of surface layers was that at decreasing 90° ply thickness the characteristic strength and the shape parameter increase. Further it was shown that the crack formation in the 90° plies of $(\pm45/90_n)_s$ laminate is strongly influenced by the severe edge stresses.

Fatigue behavior of $(0/\pm45/90)_s$ Glass/Epoxy laminate has been characterized in terms of the following parameters: static properties; S-N relationship; reliability; effect of thickness variation; damage initiation and growth; temperature increase; secant modulus change; effect of preloading on residual modulus and strength; and effect of ply failure on compression buckling strength [9]. Hojo et al. [10] presented the effect of the stress ratio on near-threshold growth of delamination fatigue cracks with unidirectional laminates of CFRPs. Their tests of delamination fatigue crack propagation were carried out under mode I loading by using double cantilever beam specimens. In the region of crack growth rates above about 5×10^{-10} m/cycle, growth rate was expressed as a power function of fracture mechanics parameters. A new phenomenological law of fatigue crack propagation was derived. Reifsnider and

Jamison [11] examined the complexity and made an attempt to assess the manner in which pre-fracture fatigue damage affects residual strength and the fracture event. They presented a thorough chain of physical evidence in support of this new approach. Growth of edge delamination across the specimen width was followed with penetrant enhanced X-Ray radiography.

Non-linear elastic behavior of fabric composites has been extensively studied by Ishikawa and Chou [12]. Fiber undulation and bridging models were applied along with the application of the non-linear constitutive relation developed by Hahn and Tsai [13]. They summarized that the non-linear effects were less pronounced for fabrics assuming larger geometric repeating length due to increasing influence of bridging effect. This bridging model simplifies the analysis of satin weave composites by dividing and isolating different regions of a selected square section with undulated and other unidirectional fibers crossing into a single lamina representing one major fiber direction. The section with dominant undulations have similar sections on its sides. It has been verified that these neighboring regions carry more load than the undulated central section and hence act as load transferring bridges which is termed above as the bridging effect. Fatigue damage development in carbon fiber reinforced composites has also been investigated by Schulte [14] who compared the behavior of a woven CFR laminate in a balanced 8-shaft satin weave style to non-woven laminates with an equivalent cross-ply lay-up. Carbon fiber prepregs of non-woven nature were investigated both consisting of continuous and aligned discontinuous

fibers. The static and fatigue strengths were measured and stiffness reduction was monitored. This study showed that the fatigue damage is caused by an interaction of a dense crack pattern and failure of 0° fibers. The sudden failure (termed as "sudden death") was observed with a rapid reduction in stiffness at the end of the fatigue life. Rotem [15] said that laminated composite materials can arrest the propagating crack to within a single lamina contrary to conventional materials, thus avoiding immediate and such sudden failure. A hypothesis for residual strength was developed which was based on cumulative damage theory. His calculations showed that for laminated composite materials degradation of the residual strength starts only very close to the end of the fatigue life which was experimentally verified.

The influence of strength of the fiber-matrix interface on strength and failure process in the uniaxial arrays of carbon fibers in an epoxy-resin has also been studied [16]. Different oxidative surface treated batches of carbon fibers having various interface strengths were tested in tension. A zone of debonding was observed to form between the carbon fiber and the epoxy matrix. In the regions close to the fracture path optical photomicrographs showed additional fiber fracture. They concluded that though fiber surface treatment had only marginal effect on the strength, mode of failure varied significantly.

Talreja [17] proposed an alternative approach for Weibull parameter estimation. He reviewed the two classical methods of moment estimation and maximum likelihood estimation and demonstrated that error made in estimating both

the scale and the shape parameter by these methods increase linearly with the absolute value of the location parameter. His proposed method estimated the scale and shape parameter more accurately than others. Statistical analysis of carbon fiber strength distribution with the help of Weibull distribution was done for the Thornel™ P fibers similarly [18]. The author considered only one mode of failure whereas his experimentally determined strength distributions exhibited several modes. The author therefore presented a new statistical analysis which allowed the possibility of multiple modes of failure. His approach was of maximum likelihood method and not method of moments but his estimates of mean fiber strength were more accurate for short gauge length. Whitney [19] gave a procedure that allowed the generation of the S-N curves with some statistical value without resorting to an extremely large database. The latter procedure was based on a Power Law representation for the S-N curve and a two-parameter Weibull distribution for time-to-failure at a specific stress level.

Series of angle-plied Graphite/Epoxy laminates was prepared and tested in tension to investigate the effects of overaged or "advance-cure" materials in the degradation of laminate strength by Ginty and Chamis [20]. Their work also included Scanning Electron Microscope (SEM) investigation of the fracture surface which revealed flat surfaces containing alternate rows of fibers and hackles. Similar tests of uniaxial tension and fatigue on cross, angle-ply, and quasi-isotropic carbon fiber reinforced epoxy laminates were carried out by Harrison and Bader [21] to show the damage development.

Curtis [22] performed tensile fatigue tests on unidirectional polymer matrix composites. He asserted that tougher materials were more sensitive to fatigue. The author also suggested that various damage phenomena were operative and related the growth of splitting along the fiber to the Paris relationship. His experiments concluded that GRP material had a much greater sensitivity to fatigue loading as compared to CFRP.

Influence of stacking sequence on laminate strength was studied, and, optimization for protection against delamination under uniaxial tension and fatigue loading by specific layer orientation was presented by Pagano and Pipes [2]. This was based on the understanding of the interlaminar normal and shear stresses. Also the effect of stacking sequence on the damage propagation and failure modes in composite laminates has been studied [23]. The authors used Graphite/Epoxy coupons with 0, 90 and ±45 degree plies in four different lay-up sequences. They used X-Ray radiographs to study the effects of testing and summarized that damage propagation direction is strongly dependent on the stacking sequence.

Onset and growth of delamination in an unnotched $(\pm 30, \pm 30, 90, 90)_s$ Graphite/Epoxy composite laminates was quantitatively characterized by O'Brien [24]. Stiffness loss was monitored and strain energy release rate, G, associated with delamination growth was calculated. Characterization and analysis of the damage mechanism in T300/5208 and T300/914C Graphite/Epoxy laminates was done with

close examination during tension-tension fatigue loading [25]. Stiffness reduction and damage induced was presented as curves. Masters and Reifsnider [26] also forwarded an experimental investigation of cumulative damage development in two unnotched quasi-isotropic Graphite/Epoxy laminates loaded in quasi-static tension and tension-tension fatigue. Surface replication was done to monitor damage. A damage model based on a concept of a characteristic damage state (CDS) was also developed.

2.3 Fatigue Damage Characterization

Xian et al. [27] carried out fatigue tests on 156 specimens of 0°, ±45 and 0/90 orientation lay-ups in the tension-tension regime on Carbon/Epoxy plastic composites. Their results were presented as deformation diagrams and Acoustic Emissions (AE) recordings. As a result they found CFRP with higher fatigue resistance than metals and glass fiber reinforced plastics. Also it was seen that the load carrying capacity of the CFRP did not exhaust on the appearance of the first damage. It was shown that the microfailure was preceded by a significant reduction in stiffness. They pointed out that the stiffness reduction could be utilized in inspecting and predicting failure in the composites.

Fatigue damage characterization as initiation and growth of specific damage modes on tension-tension fatigue of CFRP laminates was presented by Wevers et al. [28]. They devised a method to study AE signals released from each individual

damage source. Their specimens were of $(0)_8$ UD, angle plied ±45 and cross-plied $(0_2,90_2)$ with a fiber fraction of about 60%, with R ratio being 0.03. NDT techniques; X-Ray Radiography, Edge Replication and Acoustic Emissions were used to monitor the damage initiation. They have highly recommended Energy Discriminating Acoustic Emission Method (EDAEM) for monitoring fatigue damage in the CFRPs. In a similar type of study Bhat and Murthy [29] defined the composite fatigue damage stages. For this study Acoustic Emissions techniques was suggested as the best one. They carried out experiments on unidirectional (UD) glass fiber reinforced plastics coupons.

Interlaminar fracture and cracking has been recognized by researchers as an important mode of fracture in CFRP [30]. The energies associated for one Glass/Fiber Epoxy and two Carbon/Fiber Epoxy composites under mode I (tensile) loading conditions have been documented. The interlaminar fracture energy G_C was much higher than fracture energy of a neat epoxy matrix. Also the fracture surfaces of the specimens under SEM were shown to be a strong evidence for characterizing the failure process. Some test results of simple (0,90,0), ±45 and quasi-isotropic carbon fiber reinforced epoxy laminates in uniaxial tension have been presented [31]. According to them the first sign of damage was fiber/epoxy resin debonds in the transverse plies. The failure mode in the quasi-isotropic laminate was found to depend on the ply stacking sequence. Overall it was shown that thinner plies were able to support higher loads in all type of laminates. SEM, C-Scan and Acoustic Emission

signals monitoring techniques were employed for material damage assessment as well as pre-test material integrity checkup. Fatigue response of $(\pm 45, 0_2)_{2s}$ laminate of T800/5245 composite system was determined in repeated tension, repeated compression and mixed tension-compression at constant stress levels over a wide range of R values by Gathercole et al. [31]. They analyzed the results in terms of constant life diagrams and discussed the use of such diagrams for life prediction purposes.

Fractographic study of fatigue of CFRP was carried out by Prakash [32] with scanning electron microscope and fatigue failure phenomena is explained based on these fractographs. Similarly Cruse and Stout [33] made use of SEM at a magnification as low as 90 X for the study and explanation of very high variability of local fracture processes. Use of SEM was explored in the fields such as application in fracture mechanics during fiber pull-out for CFRPs by Chou et al. [34]. Their study was to investigate pull-out and failure of carbon fibers that had untreated and treated surfaces.

Carbon fiber Reinforced Epoxy Laminate composites with and without edge notch were loaded under tension-tension fatigue by Xian and Li [35]. The results showed that these composites have much higher fatigue lives and significantly well fatigue strengths. Their findings highlighted delamination as one of the severest failure modes. In notched specimens the cracks initiated from the notch tip and propagated along the fibers and after the first crack appearance, the specimen

sustained a long time fatigue till complete fracture. Fatigue damage in the specimens were examined by acoustic emissions, strain gage extensometry and SEM. Their notched and unnotched specimens were examined for stiffness and strength degradation.

Selden [36] used X-Ray radiograph along with SEM for study of fracture of angle-ply Carbon/Epoxy laminates. Delamination, matrix cracking etc. as damage growth criteria were physically observed using motor-driven cameras. Microscopic examination was carried out by Frandsen and Naerheim [37] for Graphite/Epoxy failure layer delamination that occurred in three point bending fatigue. Microstructure of the composite was then related to the surface morphology. The dominant failure surface features were found to be matrix cleavage, hackle formation and wear region. Damage growth has also been suggested as to be measured by the stiffness measurement indirectly by O'Brien [38]. He highlighted different laboratory applications of stiffness reduction measurement for indirect assessment of damage growth.

Scanning electron microscope these days is also being used to determine failure origin and fracture direction. Cross-ply Graphite/Epoxy laminates tested under fatigue were examined and hackles that characterize overload failure were observed by Morris and Hetter [39]. The damaged surface topography was interpreted in order to assess the failure initiation. Razvan et al. [40] investigated the fiber fracture in composite laminates with the help of SEM. Their experiments were on center-

notched, AS4/1808 Carbon Fiber/Epoxy laminates with quasi-isotropic $(0,45,90,-45)_{4s}$ and orthotropic $(0,45,0,-45)_{4s}$ stacking sequences. Their effort was to identify fundamental mechanism of damage growth in fiber reinforced composites under fully reversed cyclic loading. X-Ray radiography was used to map the internal delamination and matrix cracking for each individual ply. Theocaris and Stassinakis [41] used SEM for locating crack propagation and observing fracture surface of carbon fiber reinforced composites. Also micrographs showed conclusive crack propagation which assisted in explaining the different modes of failure of the CFRP. Similar detailed study was carried out by Purslow [42] for finding fracture modes in multidirectional carbon fiber reinforced plastics using SEM.

Reifsnider and Jamison [11] used ZnI_2 solution for their dye penetrant enhanced radiography of quasi-isotropic specimens. Their X-Ray unit operated at 25 kV and 25 mA for approximately 0.5 minute exposure with Kodak Industrex film and the exposures were taken at different stages of life till fracture. Another dye penetrant enhanced radiography was done with diiodobutane by O'Brien [38] for characterizing delamination in Graphite/Epoxy laminate. Their X-Ray exposure generated 18 kV for 5 seconds. Similar dye was used by Ratwani and Kan [23] for examining the stacking sequence effect. The same process was used by others such as Ramakumar [43] and Crossman and Wang [44].

Damage development near the edges of the composite material during quasi-static and fatigue loading was studied with the edge replication technique together

with SEM by Schulte and Stinchcomb [45]. The specimens used were T300/914C Carbon Fiber Reinforced Plastic system. This technique is explained in detail in the chapter 4. Replication technique was also used by Stalnaker and Stinchcomb [46] for the edge damage study of two quasi-isotropic Graphite/Epoxy laminates by recording the damage details along the edges of the stressed specimen after tension-tension fatigue loading. They presented a chronological order of damage events for each cyclic stress level and type of laminate.

2.4 Life Prediction Methodologies

At the Service Life Laboratories at Moscow Institute of Civil Aviation Engineers (MICAE), Strelyacv et al. [47] analyzed the relationship governing fatigue resistance of CFRPs in axial loading using data published and results obtained earlier. They mentioned main factors influencing the fatigue resistance of CFRPs as: type of filler, degree of filling, treatment of fiber surface, strength of matrix and loading regime. Equations were derived for the fatigue curves of CFRP based on high-modulus and high-strength carbon-fiber with surface treatment and a volume fraction of 60% of the fibers. The basic equation used was $N = A\sigma^{-m}$. The constants A and m were found by Regression Analysis.

Residual strength degradation model by Yang [48] was a statistical approach towards treating experimental fatigue data in different conditions to evaluate and

predict the life of composites like Graphite/Epoxy laminates. The basic assumption was that the residual strength decreases monotonically. Then Yang et al. [49] also forwarded a stiffness degradation model for Graphite/Epoxy laminates. Here again the model predicted the statistical distribution of residual stiffness of a particular composite laminate subjected to fatigue cycling. As before, the life predicted by the model correlated reasonably well with the experimental results. Considerable work has been done to back this proposed model. Also some improvements to it have been suggested by Yang et al. themselves and others. Radhakrishnan [50] tested the validity of the generalized residual strength degradation model for tension-tension fatigue of unnotched carbon epoxy composites. Moreover, load effects were studied under the same model which proved satisfactory later.

Theoretically Lee et al. [51] predicted fatigue life for matrix-dominated composite laminates under constant amplitude tensile fatigue loading on the basis of a fatigue modulus degradation model along with an appropriate failure criterion. For this analysis an analytical model was derived for the statistical distribution of fatigue lives for matrix-dominated composites. Their correlation between the analytical predictions and experimental results were shown to be reasonable. In matrix dominated composites, it was stressed that the stress-strain relationship is non-linear. Moreover, they highlighted that laminated specimen fail when their Fatigue Modulus reduces by a certain amount. This concept was first put forward by Hwang and Han [52] when they used the idea of "Fatigue Modulus" for the first time for analytical life

prediction of Glass/Epoxy composite under fatigue cycling assuming the fatigue modulus degradation rate followed a power function of fatigue cycles. Theoretical equation for predicting fatigue life was formulated using fatigue modulus and its degradation rate. It was claimed that their final formula predict fatigue life of glass fiber reinforced epoxy composites better than S-N curve or Basquin's equation.

Hahn [53] summarized two life prediction models which were statistical in nature and came from a very large pool of experimental data for both static and fatigue test behavior of unidirectional laminae in terms of static failure and fatigue limit strain of constituents. He used the material "age" for this model. Highsmith and Reifsnider [54] used the mechanics of a composite laminate rather than statistical approach and justified stiffness reduction relation with damage. Their basis for stiffness reduction was the matrix cracking which occurs early in the life of the specimen.

Poursartip et al. [55,56] developed the mechanics of fatigue damage of a carbon fiber reinforced laminate. They used a damage accumulation approach for fatigue of composites. They said that damage consists of a delamination front, with associated matrix cracking, which propagates inwards from the sample edges. They measured the elastic stiffness of the laminate to assess the current level of damage. A model was developed which summarized that the growth damage rate is a power function of the stress amplitude and of the mean stress and is independent of damage when cycling in a constant stress amplitude. They found that the SN curves they

plotted at various mean stresses for constant stress amplitude for life prediction were in good agreement with the experiments. Their predictions turned out much better than those of Miner's rule which are seriously non-conservative. They also quantitatively related different failure modes to the damage accumulation and showed that the damage growth rate dD/dN can be expressed as

$$\frac{dD}{dN} = f(\Delta\sigma, R, D) \tag{2.1}$$

Their basis was the relation of stiffness reduction to the damage as

$$E = E_o\, g(D) \tag{2.2}$$

The function in equation (2.1) was assessed by different methods to find fatigue life N_f of the composite as:

$$N_f = \int_{D_i}^{D_f} \frac{dD}{f(\Delta\sigma, R, D)} \tag{2.3}$$

Spearing and Beaumont [57] presented a new approach for modeling post-fatigue strength and stiffness of notched fiber reinforced composite laminates. It was based on the growth of the notch tip damage zone. Dye penetrant enhanced radiographs were used to characterize notch-tip damage zone and to establish a quantitative relationship between post-fatigue strength, cyclic stress, damage size and the number of cycles. Optical microscope in combination with Scanning Electron

Microscope (SEM) and the specimen Deply technique were used to assess the damage. Their observations showed that the extent of damage growth depends on the lay-up geometry of the laminate and the loading conditions. They also developed a model of fatigue damage of CFR Epoxy Laminate.

Petitpas et al. [58] determined the transverse cracking which occurs during the fatigue of crossply materials with different fibers (T300 or T400). They improved the solution of the well known Shear Lag Analysis concerning stress distribution in crossply composites after transverse cracking. Their treatment was experimental as well as theoretical containing both analytical and numerical approaches for modeling observed stiffness reduction. Their finite element (FE) analysis showed that the longitudinal stress in the cracked 90° layer is non-uniform. Also a mathematical model was proposed by Kobelev [59] for the micromechanism of failure of a composite material randomly reinforced with whiskers or in fiber-reinforced polycrystalline materials.

Studies have been presented for another category of components that have stress concentration sites. Spearing et al. [60] utilized fatigue damage mechanics of composite materials and developed a model for the damage growth at a notch tip in carbon fiber epoxy laminates. They explained damage as a series of interacting matrix cracks in various forms; splitting, delamination and transverse ply cracking. The extent of fatigue damage was successfully predicted for a family of $(90_i/0_j)_{ns}$ and (90,

$\pm 45, 90)_s$ laminates. Also the effects of cyclic tensile loading on the post-fatigue strength and stiffness of a notched laminate were explained. They also used Finite Element method for representing the damaged cross-ply $(90,+45,-45,0)_s$ laminate. Fracture mechanics was applied by Bathias et al. [61] to multi-orientation layered graphite fiber reinforced composite to provide a rudimentary tool with which the design engineer can assess the material. Their specimens were Graphite/Epoxy notched and the fatigue behavior at the notch root was studied extensively. Wright and Iannuzzi [62] also applied linear elastic fracture mechanics to notched carbon fiber reinforced epoxy matrix composites and used the mean stress value in fibers to predict coupon strength.

Kortschot and Beaumont [63,64] used a new approach for modeling strength of notched composites. This was based on the assumption that subcritical damage modifies the notch-tip stress field and that the state of subcritical damage just before failure, referred to as the Terminal Damage State (TDS), must have a significant influence on the notched strength. TDS was monitored for a wide range of cross-ply graphite reinforced epoxy specimens using real-time radiography. Also FE model incorporating TDS was used to determine modified notch-tip stress field. Furthermore FE model was used to simulate observed subcritical notch tip cracking patterns in cross-ply laminates. It was found that all the specimens failed when the maximum tensile stress in the 0° ply exceeded the tensile strength of that ply. Statistical evaluation of fatigue life and fatigue strength in a circular notched specimen of

Carbon 8-Harness Satin/Epoxy laminate was done by Shimokawa and Hamaguchi [65].

Significance of defects in the fatigue failure of CFRPs was highlighted by Prakash [66]. He employed ND evaluation techniques such as measuring ultrasonic attenuation for percentage of voids (defects) in a number of CFRP specimens being tested in fatigue. After failure SEM analysis showed presence of defects such as voids, interlaminar cracks etc. on fatigue fracture surfaces of specimens which failed at lower stress levels. He also presented a hypothesis for failure of CFRP along with fractographic evidence. Also Fatigue response of a $(\pm 45, 0_2)_{2s}$ laminate was described by Adam et al. [67] for the T800/5245 composite system and the results of Gathercole et al. [31] were used to define a program of four and two-block variable loading experiments in an attempt to derive predictive methods for such loading conditions. Formula have been developed to predict life under non-linear cumulative damage conditions and empirical data derived to validate procedures.

A review of fatigue damage mechanism based on the comparison between composite and homogeneous materials was forwarded by Stinchcomb and Reifsnider [68]. Many characteristic differences between the two were pointed out and explained in detail. The differences between the treatment of damage accumulation and fatigue for various types of advanced composite systems e.g. polymer matrix composites (PMC), ceramic matrix composites (CMC) and metal matrix composites (MMC) in general was discussed by Kedward and Beaumont [69]. A comparative analysis of

data for CFRP, GFRP and metal-matrix composites being used in aircrafts was presented by Vol'mir [70]. He summarized the trends in the use of these composite materials in the aircrafts and engines.

Some research work was also done on the Quality Control awareness in processing parameters of the test materials and coupons. Green and Pratt [71] determined SN-curves for the axial zero-tension fatigue behavior of uniaxial lay-up Morganite IIIs carbon fiber/CIBA LY558: HT973 epoxy resin composites. Large discrepancies were shown between nominally identical batches of fiber. The authors associated these with observed differences in degree of surface damage in the as-received fibers. This anomaly forced them to ask for careful quality control in manufacturing and treatment of reinforcing fibers.

Chapter 3

Analytical Model for Fatigue Life Prediction

3.1 Life Prediction Model

This model by Poursartip et al. [72] was forwarded along with the assertion that fatigue data is better to be presented as stiffness reduction vs number of cycles rather than as Stress vs Number of Cycles to failure or S-N curves. This model was based on accumulation of damage in the composite material during fatigue loading. This damage may be a combination of a number of sub-damage processes such as fiber breakage, matrix cracking, decohesion between matrix and fiber, delamination etc. Damage grows with the cycling until the net section stress (allowing for the loss of

section caused by the damage) reaches the ultimate strength, or until a critical crack, formed by the aggregation of damage, forms and propagates catastrophically.

The damage can be monitored by measuring properties other than moduli of the composite, for instance the electrical conductivity, or the light scattering, or the X-Ray absorption, or the ultrasound attenuation, or the damping coefficient. The moduli are particularly attractive because, being a tensor of the fourth rank, they offer the possibility of distinguishing and monitoring different components of damage. In the following section is presented the differential damage accumulation model.

3.1.1 Damage Model based on Stiffness Reduction

Let the fatigue damage be measured by a variable D. At the start of life D is zero unless damage D_i has been introduced during fabrication, or by earlier history. Cyclic loading causes damage to increase from D_i to D_f at which fast fracture occurs, either by the aggregation and linking of general damage, or by the propagation of a single crack. The model can be generally formulized as folows:

Let the damage depend on cyclic stress amplitude $\Delta\sigma$ and on the current value of D. Then:

$$dD/dN = f(\Delta\sigma, D) \tag{3.1}$$

This can be integrated to give the life, N_f (the number of cycles required to increase D from D_i to D_f), then:

$$N_f = \int_{D_i}^{D_f} \frac{dD}{f(\Delta\sigma, D)} \tag{3.2}$$

The difficulty, of course, is that we do not know the function f. But the modulus can be used to monitor damage. If a relation exists between modulus E and damage D:

$$E = E_o\, g(D) \tag{3.3}$$

where E_o is the undamaged modulus, then we have that:

$$\frac{1}{E_o}\frac{dE}{dD} = g'(D) \tag{3.4}$$

where g′ is the derivative of g with respect to D. Substituting into equation (3.1), we have:

$$\frac{1}{E_o}\frac{dE}{dN}\frac{dD}{dN} = g'(D)\cdot f(\Delta\sigma, D)$$

or

$$\frac{1}{E_o}\frac{dE}{dN} = g'\left(g^{-1}\left(\frac{E}{E_o}\right)\right) f\left(\Delta\sigma, g^{-1}\left(\frac{E}{E_o}\right)\right) \tag{3.5}$$

where g^{-1} is the inverse of g:

$$D = g^{-1}\left(\frac{E}{E_o}\right) \tag{3.6}$$

This equation suggests two alternative approaches to evaluate damage in composites. First, a damage-accumulation function, $f(\Delta\sigma,D)$, can be guessed or inferred from a model, inserted into equation (3.5), and the result compared with the experiment. Alternatively, data can be gathered for E/E_o as a function of N and, knowing $g(D)$, $f(\Delta\sigma,D)$ can be determined empirically, using:

$$f(\Delta\sigma, D) = \frac{1}{g'\left(g^{-1}\left(\frac{E}{E_o}\right)\right)} \frac{1}{E_o} \frac{dE}{dN} \tag{3.7}$$

To do so the right side of the equation (3.7) is evaluated from experiments. Tests are run at constant $\Delta\sigma$ to get a range of E/E_o values and similarly at different stress levels. For each test, rate of stiffness degradation (dE/dN) is obtained. Using this dE/dN value in the above equation the function f i.e. dD/dN (the damage rate) is found for each test. The damage rate dD/dN as a function of stress range $\Delta\sigma$ was plotted on a log-log graph. A power law is fitted through the data to obtain a relation between the damage rate dD/dN and stress range $\Delta\sigma$. The function f is thus determined from this plot.

Consider a unidirectional composite which is under uniaxial loading parallel to the direction of the fibers. This cyclic loading induces cracks in the matrix and the weft bundles which lie normal to the axis of loading. Due to the partial elimination of a continuum in these weft bundles the result is that the cracks reduce the axial

modulus E of the fiber reinforced composite. A number of analysis exist for the moduli of cracked solids. Eshelby [73], Bristow [74], Budianski and O'Connell [75] agree that for small D ($D < 0.1$), Elastic Modulus E_o (at N = 0) for an isotropic solid is reduced by a distribution of cracks to the value of E as:

$$g(D) = E/E_o = 1\text{-}cD \tag{3.8}$$

For the isotropic solid the above authors proposed a value of 1.5 for the constant "c". But for an anisotropic solid (e.g. a unidirectional composite) with a distribution of cracks all lying in the plane normal to the tensile axis, Gottesman, Hashin and Brull [76] proposed the following relationship to evaluate the constant "c":

$$c = \pi \left(2\frac{E_A^2}{E_T}\right)^{1/2}\left[\frac{1}{(E_A E_T)^{1/2}} + \frac{1}{2G_A} - \frac{\upsilon_A}{E_A}\right]^{1/2} \tag{3.9}$$

where E_A, G_A and ν_A are the Young's modulus, the shear modulus and the Poisson's ratio associated with loading in the axial direction, whereas E_T is Young's modulus in the transverse direction of the undamaged solid.

The values of these moduli and Poisson's ratio in equation (3.9) can either be obtained form literature or they can be evaluated empirically by the help of the Rule of Mixtures as under:

$$E_A = E_f V_f + E_m V_m \tag{3.10}$$

$$E_T \cong \frac{E_{ml} E_f}{E_{ml} V_f + E_f V_{ml}} \tag{3.11}$$

$$\nu_A \cong \nu_f V_f + \nu_m V_m \tag{3.12}$$

$$G_A \cong G_f V_f + G_m V_m \tag{3.13}$$

or

$$\frac{G_A}{G_m} = \frac{G_f\left(1+V_f\right) + G_{ml}\left(1-V_f\right)}{G_f\left(1-V_f\right) + G_{ml}\left(1+V_f\right)} \tag{3.14}$$

The values of these constant as calculated by using the above equations are represented in Table (1). Further refinement in evaluation of the constants is possible for woven fiber composite materials such as the plain weave carbon-carbon fabric reinforced composite. The change in the elastic modulus in periodically bent fibers in the woven fabric is given by [77]:

$$\frac{E_A^{\beta}}{E_A^{o}} = 1 - 2\left[1 - 2\frac{G_{ml}}{E_f} \cdot \frac{1}{V_f\left(1-V_f\right)}\right] \cdot \beta^2 \tag{3.15}$$

where E^{β}_A and E^{o}_A are the axial moduli with and without undulations respectively. Equation (3.8) can then be used with the value of "c" obtained from

equation (3.9) and after combining equations (3.1), (3.7) and (3.8) expression for the damage function is obtained as:

$$f(\Delta\sigma, D) = -\frac{1}{c}\left(\frac{1}{E_o}\frac{dE}{dN}\right) \tag{3.16}$$

E_o is taken to be the highest measured modulus to allow for the initial increase in stiffness usually observed in the beginning of fatigue loading accompanied by a sharp drop to a steady E value. After approaching this value the stiffness degradation is predominantly linear for a large portion of fatigue life until the last few cycles. Here the failure is usually sudden and the stiffness value also drops rapidly. In effect the distinct three zones in the stiffness degradation plot are more or less typical of fiber reinforced composite materials.

3.1.2 Maximum Stress Effect on Damage

It has been established that the terminal damage and the failure criterion is determined by the maximum stress and not by the mean stress level applied during loading. It is also established that there is a linear relation between maximum stress and damage at failure. Talreja [17] has postulated that the critical failure parameter is the applied strain. In load controlled fatigue test, as E decreases with cycling, the maximum strain increases. When $\varepsilon = \varepsilon_c$ failure occurs.

Under static loading, assuming no stiffness reduction,

$$\varepsilon_c = \frac{\sigma_{TS}}{E_o} \tag{3.17}$$

After cycling at some maximum stress, σ_{max}, the maximum strain is given by:

$$\varepsilon = \frac{\sigma_{max}}{E} \tag{3.18}$$

where E is the reduced modulus due to damage. Failure occurs when the maximum strain during the fatigue cycle equals 'ε_c'. Equating equations (3.17) and (3.18) and substituting for D_f from equation (3.8) we have, at failure:

$$D_f = \frac{1}{c}\left(1 - \frac{E_f}{E_o}\right) = \frac{1}{c}\left(1 - \frac{\sigma_{max}}{\sigma_{TS}}\right) \tag{3.19}$$

For equation (3.16) the stiffness reduction rate *dE/dN* for all specimens is calculated by fitting a least-squares regression line to the linear section of the stiffness reduction-cycle curves. The function f or the damage rate, *dD/dN*, is then calculated using equation (3.16).

Poursartip et al. using the above mentioned analysis proposed that the relationship between E/E_o and the fatigue damage can be evaluated assuming that;

(i) Initially there is no damage and, $E = E_o$;

(ii) Physically the total damage is a mixture of delamination and matrix cracking;

(iii) the relation between E/E_o and damage is linear; and.

(iv) When delamination and matrix cracking are complete, $E = 0.65\ E_o$

Figure (1) which represents the work of Poursartip et al. [55] shows the damage rate dD/dN as a function of stress range $\Delta\sigma$. All the data is for nominal load ratio $R = 0.1$ and each point represents a different test. There are three regimes of behavior:

(1) Over most of the stress amplitude range, there is a power-law relation between dD/dN and $\Delta\sigma$. The log-log plot is clearly showing this by the straight line in Figure (1).

(2) At stresses approaching the tensile strength of the material, the damage rate is much higher and we observe what is effectively a static failure.

(3) Below a stress of about 250 *MPa*, the damage rates are much lower than would be expected by extrapolating the power-law prediction and there are indications of the threshold $\Delta\sigma$ below which no damage occurs.

A least-square regression line fitted to 21 data points between stress ranges of 240 *MPa* and 480 *MPa* for R = 0.1, gives the following empirical equation:

$$\frac{dD}{dN} = 9.189 \times 10^{-5}\left(\frac{\Delta\sigma}{\sigma_{TS}}\right)^{6.393} \qquad (3.20)$$

The stress range has been normalized by the mean tensile strength so that the equation becomes more generalized in nature and is not restricted to a specific material with a constant tensile strength. This way materials having many different stress range to tensile strength ratios can be represented by this one equation easily.

Equation (3.2) can then be integrated between $D = 0$ and $D = D_f$ to evaluate the number of cycles to failure N_f.

$$N_f = \int_{D_i}^{D_f} \frac{dD}{9.189 \times 10^{-5} \left(\Delta\sigma / \sigma_{TS} \right)^{6.393}} \tag{3.21}$$

where D_f is calculated by using equation (3.19).

Chapter 4

Experimental Setup and Data Collection

4.1 Material and Specimen Geometry

The composite material under investigation was a prepreg plain weave woven Carbon-Carbon Fabric Reinforced Plastic with polyester resin as the matrix material. The carbon-carbon worked plain-weave fabric had a fiber density of 208 g/mm^2. The carbon fiber was high tenacity/high strength fiber with 3000 filaments per yarn or tow of the warp and weft of the fabric. These high strength fibers were Thornel™ T-300 type in the graphite crystal form having a density of 0.0017625 g/mm^3. The fibers have a Young's modulus of 235 *GPa*, approximate elongation of 1.6% and has a tensile strength of 3.7 *GPa*. The yarn had a twist of 15 *TPM* (turns per meter) and a

fineness (tex) of 200 *g/km*. The properties of the fabric, resin, a single ply and the composite are given in Table (2). For the monotonic properties of the material sample graphs for each class of composite are given in Figures (2-4). The value of the elastic moduli were evaluated using linear fits of the stress-strain curve of the tensile tests. The properties of the composite material were estimated using STRAN; a software used for the analysis of mechanical properties of multilayered hybrid fiber composites. These values are given in Table (2).

A number of Eight-ply carbon fiber reinforced plastic composite laminate panels with a density of 0.0016075 g/mm^3, 66% volume fiber fraction and approximately 250 X 250 *mm* size were prepared in an autoclave under vaccum bagging. A curing temperature of 120-130°C and a curing pressure of 8 Bars was used. The fiber orientations selected for investigation were unidirectional $(0)_8$, $(0,0,45,-45)_{2s}$ and $(45,-45,0,0)_{2s}$. All test coupons were machined using ASTM standard D-3039 [78] with a dimension of 200 X 25 *mm*, having a thickness of approximately 1.6 *mm* as in Figure (5). End tabs of 30 X 25 *mm* size were made of the same composite material with the same thickness and bonded with *ACE*™ 2 Ton Epoxy. The tabs were left to harden overnight and excess epoxy was scraped off for dimensional accuracy.

4.2 Fatigue Testing

The machine used in order to obtain fatigue data for the carbon fiber reinforced plastic composite was the Instron 8501 material testing system. It is a closed loop servo-hydraulic, dynamic, single axis fatigue testing system. This machine (see Figure (6)) was used to generate constant amplitude loading histories. The main controlling modes of the system are strain (±10%), load (±100 *kN*) and position (±75 *mm*) with a frequency range from 0 to 200 *Hz*. The controlling limits can be viewed on the digital control panel any time during the test along with all other test variables (e.g. maximum/minimum limits of each cycle or the safety limits set or number of cycles or elapsed time etc.).

The machine is equipped with a hydraulically actuated self-aligning gripping system. To ensure the vertical alignment of the specimen specially machined inserts were used during the tests. Any pre-loading induced during clamping was adjusted to zero prior to testing by the re-calibration of the load cell after clamping.

All tension and fatigue tests were carried out in the ambient laboratory conditions using a specialized Fatigue Laboratory APplications Software (FLAPS™) which provides the complete machine control, data acquisition, reduction and analysis capability. All the constant amplitude loading histories were designed in FLAPS™ as well as the ramp tests for mean stress level application or static load or position increments for the tension tests. The software contained all options for designing a

comprehensive test. A complete test consisted of one or more than one event or in software language "task". Position and Load control mode programs were fed into a customized multitask test for a variety of Constant Amplitude Loading (CAL) histories.

The tension tests were carried out in the position control mode with a constant displacement rate of 2 *mm/min* (ASTM Standard D-3039). The software logged position and corresponding load of the test with a constant position increment till fracture at the ultimate tensile strength which was logged along with the final position before fracture. The stress and strain were calculated from the load and position data and hence the elastic modulus for the carbon fiber reinforced plastic composite was obtained. The final position of the actuator gave the strain at failure ε_f and the final stress value obtained just before failure was selected to be the tensile strength of the specimen. The results of the tension tests are given in the tabular form in Table (6). The obtained mechanical properties were later used in the fatigue test data manipulation.

The fatigue tests used the following load history. Initially a ramp to the mean stress level and then a sinusoidal loading between the P_{max} and P_{min} with an amplitude of P_a. The second loading task was set at a constant frequency of 20 *Hz* and a constant stress ratio R of 0.1 for all tests. The P_{max} ranged from 10 *kN* to 25 *kN* for different types of specimen i.e. unidirectional or angle-ply coupons. The level of mean stress

and the P_{max} to be programmed for the test was estimated from the tensile strength obtained in the tension test. Normally P_{max} ranged between 50-80% of the tensile strength i.e. failure load.

Data collection was done by FLAPS™ for both the tensile and fatigue tests. The logging of position and load along with elapsed time was done at position increments of 0.0333 *mm* for the complete tensile test.

For the fatigue test, logging was done only for the constant amplitude and frequency cyclic loading at a rate of 40 *Hz* for peak/trough values of load and position along with the logged cycles after an interval ranging form 100 to 5000 cycles for different tests depending upon the expected life of that particular type of specimen under the applied load history. The 40 *Hz* frequency logging stored two data points (peak and trough) in each cycle after the specified interval.

4.3 Fatigue Damage Characterization

The equipment used for the non-destructive and destructive testing of the fatigue damaged CFRP specimens are given below:

- Jeol *JSM* T-300. Scanning Electron Microscope
- SEIMENS Polyphos-30. X-Ray machine

- Olympus, Reflected Light Microscope for Photomicrography
- Leitz Ortholux 2™, Transmitted Light Microscope for Edge Replica Examination

The surface morphology of the damaged CFRP specimen was studied under Jeol JSM T-300 scanning electron microscope to investigate the fatigue damage. The specimen were reduced to the appropriate size by Buehler Isomet™ low speed saw using a diamond wafer (15 *HC*), in order to eliminate the possibility of inducing any post fatigue damage near the fractured surface.

To suppress charging and increasing electron emission, gold coating of the fracture surface was also done. This process provided very fine uniform coating of a conducting material (i.e. gold), so that the surface after coating was an exact replica of the underlying material. The coating was done by vacuum depositioning in several stages provided by rotary and diffusion pumps of Jeol Fine Coat Ion Sputter JFC-1100 with a vacuum of 0.1 *Torr* at 1-1.5 *kV*. The time and amperage were selected with the constraint of the coat thickness and the specimen surface area.

X-Ray radiography technique was used to examine internal damage features of the fatigue fractured coupons. A special Zinc Iodide solution was used to infiltrate the damage zone and enhance the visibility of the damage on the radiographs. The composition of this solution was 60 *g* Zinc Iodide (ZnI_2), 8 *ml* Water (H_2O), 10 *ml*

Isopropyl Alcohol (2-Propanol) and 3 *ml* Kodak photoflo-200. The equipment used was a commercial Seimens PolyPhos-30 available at KFUPM medical center. X-Rays at 40 *kV* with a rate of 0.2 *mA/sec* were used. The best X-Rays with clear contrast had exposure distance from the source to the target coupons between 135-145 cm.

In order to see the time effect of submersion in dye on the material to the contrast and resolution of the radiograph, different amounts of dye and different periods of dye immersion were tried, but the differences proved to be undistinguishable and hence one unique method was adopted for use on all coupons. A hypodermic syringe was used to inject the dye at the edges of the coupons and in the damage sites visible outside. Reasonable amounts were injected in , and excess amount removed with a clean cloth. It was useful to inject with certain tensile static load being applied on the coupon to allow the dye to penetrate deeper inside the cracks.

The X-Ray radiographs provided excellent delineation of matrix cracking and delamination which could be qualitatively linked to the reduction in the strength and stiffness of the material. These radiographs identified matrix cracks, fiber fracture and delamination. Nascent coupons were also randomly radiographed to observe the presence of initial flaws, if any, that may have been introduced during manufacturing, machining or handling before the test. All random checks proved the coupons to be generally free of any initial damage.

The optical examination of the specimen edges was possible with the Olympus light microscope. For this purpose the specimen edges were metallographically prepared. They were manually polished with increasing grit size from 240, 320 to 400 and then 600 grit emery paper having alternate perpendicular rotation at the change of a lower grit to the higher one till 600. The sequence was followed in such a way that the 600 grit was used to polish for the last time along the direction of the fibers which is along the length. Then 0.3 micron Alpha Alumina powder with water was used on a microcloth on a polisher for polishing in order to produce a mirror-like surface on the coupon edge.

In the study of sequential damage it is essential to have a quick and reliable method of permanently recording in-situ damage during the entire period of fatigue loading from N = 0 to N*f*. An essential requirement of any such technique is that it must be capable of being performed on the specimens during the fatigue test. This provides permanent recordings of the damage at specified intervals throughout the test. The surface replication was done using cellulose acetate replicating tape manufactured by Buehler™. The replica were made by softening one side of the strip of approximately 5-mil with methyl acetate and pressing against the edge of the specimen. In order to avoid slippage of the replica scotch tape was used to hold the acetate tape to the specimen edges. Methyl acetate was introduced at the specimen-tape interface with a hypodermic syringe. The tape was pressed with a soft eraser for at least 30 seconds to obtain a good impression of the specimen surface. The replica

was allowed to dry and harden for 2 minutes. After removing the replica from the specimen they were placed in a set of clear glass slides to avoid their curling up. The replicas were examined under a transmission light microscope, Leitz Ortholux-2™ in the Research Institute of KFUPM to investigate damage along the edges of the surface.

Chapter 5

Results and Discussions

5.1 Fatigue Damage Characterization

It is well established that the composite materials are significantly different from their metal counterparts in the manner in which fatigue fracture initiates and develops during the load cycling. We must deal with a number of considerations which are unique to the composite materials. Whereas only one or two fatigue damage characterization techniques (destructive or non-destructive) may be sufficient to completely characterize the damage in metals, the unique phenomena by which the damage occurs in composites necessitates the use of several damage characterization techniques to fully understand the damage mechanism in this class of materials.

The specific elements that need to be carefully examined are:

- The typical failure modes
- The interplay of various failure modes
- Initiation and propagation mechanisms during various stages of fatigue life

Since our knowledge of composite failures is still lagging significantly behind the rate at which these materials are being used in the modern engineering components and structures, the need to develop new life prediction methodologies or to extend the application of the existing methodologies to new composite materials can not be over emphasized.

The following presentation of results of the present study and ensuing discussion is an effort to add on to the existing knowledge of not so well studied class of carbon fiber reinforced composites, namely the woven Carbon-Carbon fabric reinforced plastic composite.

5.1.1 Generalized Fatigue Behavior

The results of all the fatigue tests are provided in the tabular form in Table (3) and graphically represented as the conventional SN curves in Figures (7-9). An examination of Figure (10) which shows the fatigue test results of all the three classes of composites, indicate that the fatigue strength of the composite is only moderately

affected by the stacking sequence but it is significantly affected by the ply orientation. Class 1 $(0°)_8$ composite having all plies in the 0° direction show significantly high fatigue strength as compared to the class 2 $(45,-45,0,0)_{2s}$ and also the class 3 $(45,-45,0,0)_{2s}$ composite. The class 2 specimens having $(0,0,45,-45)_{2s}$ orientation exhibit higher fatigue strength than the class 3 with $(45,-45,0,0)_{2s}$ orientation.

It was seen that class 1 $(0°)_8$ i.e. unidirectional composite was predominantly failing with lateral fractures usually coded as LAT(lateral At-tab Top), LGT(Lateral Gage Top), LGB(Lateral Gage Bottom), LAB(Lateral At-tab Bottom) as per ASTM D-3039 [78]. Some of these typical failures are shown in Figure (11). Some fractures were observed to occur inside the tabs. Shulte [14] has mentioned the phenomenological final rupture as 'sudden death' failure of the composite. As compared to unidirectional $(0°)_8$, the class 2 and class 3 CFRPs have shown a range of failure modes. Class 2 having 0° on the outside fails partially as unidirectional but the modes of failure are intermixed. Failure codes are mostly LGM(Lateral Gage Middle), MGM (Multi-mode Gage Middle), LGB on the outside and SGM (Splitting Gage Middle), SGT(Splitting Gage Top), or sometimes AGM(Angular Gage Middle), MGM, AGT(Angular Gage Top) etc. on the inside for the 45° fiber bundles. The shearing of inner 45° fibers in class 2 is a result of a series of events that take place sequentially. Initially transverse matrix cracks appear through the weft of the 0° fiber bundle which is at 90° to the loading direction. These transverse cracks travel inward

from the edge of the composite. The transverse cracking through the matrix increase with increasing fatigue cycling. Subsequently fibers in the 45° ply start splitting in the transverse direction. Upon further loading these cracks link up with the neighboring 90° weft cracks and jog to the other to ultimately create a major edge delamination which spans the complete length of the specimen. Further cycling extends this delaminated area more as the separation propagates more and more inwards. Same is the situation in class 3 CFRP specimen where the 45° fibers are on the outer edge. Here the ultimate failure is less severe. The surface of the class 3 composite at failure is fractured as AGM, AGT, SGM, SGT, MGM on the outer side, and, LGB or LGT on the inside for 0° fiber bundles. The fiber splitting and fractures are more visible on the outer ply and much more abundant as compared to class 2. The complexity of the fracture has been clearly demonstrated by the SEM figures and the edge replicas in the coming sections.

The laminates that have off-axis plies, such as the $(0,0,45,-45)_{2s}$ and the $(45,-45,0,0)_{2s}$ quasi-isotropic stacking sequence, the fatigue damage is initiated through matrix cracking. Although the toughness and ductility of the matrix material may accelerate or retard the initiation of such cracks, even to the extent of suppressing matrix crack formation entirely for quasi-isotropic loading in some cases, cyclic loading is known to have initiated the fatigue damage via matrix cracks in virtually every laminated high modulus or high strength continuous fiber composite materials. These cracks usually form through the thickness of the plies in a direction parallel to

the fibers and perpendicular to the dominant load axis (the 0° direction). The Figure (12a) is a schematic diagram of such fiber fracture near primary matrix crack tips. It also includes schematic diagram of the internal distribution of the fiber fracture in the warp direction in Figure (12b). The behavior of the weft fibers is somewhat similar to that of a 90° fiber bundle but here the woven nature increases the failure time and so the failure localities of the warp 0° fibers are determined more or less by the peak of undulations as maximum bending stress in the fibers occur here. The schematic also shows the local debonding that occurs near the tip of fractured fiber, Figure (12c).

A photomicrograph in Figure (13) shows multiple cracks in off-axis plies, coupled together with delamination. Figure (14a) shows the delamination joining with a matrix crack in order to pass to the adjacent interface and continue delamination (A) and damage to the composite material. Figure (14b) shows the matrix cracks (arrows) inside the fiber bundle in class 3 $(45,-45,0,0)_{2s}$ composite. Under cyclic loading the appearance of the primary cracks, the first crack along the matrix, is the beginning of the causative sequence of the micro-damage events which ultimately determines the residual strength and life of a given composite laminate. This subsequent damage sequence is responsible for the strength reduction during fatigue loading. The second and most immediate cyclic consequence of these cracks is the occurrence of fiber fractures which begin to appear in adjacent plies near the crack tips.

The third major type of micro-damage event which occurs in the sequence of damage development in laminates is the local delamination where the primary and

secondary cracks are intersecting. The secondary cracks that are progressing at $\theta>0$ to the primary cracks usually will create planar separation resulting in the region of delaminated plies. Such evidence on a macroscopic scale has been substantiated by X-Ray radiographs in Figure (15) that highlights the delaminated region with contrast.

Hence, the causative sequence of micro-damage development in a fiber reinforced composite laminate under tensile fatigue loading can be thought of as a process of initiation and successive localization which includes initiation of primary matrix cracks, fiber fractures, local debonding, secondary cracking and possible local delamination which becomes more and more concentrated in a small region around the intersection of primary and secondary cracks.

5.1.2 Damage Characterization through X-Ray Radiography

Enhanced dye penetrant X-Ray radiography was conducted on a number of fatigue tested specimen for delineating edge delamination across the specimen width. The specimens failed were injected with a solution of ZnI_2 in 2-Propanol and water with a hypodermic syringe. The Zinc Iodide provided the needed opacity to the X-Rays and enhanced the contrast. Radiographs were obtained by a Seimens PolyPhos-30 equipment operating at 40 *kV* and 0.02 *mA/sec* with Kodak TME (100 NIF) film. Figure (16-18) show X-Ray radiographs of class 1 $(0°)_8$, class 2 $(0,0,45,-45)_{2s}$ and class 3 $(45,-45,0,0)_{2s}$ composite specimens after fatigue failure. These figures show

the typical fatigue damage details of each class. Figure (16 a,b,c) shows class 1 $(0°)_8$ specimens. One coupon has experienced lateral fracture whereas another has failed inside the tabs. All the three specimens showed only a negligible amount of delamination. The cracking has occurred through the matrix which extends laterally. The X-Ray radiograph in Figure (16d) shows a $(0°)_8$ specimen cured at 0.9 Bars. The fatigue damage in the specimen occured as lateral fracture along with considerable damage in the form of matrix cracks and splitting between the fibers in the gage section. The reason for testing such CFRP was to see the effect of low curing pressure on the fatigue behavior of composite. The fatigue test results of class 1 specimens are provided in Table (3a). The fatigue damage in class 2 $(0,0,45,-45)_{2s}$ as shown in Figure (17) exhibited a typical trend of a single dominant delamination front propagating to produce the final fracture. Relatively less delamination at other sites was observed and failures like AGM and AGM were noted. Similarly class 3 $(45,-45,0,0)_{2s}$ showed delamination but here it was scattered over all the gage section and the damage was completed when one of these delamination fronts dominated and passed into the composite material far enough to cause final fracture. Figure (18) shows specimens of class 3 $(45,-45,0,0)_{2s}$ fatigued to failure. The delamination can be clearly observed. The well defined serrated feature of the fracture surface produced provides evidence of the fiber breakage that has taken place after the delamination of the 45° ply.

An approximate measurement of the observed delaminated area seen could also help in estimating the reduction in the stiffness of the composite material. This method was used by Poursartip et al. [55] for determining reduction in stiffness due to delamination. The delamination process was recorded by the use of C-Scan and reduction in the laminated area was measured. They related this area reduction to the reduction in the stiffness by a direct linear relation. For the class 3 $(45,-45,0,0)_{2s}$ specimens where the area delaminated was delineated with the help of X-Rays, the stiffness reduction was also found to be directly related to the amount of delamination. For a specimen shown in Figure (18), the area reduction was approximately 12.8% where the stiffness reduction for a material of this class of lay-up was calculated to be averaging between 10-15%.

5.1.3 Damage Characterization with Fractographic Study

The scanning electron microscope was used to examine the surface morphology of the fractured specimens. Figure (19) shows the complexity of the woven structure in $(45,-45,0,0)_{2s}$ lay-up carbon fabric reinforced composite and its complex fracture morphology. Here all the 0° and 45° fiber bundles can be seen broken as a whole and splitting is complete for the matrix and fiber bundles. Figure (20a) shows a complete delaminated region between 0° and 45° fiber bundles in a class 3 $(45,-45,0,0)_{2s}$ CFRP specimen. The fracture can be observed to have taken place after a large amount of

delamination. Similarly in Figure (20b) 45° fiber bundle can be seen separated due to substantial interfacial delamination and fiber splitting. Figure (21) shows the pull-out of a complete bundle of 0° fiber bundles which indicates that the stress applied had reached the second stage of the damage development without any major fiber pull-out. A complete bundle of fibers has been removed which also highlights the presence of delamination among 0° and 45° adjacent fiber plies. This means that macroscopically in terms of final fracture, the warp fibers can be considered 0° laminae of non-woven nature but again the periodic undulations provide bending stresses even in monotonic loading state. Hence the analysis of a carbon-carbon woven fabric composite cannot be generally understood with the analogy of a non-woven fiber composite given that all properties remain the same. High magnification of 120X reveals that the fibers that have pulled-out of the matrix contain some polyester on the surface which is indicative of the matrix cracking going on in between the warp fiber bundles in a $(0°)_8$ CFRP specimen (see Figure (22)). The fiber bundles have fractured as a whole and no significant fiber splitting has taken place. The close-packed state of the internal structure proves the absence of delamination before fracture. Therefore one can summarize the failure of class 1 $(0°)_8$ CFRP as simply the matrix cracking with fiber fracture dominance till the end of life.

Somewhat different fracture morphology is seen in class 3 $(45,-45,0,0)_{2s}$ specimens where the excessive load cycling breaks the matrix in small pieces and the fibers are splitted easily from the matrix. Such fiber pull-out is shown in Figure (23b).

Figure (23a) shows the macroscopic view of the fiber breakage (A) and major delamination (B) between the 0° and 45° fiber bundles. Figure (24a) and Figure (24b) show the fractured fibers with very little matrix on the surface indicating clean fiber-matrix debonding before fiber fracture. A lateral view of the broken fibers and broken matrix in the form of debris is shown in Figures (25) and (26a) where broken fibers are seen well attached to the remains of the matrix exhibiting the high cohesive strength and strong fiber-matrix bonding at this site. Figure (26b) shows a special matrix feature called "Hackle" (see arrow). These are produced by the shearing action of the matrix during cyclic loading and look the same as fatigue striations in an isotropic metal as shown with high magnification of 3,500X in Figure (27b).

The fracture surface morphology according to the SEM analysis has highlighted the complex nature of the damage as well as its characterization in CFRPs. It was established that in angle-ply composites, different fiber lay-ups display different sequences of damage. Pagano and Pipes [2] have optimized the stacking sequence which led to the optimum protection against damage such as delamination and subsequent strength degradation. Ratwani and Kan [23] have also substantiated this with experiments and highlighted that damage propagation direction depends upon the stacking sequence with the accompanied orientation. According to these authors, the fatigue or static behavior of the unidirectional composites is relatively more consistent, simple and reproducible. In angle-plied specimens as of class 2 and class 3, the damage starts from the shearing at the matrix and unidirectional 0° fiber

bundles. Gradually this shearing gives rise to complex failure mechanics for the fracture of the 45° bundles, leading to the failure of these fibers and transfer of load to the remaining 0° fibers. But as far as their fatigue resistance is concerned, their limit is the ultimate tensile strength of the carbon fibers of the warp.

5.1.4 Damage Characterization through Optical Microscopy

Polished specimens were viewed under the light microscope at different magnifications ranging from 50 - 400X. In Figure (28) it can be clearly seen that even the untested specimens have a really complex structure because of the use of fabric instead of fiber laminae in the CFRP. The interwoven nature of the fabric provides some extra components of stress because of the presence of the extra weft fibers (B) in the transverse direction. The micrographs shown provide a summary of events taking place in a variety of combinations. They reveal matrix cracking, delamination, splitting of fibers and matrix, and breaking of fiber bundle. In Figure (29a) the crack-like front of delamination which might have started at some defect or void at one location, is seen propagating along the edges of the 0° fibers. Then because of the complex nature of the normal stresses the crack 'jogs' almost perpendicular to the 0° fiber into the 45° fiber bundle breaking the interface, resulting in fiber-matrix debonding inside the bundle. After passing along the bundle width the crack confronts the fiber surface, and can not proceed further, hence adjusts its path along the 0° fiber bundle. The detail of the fiber-matrix debonding is clear in Figure (29b) where the 45°

fibers are being pulled apart from the matrix (arrows). Small matrix cracks can also be seen responding as matrix failure to the localized severe tensile loading in that small region.

The transverse cracking of the fiber-matrix interface for an angle-ply coupon $(0,0,45,-45)_{2s}$ is clear in Figure (13). The four plies of 45° are sharing the stress and responding with matrix cracking across the 45° bundle. This situation continues along the bundles till the propagating pseudo-crack i.e. the shearing of matrix, encounters the outer layers of 0° fiber bundles.

Complete failure of a angle ply $(45,-45,0,0)_{2s}$ specimen is shown in Figure (30) where total splitting and delamination is clearly visible (arrows). The major stiffness reduction is because of the interface failure to strengthen the complete laminate structure and only the 0° fibers take the load at the end. When those fibers are debonding from the matrix, the integrated form of their existence is lost and the debonded fibers stand alone to bear all the tensile stresses. Hence the applied stress gradually reaches the ultimate tensile strength of the carbon fibers in the 0° fiber lamina, and the lamina breaks catastrophically.

5.1.5 Damage Characterization through Edge Replication

Edge replication technique was used to examine the progressive damage growth with the number of fatigue cycles. All the damage on the edges of the coupons, polished to

a metallographic mirror (0.3 micron Alumina) finish, was recorded for class 1 $(0°)_8$ specimen at 10%, 20%, 25%, 50% and 75% life with N_f = 40,000 cycles. Another one of class $(0°)_8$ with N_f = 1,100 cycles was recorded for 10%, 25%, 50% and 90% of the fatigue life. For the class 2 specimen $(0,0,45,-45)_{2s}$ replicas were made 10%, 20%, 30%, 50%, 70%, 90% life which failed at almost 450,000 cycles and for class 3 $(45,-45,0,0)_{2s}$ sample, at 1%, 10%, 20%, 30%, 50%, 70% and 90% life which failed at almost 80,000 cycles. Replica production was carried out while the specimen were held under a slight tensile load as it helped the micro-cracks to remain open which might have gone undetected in zero-load conditions.

Sequential damage in class 3 CFRP can be examined from the edge replicas shown in Figure (31). At zero cycles in Figure (31a) no damage has been recorded and the surface is free of cracks. After a few hundred cycles first transverse cracking in weft bundle of the 0° fabric have taken place. These cracks have initiated because the loading axis is perpendicular to the fibers of weft bundle. The only continuum that could bear the load is the matrix within the weft bundle. Just as the stress in the matrix reaches its tensile strength which is very low as compared to the fiber, the matrix starts cracking through the weft bundle and these cracks start propagating along the outer surfaces of the weft fibers till they reach the boundary such as the other weft bundle or the 0° warp fibers. At 10,000 cycles, this damage has transformed from the transverse matrix cracking to the longitudinal fiber-matrix

debonding along the length of fibers and the loading axis. Further cycling till 15,000 induces more transverse cracks that tend to link with each other and separation between the matrix material and the 0° fiber increases. This is the second stage of the sequential damage mentioned earlier when the transverse cracks are saturated and the delaminated area is increased to an appreciably large amount. At this time more cycles of loading keep introducing these cracks till saturation occurs and more crack initiation is converted into jogging of transverse cracks from one bundle to the other. Looking at higher magnification, we can observe that the fibers tend to separate from the matrix. This phenomenon, called fiber-matrix debonding, has been seen in Figure (29b) clearly. After 30% life (N=15,000 cycles), evidence of fiber breakage can be seen in Figure (31a). The boundary of the 0° fiber bundle is met perpendicularly with the progressing crack with large enough stress to break the fibers at the outer rim of the bundle and the fibers start breaking one by one along the bundle width. This carries on until the stresses reach the tensile strength of the fibers and the whole bundle breaks completely. This process carries on toward the later portion of life and the edge replica at 70% (N=39,000 cycles) of life show a substantial amount of delamination and matrix cracks, transforming the matrix continuum into two pieces rather than one. At 90% life the replica shows complete structural failure and the complex ultimate failure is evident. The delamination has completed from one end of the specimen to the other end. Enough transverse cracks have shattered the structure of the weft bundles. At 95% life (75,000 cycles) the whole structure loses the load bearing capacity completely and the composite features are all lost. The specimen is

shown in an SEM micrograph in Figure (32) where fiber fracture and fiber-matrix splitting has spread into the complete structure of the composite material.

Figure (33) shows a $(0°)_8$ specimen fatigue to failure at N_f = 1,100 cycles. Some prexisting flaws, voids and splitting in plies are observed. These pre-existing flaws must have contributed to the large scatter in fatigue test data observed especially in class 1 $(0°)_8$ material. At 100 cycles transverse cracks have appeared and they tend to move across the weft fiber bundle to reach the interface but at 1,000 cycles (90% life) the cracks have still not manage to cause any marked delamination. At a lower stress where the fatigue life is in the intermediate life regime delamination can still be one of the dominant causes of failure. Hence it is suggested that different fatigue damage processes are operative in different fatigue life regimes for class 1 $(0°)_8$ composites. Similar to class 3 $(45,-45,0,0)_{2s}$, class 2 $(0,0,45,-45)_{2s}$ exhibit the same damage modes starting with the matrix cracking, preferably from a void or defect as shown in Figure (35a) and leading to initial cracking. Delamination beginning in the first quarter of life and the fiber splitting and debonding from the matrix in the middle of the life. After three quarters of the life the delamination has covered all the specimen edge and much load carrying capacity is reduced. Any major 0° fiber bundle fracture leads to the final failure of the CFRP specimen. This behavior is consistent in both class 2 and class 3 CFRPs which is encouraging for the designers for its use in wide applications confidently.

A comparison of damage of the three classes of composites has been summarized in Figure (36) where damage is shown for each class at the same stress applied and same percentage life. It is clearly visible that class 1 has different failure sequence than class 2 and class 3. The major difference being the absence of delamination in class 1 $(0°)_8$ CFRP.

5.2 Fatigue Life Predictions

The analytical model discussed in chapter 3 was used to calculate the fatigue life in the three classes of composites. In order to examine the validity of the model a series of fatigue tests were performed on the three classes of material to generate the experimental fatigue life data. As was discussed earlier the analytical model was based on the stiffness degradation that results as the fatigue damage accumulates during the cyclic loading.

5.2.1 Stiffness Degradation Rate

The data collected was utilized in obtaining the rate of stiffness degradation per cycle of fatigue loading, *dE/dN*. Some typical plots of stiffness degradation vs cycles are graphically shown in Figures (37-39). The rate of stiffness degradation were used to calculate the damage rate *dD/dN* from equation (3.7).

The behavior of the curves obtained have a generally unique nature which varies very little from one class of composites to the other. A typical characteristic curve of the stiffness reduction with fatigue life could broadly be divided in three regions. Initially the stiffness of the composite decreases rapidly to a certain level. This is related to the formation of transverse cracks in the matrix. After a few thousand fatigue cycles this rapid decline ends and reasonably stable stiffness is reached as shown in Figure (40). This is because of the saturation of these initial cracks to the stage where the applied stress is more or less transferred to the 0° fibers of the warp weave. The initial stage of rapid stiffness reduction is categorized as stage I of stiffness degradation.

During fatigue in stage II, a constant decrease of the elastic modulus can be observed, visible in the linear part of all the curves for the three classes of laminates. The damage mechanisms occurring in stage II is the typical fatigue mechanisms. For a specimen loaded in tension, the 0° plies carry most of the load. Because of internal damage (matrix cracking and delamination) an increase in the stress of the 0° fibers occurs. Because of the Poisson's strain, a contraction within the 0° plies occurs. The contraction is hindered by the angle-plies which have higher elastic modulus into the width direction of the specimen than the 0° plies. In the 0° plies tensile stresses develop perpendicular to the fiber direction, which especially under fatigue load can lead to longitudinal cracks. Along these longitudinal cracks, failure of the 0° fibers is initiated and possibly even before the actual fracture stress of the fibers is reached.

Another important contribution is the delamination between the differently oriented adjacent stacked plies. The intersection of primary and secondary cracks is the best locality for the initiation of local delamination. Combining with the cracks and the fiber breakage, delamination contributes much in the reduction of the elastic modulus of the composite laminate.

The stage III of the stiffness reduction varies in time as well as form of decay. The fabric used in the composites are basically of two different type of laminates. The class 1 composites containing unidirectional laminae have really a short third stage (see Figure (37)) as compared to class 2 and class 3 shown in Figures (38,39). Here the major contribution towards failure is strictly matrix cracking coupled with sudden fracture of the 0° fibers. But in other classes the final failure is indicated relatively early in life where the stiffness reduction is relatively gradual because of the development of longitudinal crack growth and interior delamination at the warp and weft threads of the 0° and 45° laminae. Normally it was not easily possible to log enough data to capture that precise life span where the degradation occurred in stage III. Rather the failure occurred after stage II e.g. in Figure (37). This is not the real representation of stiffness degradation which is shown in Figure (40). During stage III the first fiber fracture occurs in the weft fibers at the center of the undulation. Later, total failure of the weft thread results in the abrupt stiffness reduction.

Our methodology involves the stage II of the stiffness degradation curve only as we need to obtain the dominant trend of stiffness reduction due to fatigue loading

in that particular type of material. The behavior of stage I has always been difficult to quantify and remains a problem of statistical nature and not empirical owing to the inherent nature of low cycle fatigue in fiber reinforced composite materials. Stage III has always been randomly varying in terms of time. Hence reduced data for stage II only has been used to obtain the *dE/dN* values for our model.

5.2.2 Damage Rate

The damage rate *dD/dN* as obtained from the stiffness reduction data is plotted against the stress range $\Delta\sigma$ on a log-log paper (see Figure (41,42)). The plot of different stress levels is furnished with a power law curve fit to obtain the relation between the damage rate *dD/dN* and the stress range $\Delta\sigma$ for the data of that certain type of composite class as in equation (3.20). There the normalization of the $\Delta\sigma$ with the σ_{TS} is a generalization for all kinds of composite materials with that class of lay-up. Such practice is also repeatable for other two classes of composite materials under investigation. The observed values of stiffness reduction and the damage rate are given in Table (4) for the two quasi-isotropic classes. The class 1 $(0^\circ)_8$ CFRP fatigue test had certain problems which forced the model and life prediction attempts to be discarded. This is discussed in the next section in detail.

5.2.3 Life Prediction

The mathematical procedure for predicting life by using the stiffness degradation model has been explained in detail in chapter 4. In this section, we use the collected data from the fatigue tests run on the two different CFRP classes to check the validity of the proposed model to predict life in the two. For this procedure, amount of stiffness reduction, stiffness degradation rate and the damage rate are used in equation (3.16) and equation (3.20) is obtained from the graph of fitted power law as shown in Figures (41,42). This relationship is different for each class of composite laminates.

The relationships obtained for class 2 and class 3 were significantly sound to predict lives which were within a factor of 3. Considering the complex behavior of CFRP exhibited under fatigue loading, this amount of scatter can be considered very good. The graphs in Figures (43,44) show plot of fatigue lives of all specimens tested on from class 2 and class 3, experimental and predicted. The points lying away from factor of three lines are the specimens that suffered some problems such as failure at stress concentration sites and internal defects. So these points are located in the non-conservative zone. Although the conservative region for both classes, especially class 3, is largely vacant and some points lie in the non-conservative zone, still the model suggested, not for design perfection purpose, is a handy tool for predicting the fatigue life in carbon fabric reinforced plastic composites with reasonable confidence.

Therefore for class 2 $(0,0,45,-45)_{2s}$, the relation between damage rate, dD/dN, and the stress range, $\Delta\sigma$, is:

$$\frac{dD}{dN} = 2 \times 10^{-46} (\Delta\sigma)^{16.057} \tag{5.1}$$

and for class 3 $(45,-45,0,0)_{2s}$, the relation is:

$$\frac{dD}{dN} = 8 \times 10^{-71} (\Delta\sigma)^{25.979} \tag{5.2}$$

The predictions obtained from these relations are tabulated in Table (5) for class 2 $(0,0,45,-45)_{2s}$ and class 3 $(45,-45,0,0)_{2s}$ carbon-carbon fabric reinforced plastic composites. It is a nice practice to have a generalized form of these equations as equation (3.20) making the relationship valid for all class 2 or class 3 CFRPs with varying σ_{TS} values. It is also important here to highlight that the model has been used by Poursartip et al. for composites made up of laminae and not fabric. It is considered a good agreement if the scatter in life prediction is considerably large because of the large amounts of complexity of the stresses inside a fabric composite unlike a composite with straight laminae. Also the detection of certain defects like voids as shown in photomicrograph in Figure (45) in an untested specimen explained the presence of scatter in the fatigue lives that predicted with the analytical model.

For the class 1, modulus reduction data obtained was unreliable due to failure of a large number of specimens at the tab ends where the possibility of stress

concentration exists. It is perhaps reasonable to assume that any unidirectional CFRP of class 1 turned out to be very sensitive to bending stresses which usually accompany tension-tension fatigue loading. As a result a large scatter was observed in the fatigue life of the class 1 $(0°)_8$ composite. Eventually the scatter in the observed life was too sporadic to be regressed and analytically determined within a satisfactory confidence limit.

Chapter 6

Conclusions and Suggestions

6.1 Conclusions

The following conclusions can be drawn from the experimental and analytical work carried out in the present study:

- Destructive and non-destructive techniques such as X-Ray Radiography, Fractography by SEM, Optical Microscopy and Edge Replication can be successfully employed to fully characterize the fatigue damage in the plain-weave carbon-carbon fabric reinforced plastic composite

- Delamination was found to be the major damage mode in the CFRP while matrix cracking played the secondary role of determining the type of fracture occurring in the composite material.

- The fatigue damage is initiated by the transverse matrix cracking and leads to the onset of an interactive sequence of triggering other fracture modes such as fiber fracture, fiber-matrx debonding investigated under the present study.

- The analytical model based on stiffness degradation, proved reasonably successful in predicting the fatigue lives of class 2 $(0,0,45,-45)_{2s}$ and class 3 $(45,-45,0,0)_{2s}$ Carbon-Carbon Plain Weave Fabric Composite material.

- Predicted Lives are scattered within a factor of 3 for class 2 $(0,0,45,-45)_{2s}$ and class 3 $(45,-45,0,0)_{2s}$ CFRPs.

- Tests showed class 2 $(0,0,45,-45)_{2s}$ had higher fatigue life as compared to class 3 $(45,-45,0,0)_{2s}$ which highlights the effect of the stacking sequence on the fatigue life of the CFRPs.

- Class 1 $(0°)_8$ showed higher fatigue strength but less degradation in modulus accompanied with little delamination and fiber fracture with abundant matrix cracks.

6.2 Future Work Suggestions

It is evident from the available literature on the carbon fiber composites and the results of the present study that our understanding of the fatigue phenomenon in the composites is still at an early stage of development. This is more so in the class of composite investigated in the present study i.e. the woven fabric composites. Substantial room for continued research exists to generate, analyze and understand the fatigue data and fatigue phenomena in this class of fiber reinforced composite. Following are few of the areas in which further research is needed:

- Incorporation of Stress Ratio Effect into the Stiffness Reduction Model
- Effect of Frequency of loading
- Effect of Variable and Random amplitude loading
- X-Ray radiography can be introduced as in-situ process to record delamination growth with loading cycles
- Effect of changing the processing parameters such as matrix resin, curing time and pressure in manufacturing of CFRP
- Fatigue Damage study of other fiber reinforced composite materials such as Kevlar™ Aramid

- Investigation of the involvement of bending stresses

- Simulating the real-life loading histories for realistic modeling and prediction

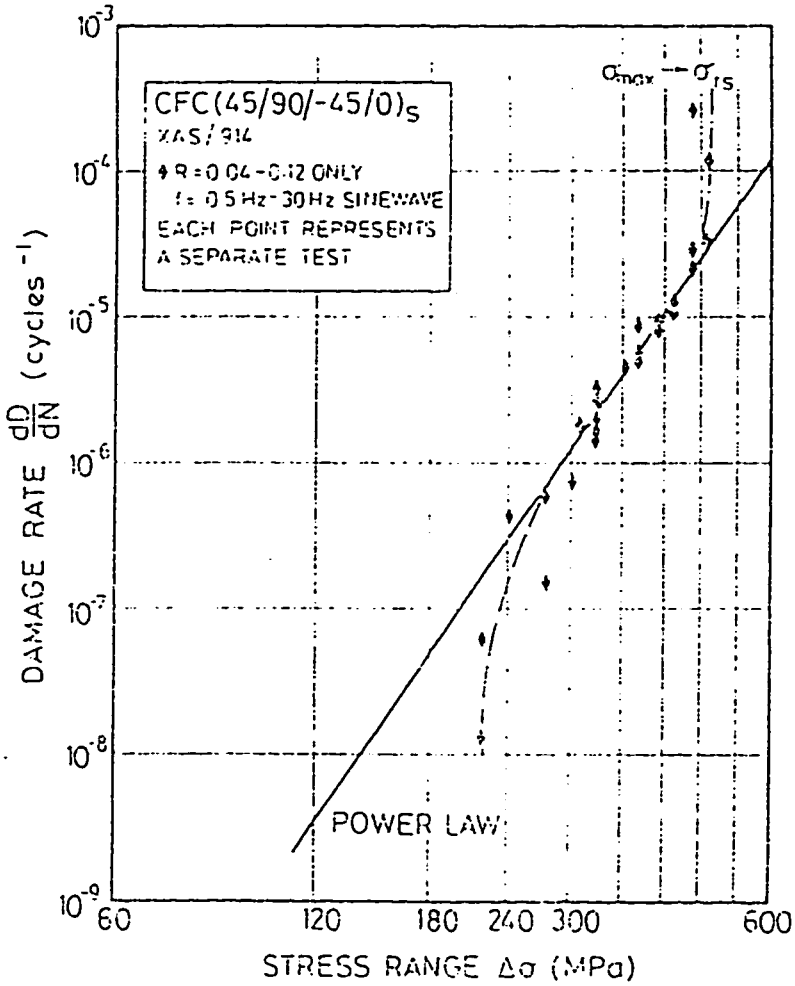

Figure 1: The Damage rate as function of the applied stress range. Only data for R<0.12 is shown [55]

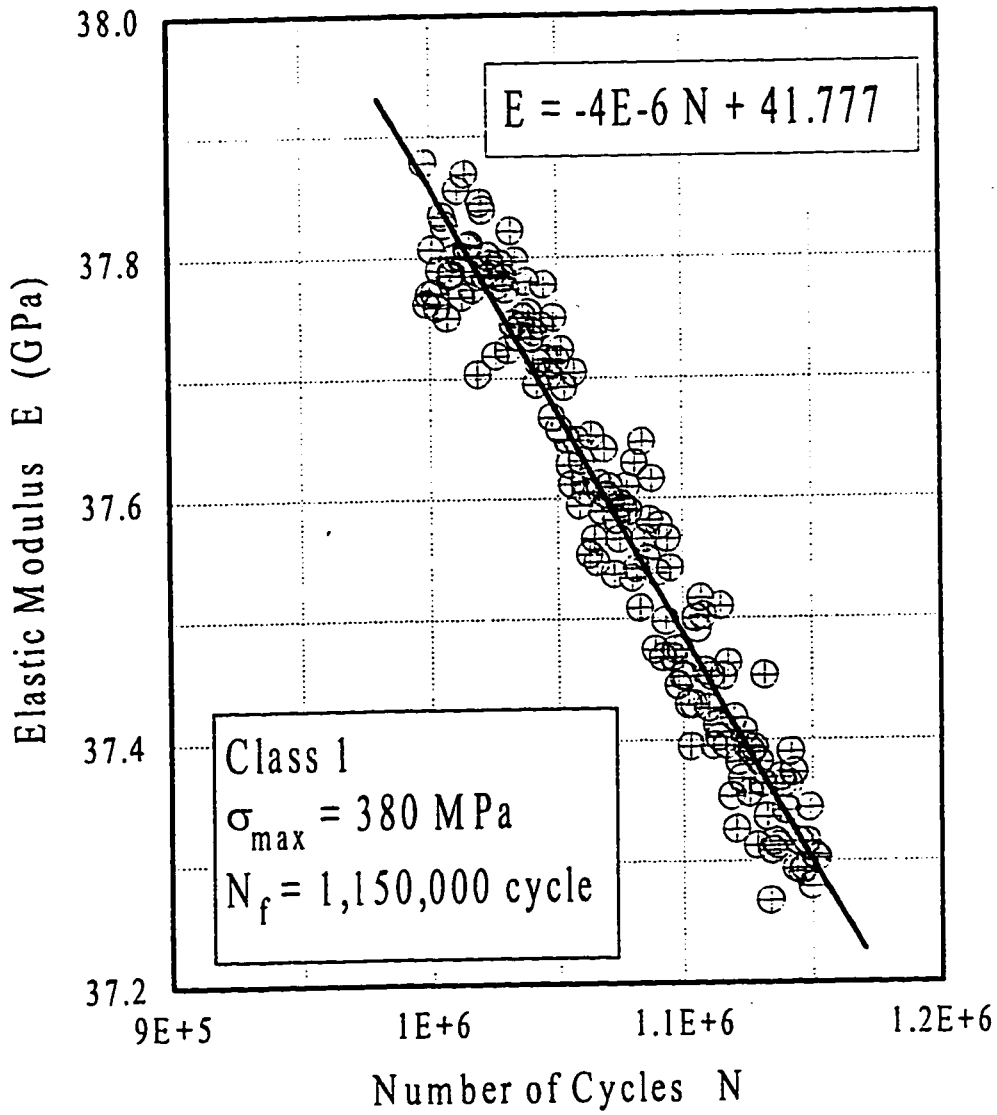

Figure 2: Plot of Elastic Modulus, E vs Number of Cycles, N for obtaining the Rate of Modulus Degradation for class 1 $(0°)_8$ CFRP

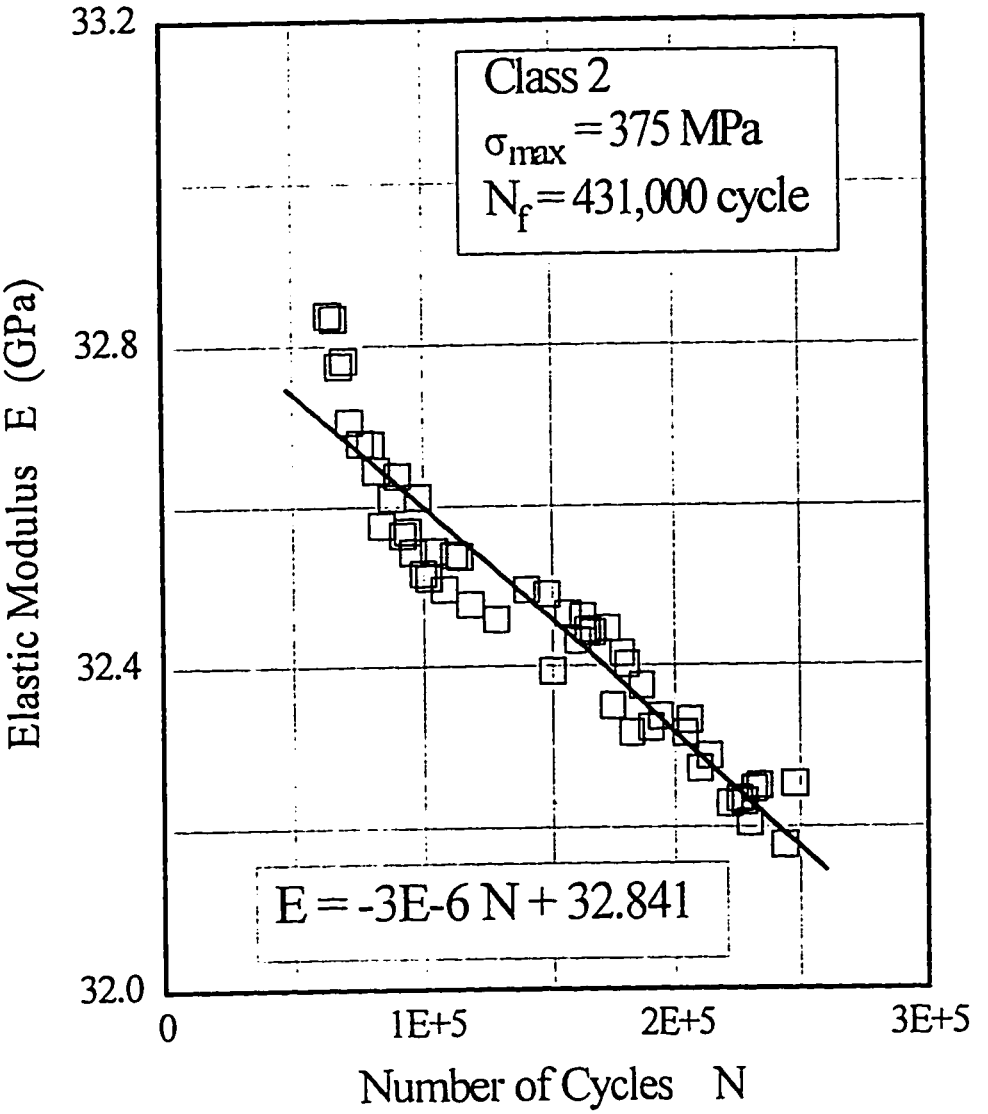

Figure 3: Plot of Elastic Modulus, E vs Number of Cycles, N for obtaining the Rate of Modulus Degradation for class 2 $(0,0,45,-45)_{2s}$ CFRP

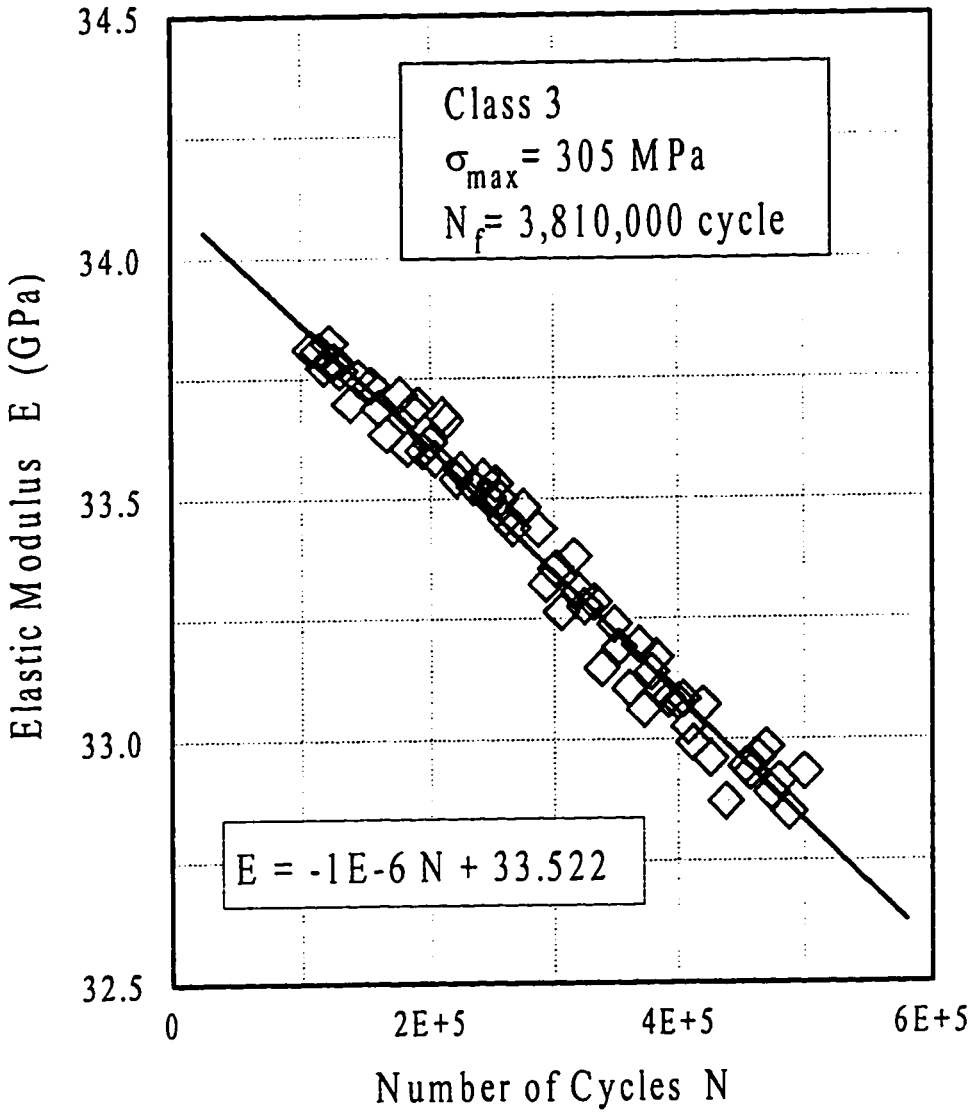

Figure 4: Plot of Elastic Modulus, E vs Number of Cycles, N for obtaining the Rate of Modulus Degradation for class 3 $(45,-45,0,0)_{2s}$ CFRP

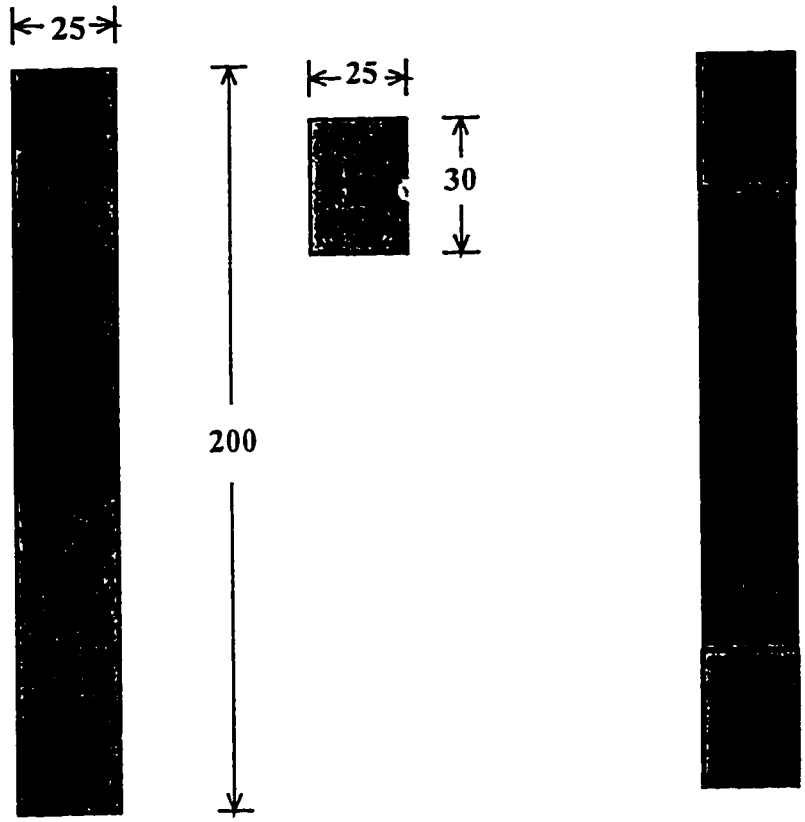

Figure 5: Carbon Fiber Reinforced Composite Coupon with and without Tabs, according to ASTM D-3039 standard (All dimensions are in mm)

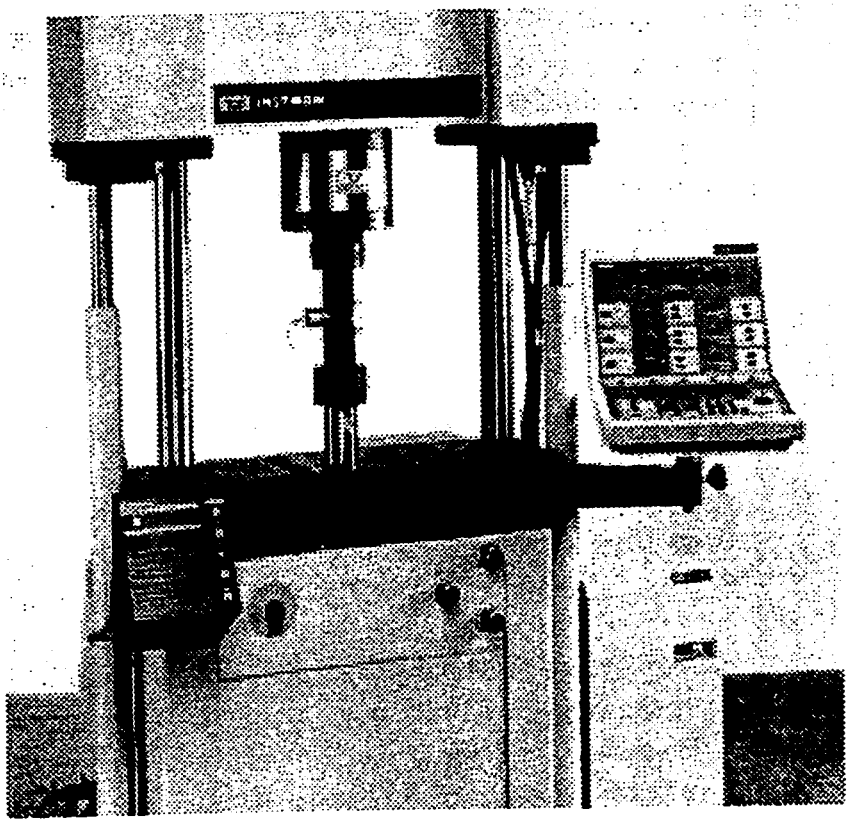

Figure 6: Instron 8501, closed-loop, servo-hydraulic material testing system

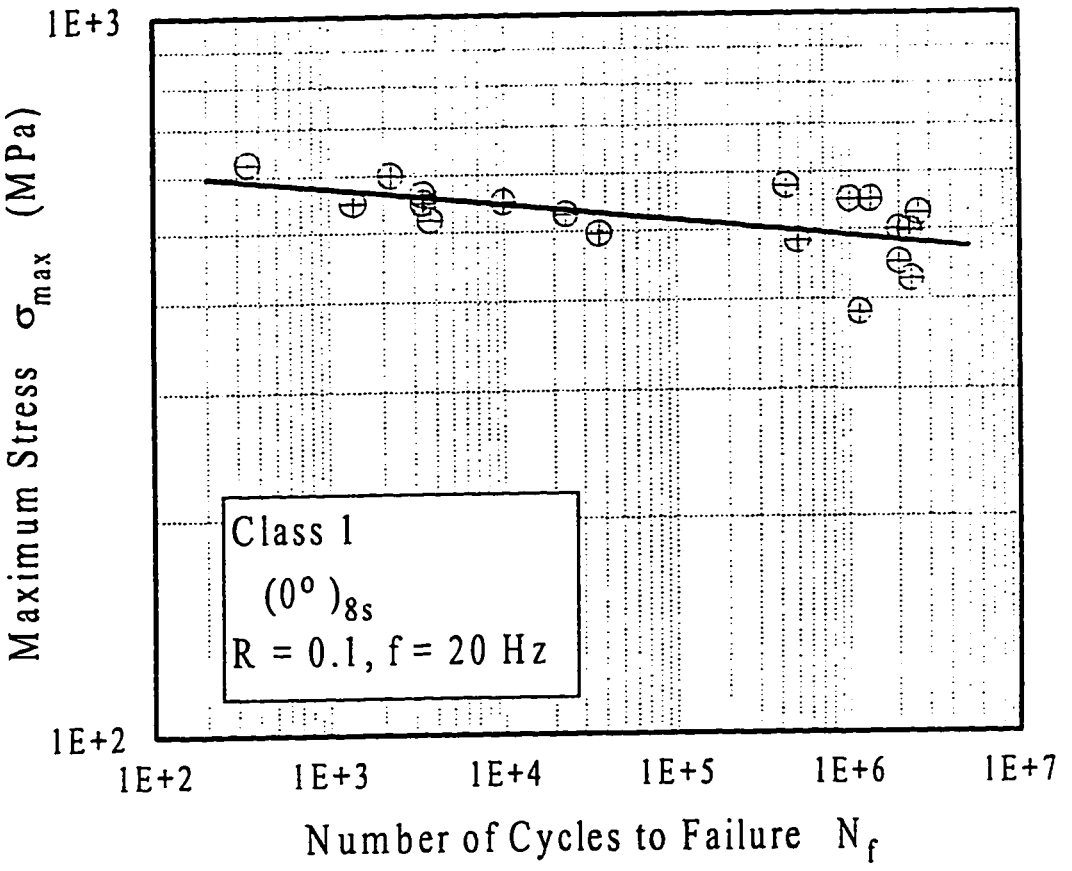

Figure 7: S-N curve for the Fatigue test data of class 1 $(0^\circ)_8$ CFRP

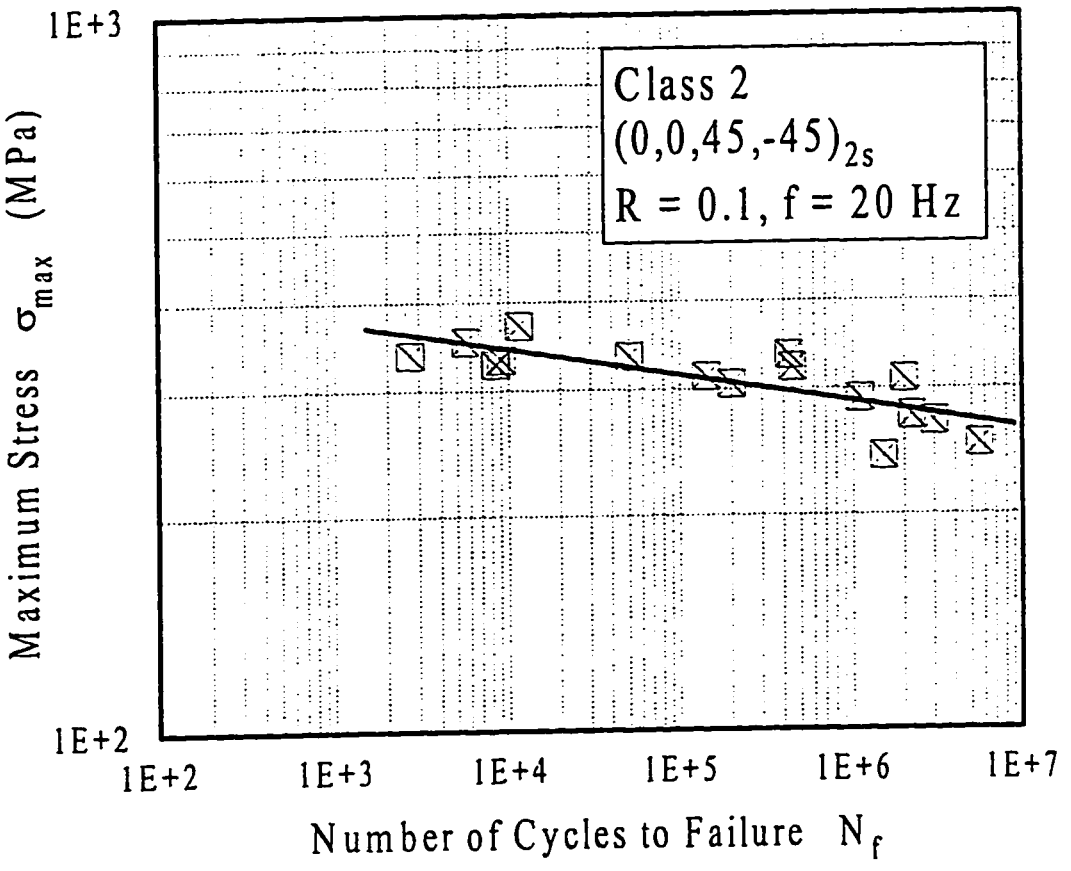

Figure 8: S-N curve for the Fatigue test data of class 2 $(0,0,45,-45)_{2s}$ CFRP

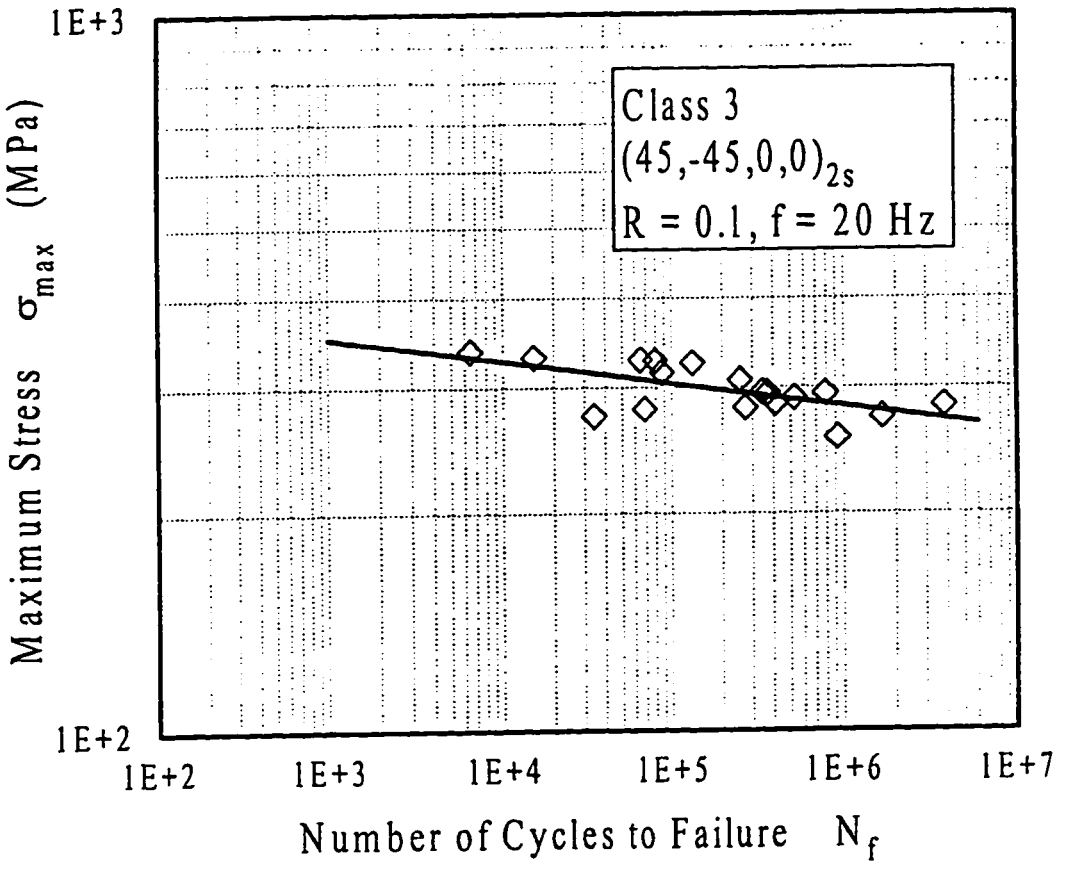

Figure 9: S-N curve for the Fatigue test data of class 3 $(45,-45,0,0)_{2s}$ CFRP

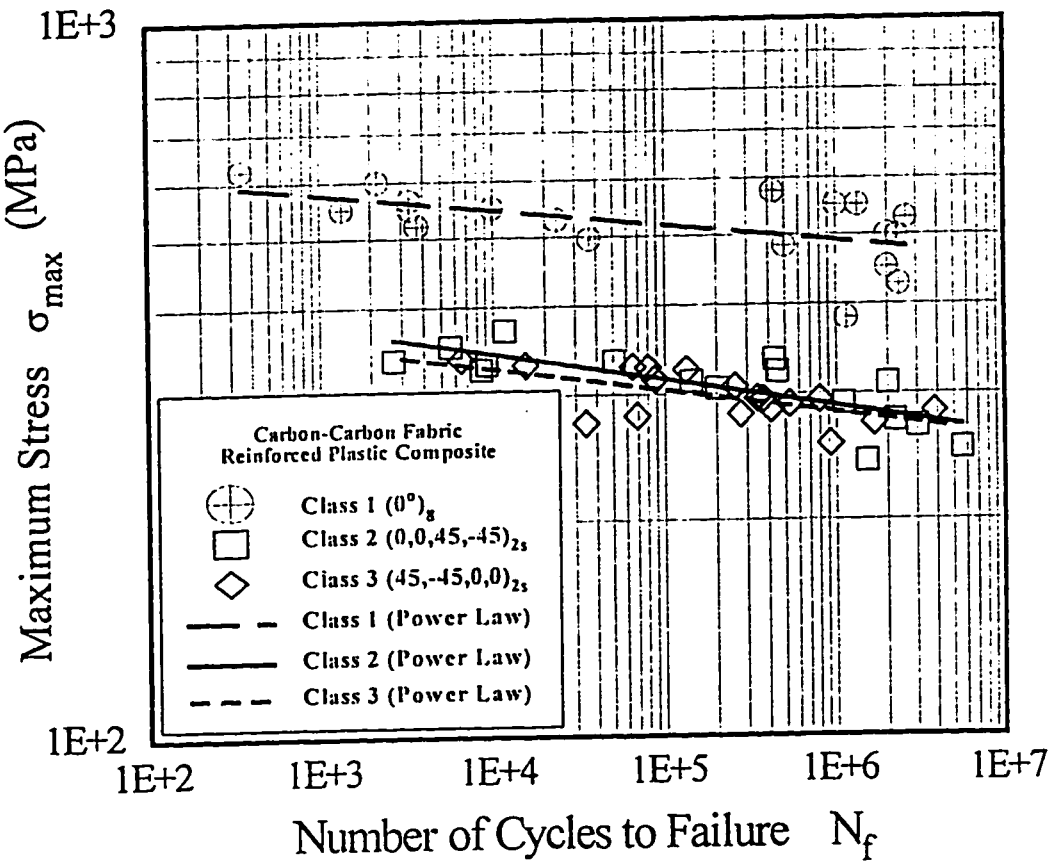

Figure 10: S-N curve for class 1 $(0°)_8$, class 2 $(0,0,45,-45)_{2s}$ and class 3 $(45,-45,0,0)_{2s}$ CFRP specimens

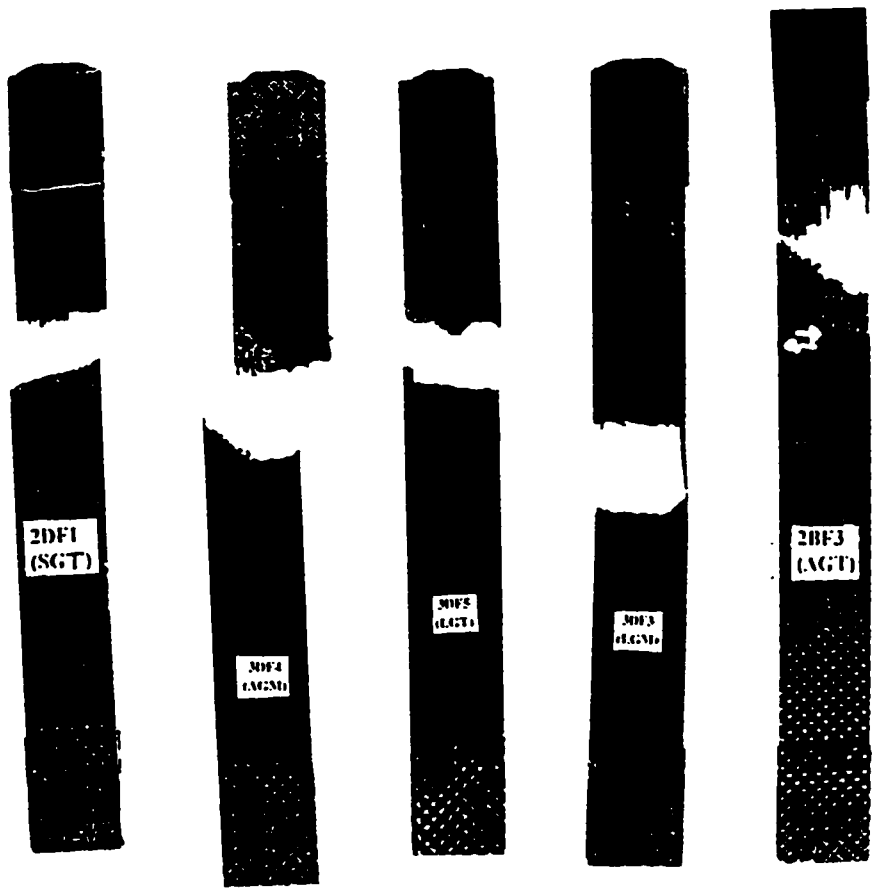

LAT-Lateral At-tab Top	LGM-Lateral Gage Middle	AGM-Angular Gage Middle
LGT-Lateral Gage Top	MGB-Multimode Gage Bottom	AGT-Angular Gage Top
LGB-Lateral Gage Bottom	SGM-Splitted Gage Middle	SGT-Splitted Gage Top
LAB-Lateral At-tab Bottom	XGM-eXploded Gage Middle	DGM-Delamination Gage Middle

Figure 11: Typical Fracture Codes for Tensile and Fatigue test specimens [78]

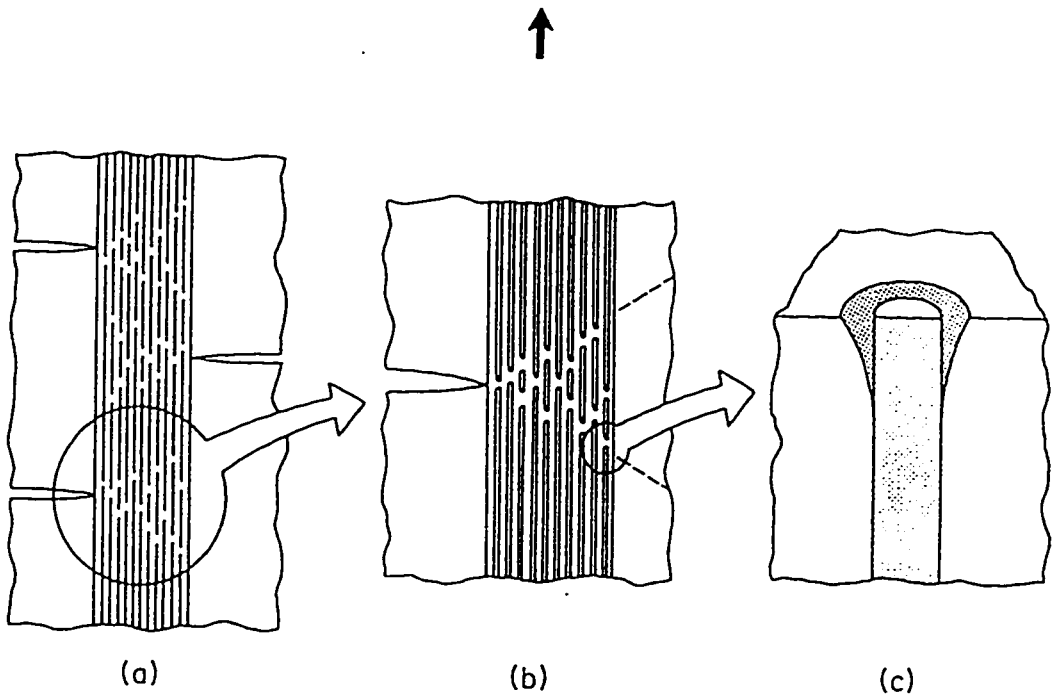

Figure 12: Schematic diagram of fiber fracture patterns associated with matrix cracks (a), the distribution of fiber fractures through adjacent plies near a primary matrix crack (b), and local debonding near the tips of the broken fiber ends (c) [79]

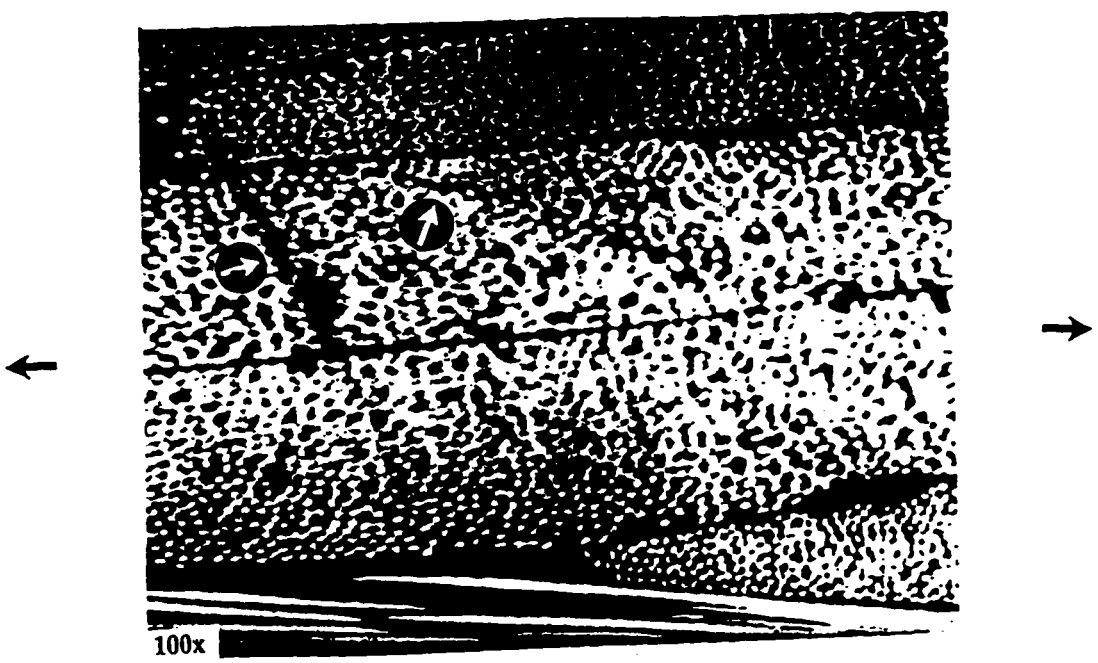

Figure 13: Photomicrograph of transverse cracks in the inside 45° bundle shown by arrows for class 2 $(0,0,45,-45)_{2s}$ CFRP

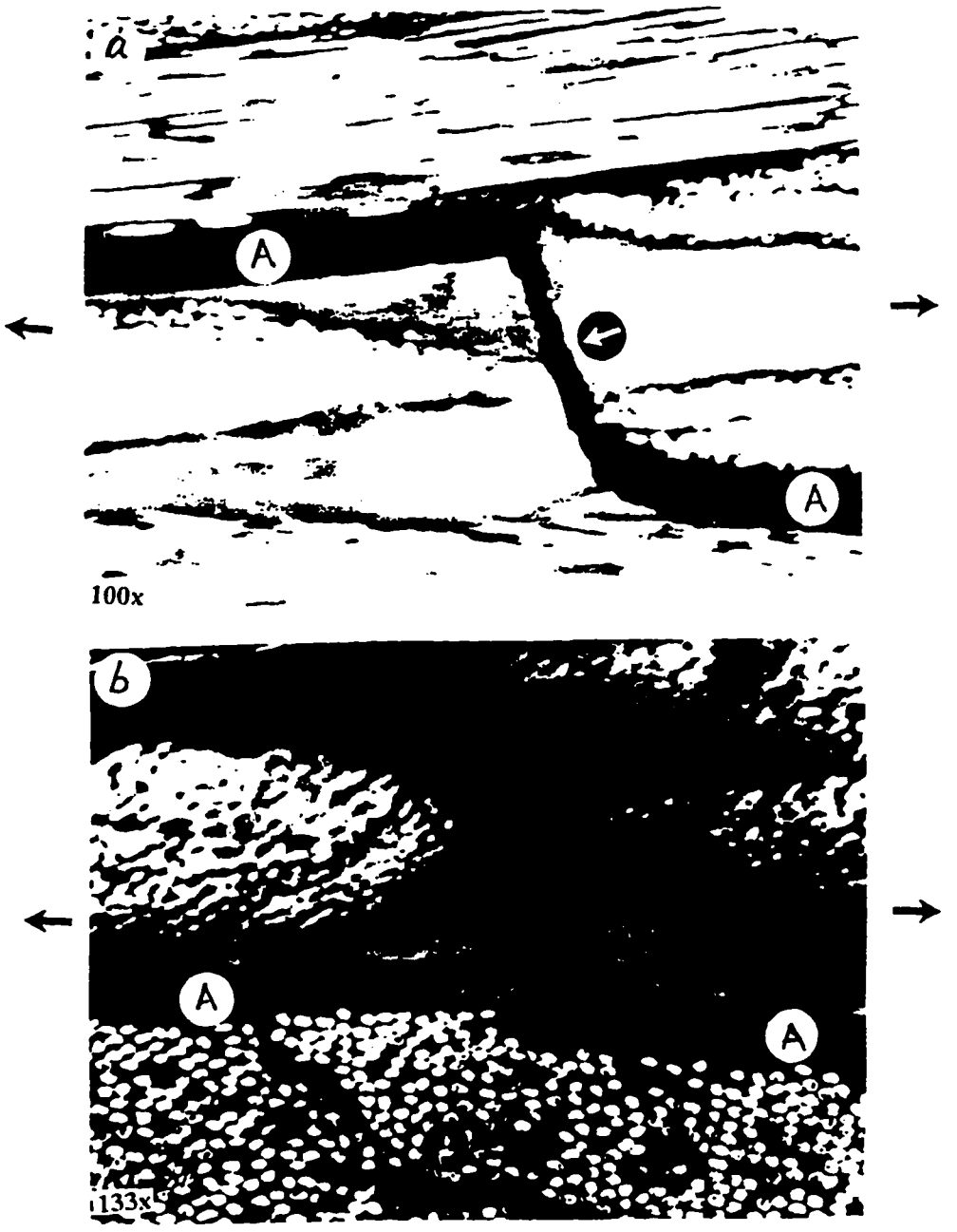

Figure 14: Photomicrograph showing matrix cracks (arrows) and delamination (A) in class 3 $(45.\text{-}45,0,0)_{2s}$

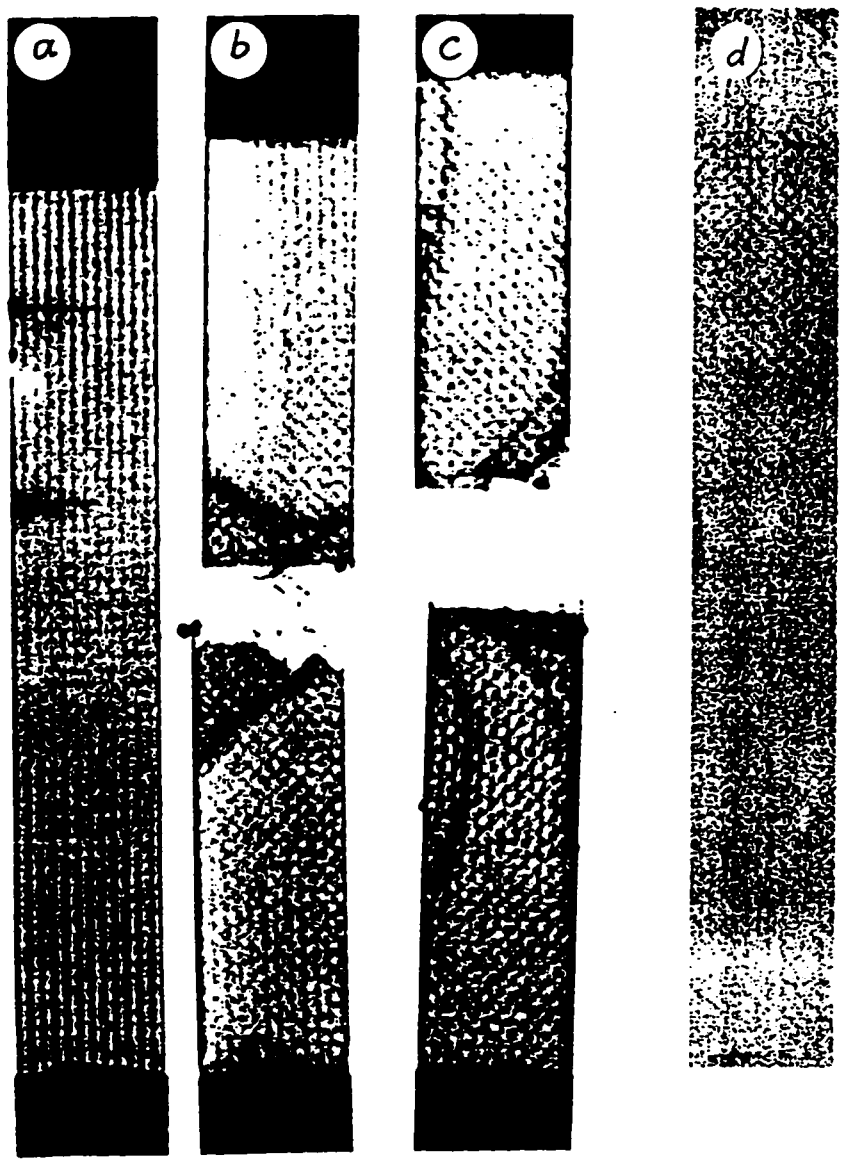

Figure 15: X-Ray Radiographs showing a comparison of fatigue damage in class 1 $(0°)_8$ (a), class 2 $(0,0,45,-45)_{2s}$ (b) and class 3 $(45,-45,0,0)_{2s}$ (c) CFRP specimens with details of typical fracture mode dominance in each class. Also an X-Ray Radiograph of an untested specimen shown (d)

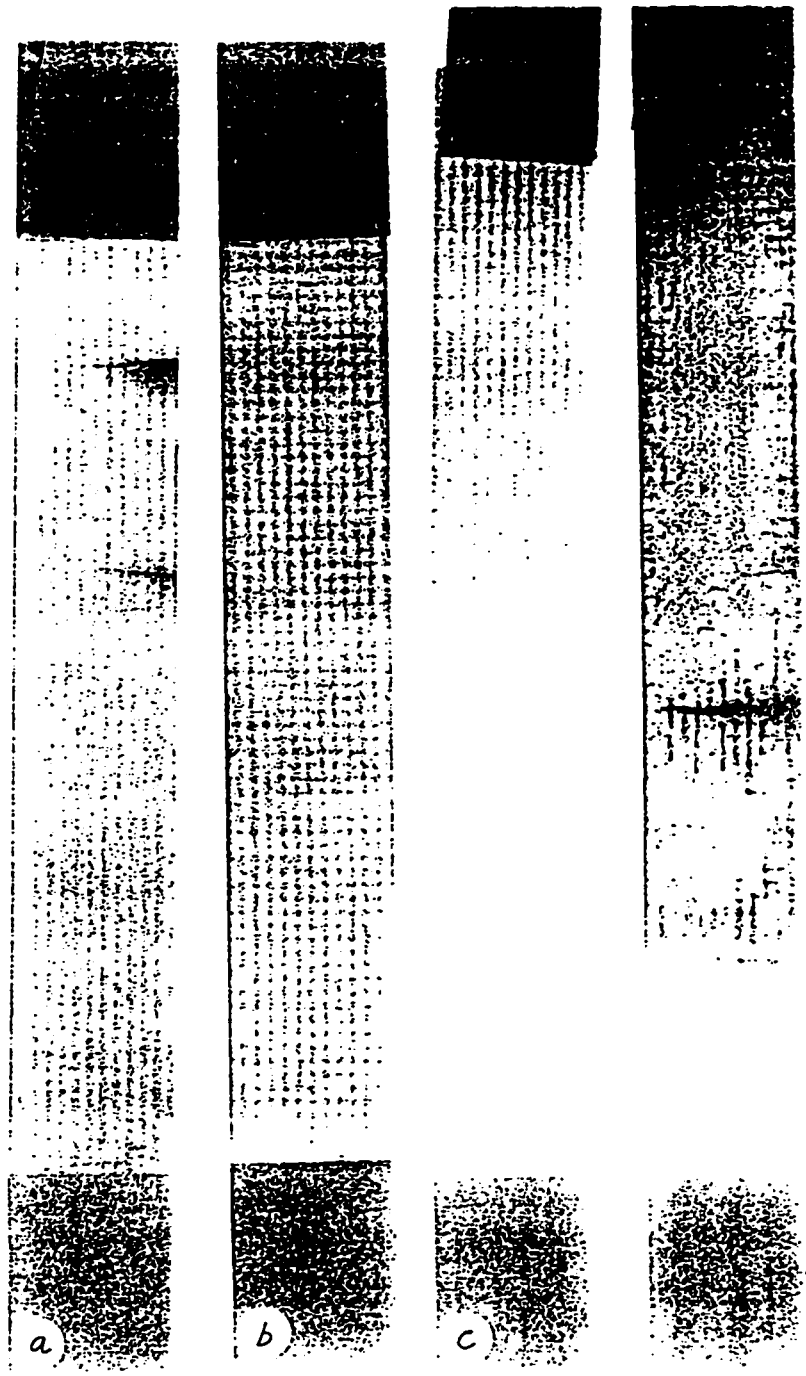

Figure 16: X-Ray Radiographs showing three class 1 $(0°)_8$ CFRPs (a,b,c) and one class 4 $(0°)_8$ CFRP manufactured at lower pressure of only 0.9 Bars, revealing more damage

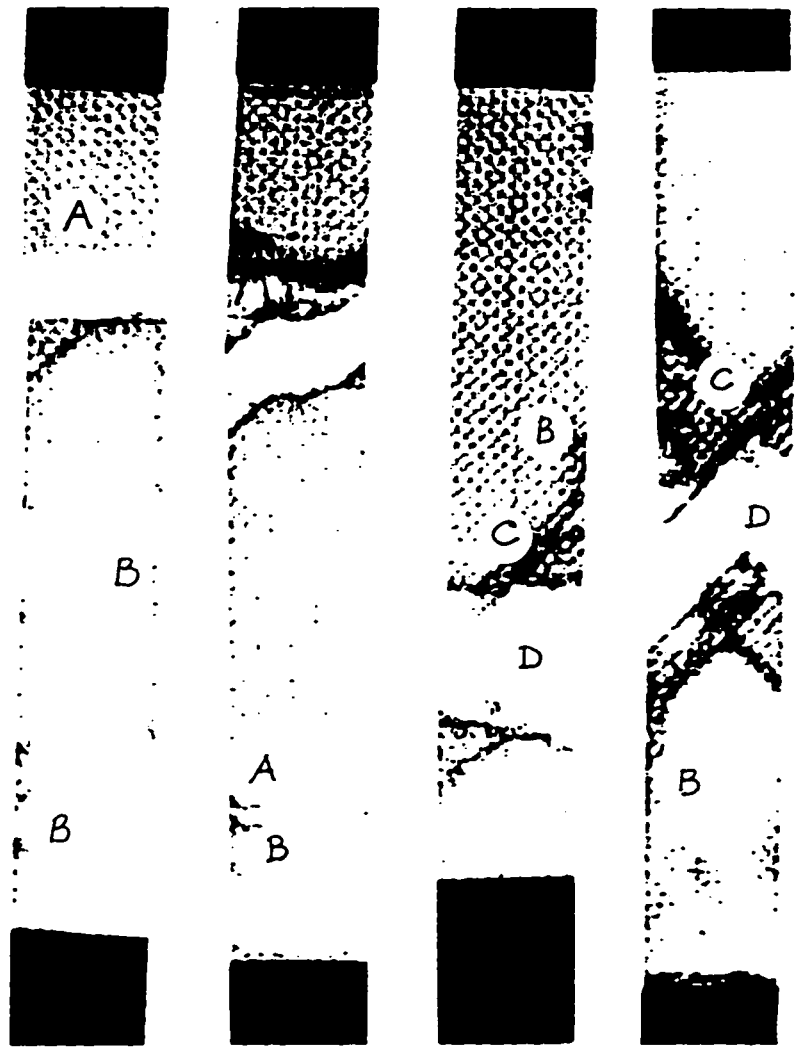

Figure 17: X-Ray Radiographs showing lateral cracks (A), edge delamination (B), matrix cracks (C) and fiber fracture (D) in class 2 $(0,0,45,-45)_{2s}$ CFRPs

Figure 18: X-Ray Radiographs showing delamination (A), matrix cracks (B) and fiber fracture (C) in class 3 $(45,-45,0,0)_{2s}$ CFRPs

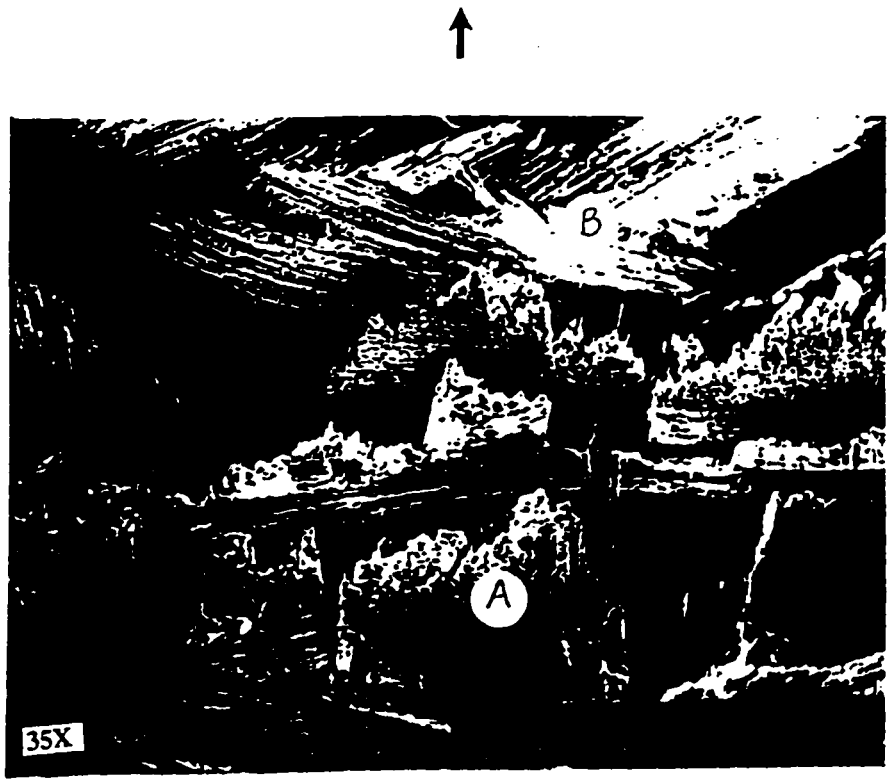

Figure 19: Complex woven structure and fracture shown in SEM micrograph with 0° fiber fracture (A) and 45°/-45° fiber fracture (B) for class 3 $(45,-45,0,0)_{2s}$ CFRP

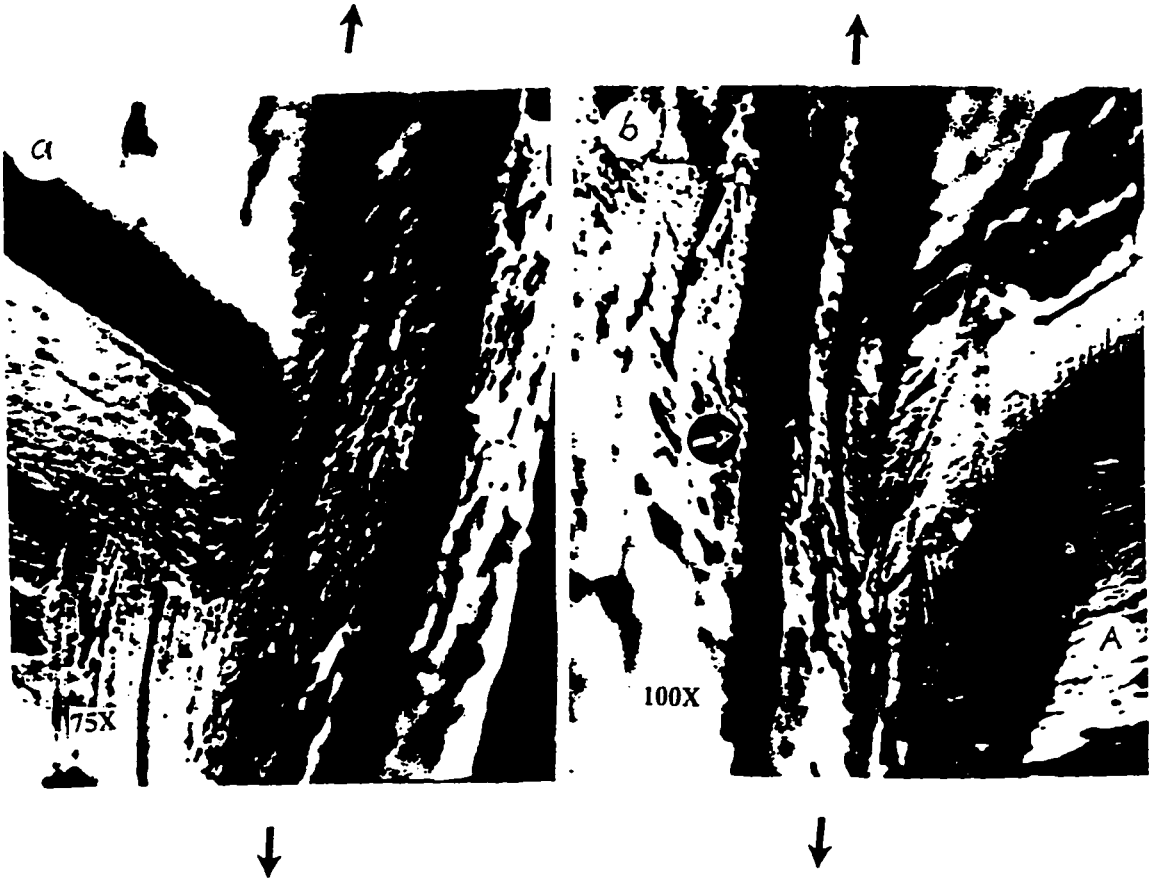

Figure 20: SEM micrograph shows delaminated plies and fiber-matrix debonding in class 3 $(45,-45,0,0)_{2s}$ CFRP (a), Isolated 45° fiber bundle from main composite structure due to fiber pull-out and edge delamination (A) and fiber-matrix debonding at 0° and 45° interface (arrow) (b)

Figure 21: SEM micrograph shows 0° fiber bundle pull-out from the matrix structure (arrow) for class 3 $(45,-45,0,0)_{2s}$ CFRP

Figure 22: SEM micrograph shows close-packed plies (no delamination) after fiber fracture and specimen failure of class 1 $(0°)_8$ CFRP

Figure 23: SEM micrograph shows fiber fracture (A) and delamination (B) between plies (a), Fiber-matrix debonding as one single fiber appears out of the bundle separated in class 3 $(45.\text{-}45,0,0)_{2s}$ CFRP (b)

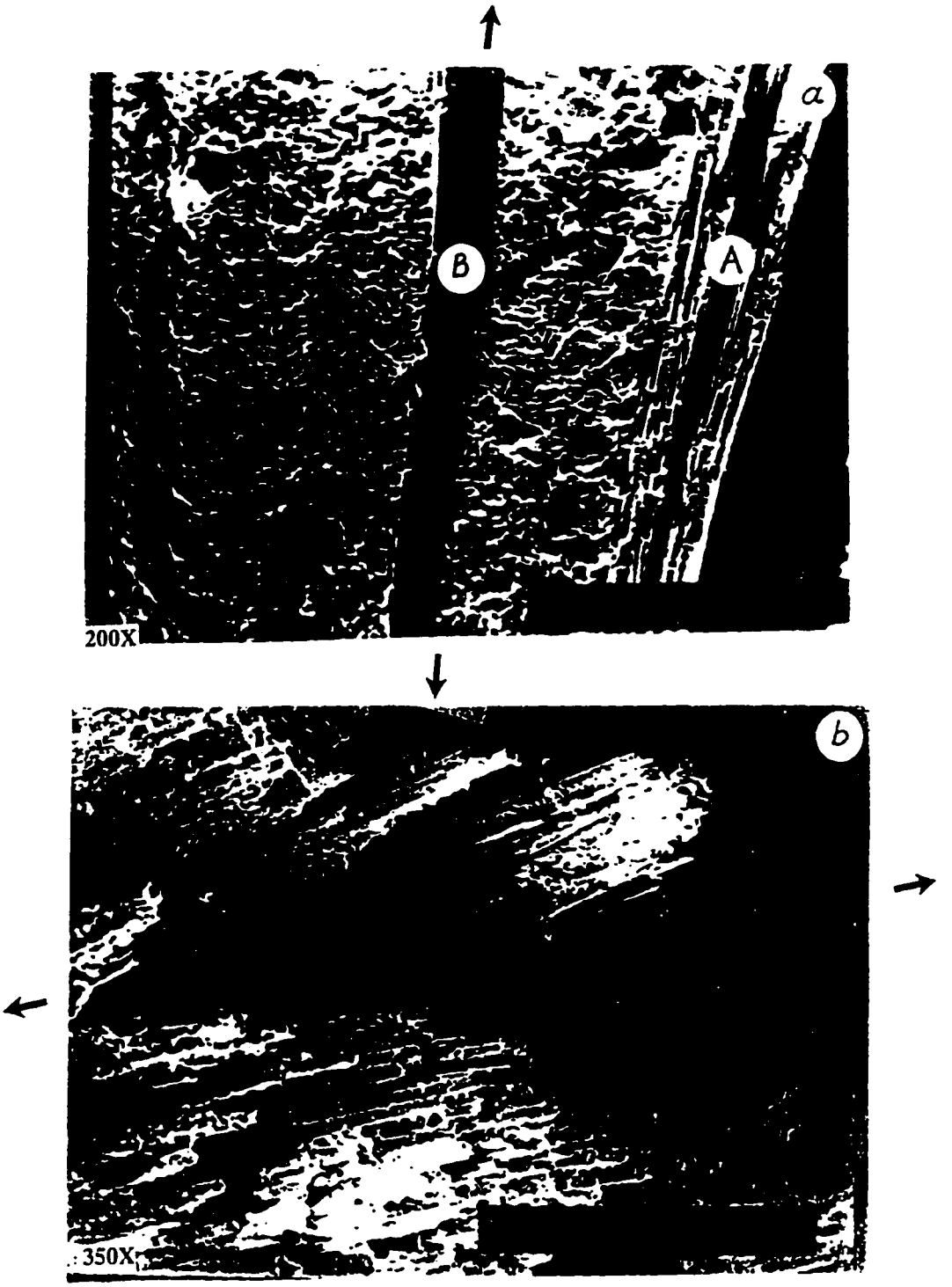

Figure 24: SEM micrograph showing fiber and matrix splitting (A) and delamination (B) at the interface (a), Excessive fiber fracture in the loading direction for class 3 $(45,-45,0,0)_{2s}$ CFRP (b)

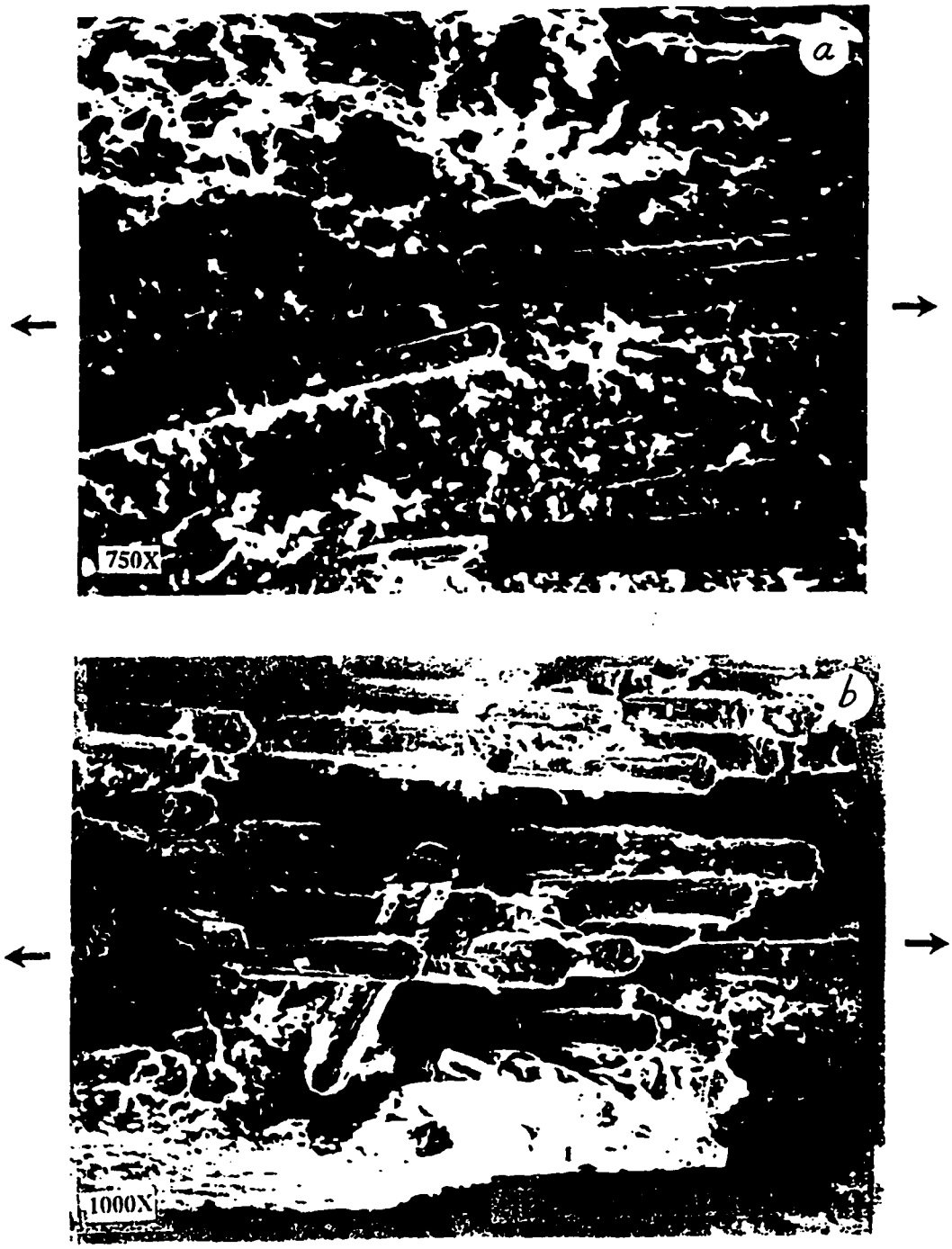

Figure 25: SEM micrograph shows matrix debris on the fiber surface due to excessive load cycling (a). Fiber fracture and pull-out shown in class 3 $(45_2/-45_2/0_2/0)_{2s}$ CFRP (b)

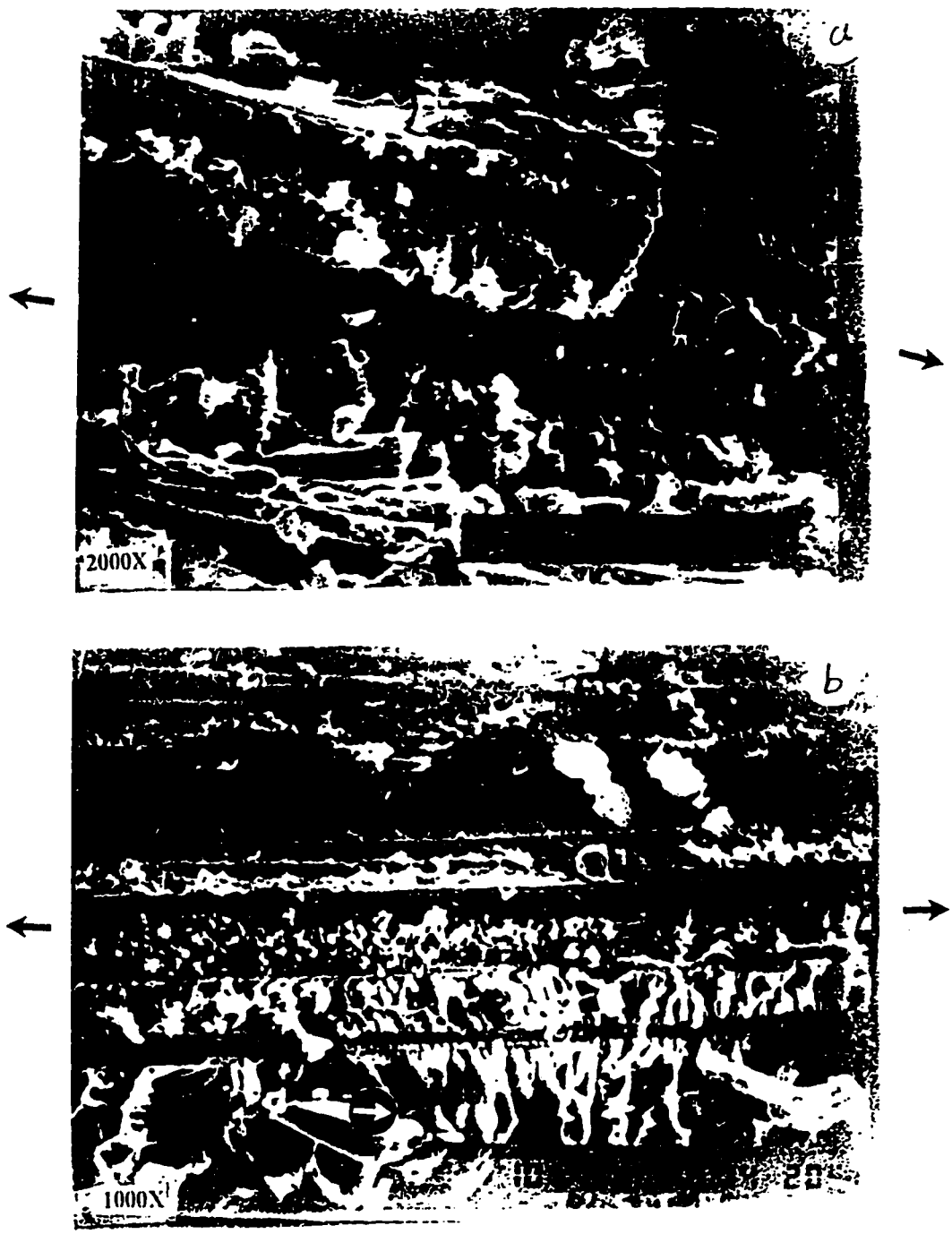

Figure 26: SEM micrograph shows debris of matrix on the fiber surface (a). Matrix Debris due to excessive load cycling and hackles (see arrow) of class 3 $(45_2/-45_2/0_2)_s$ CFRP (b)

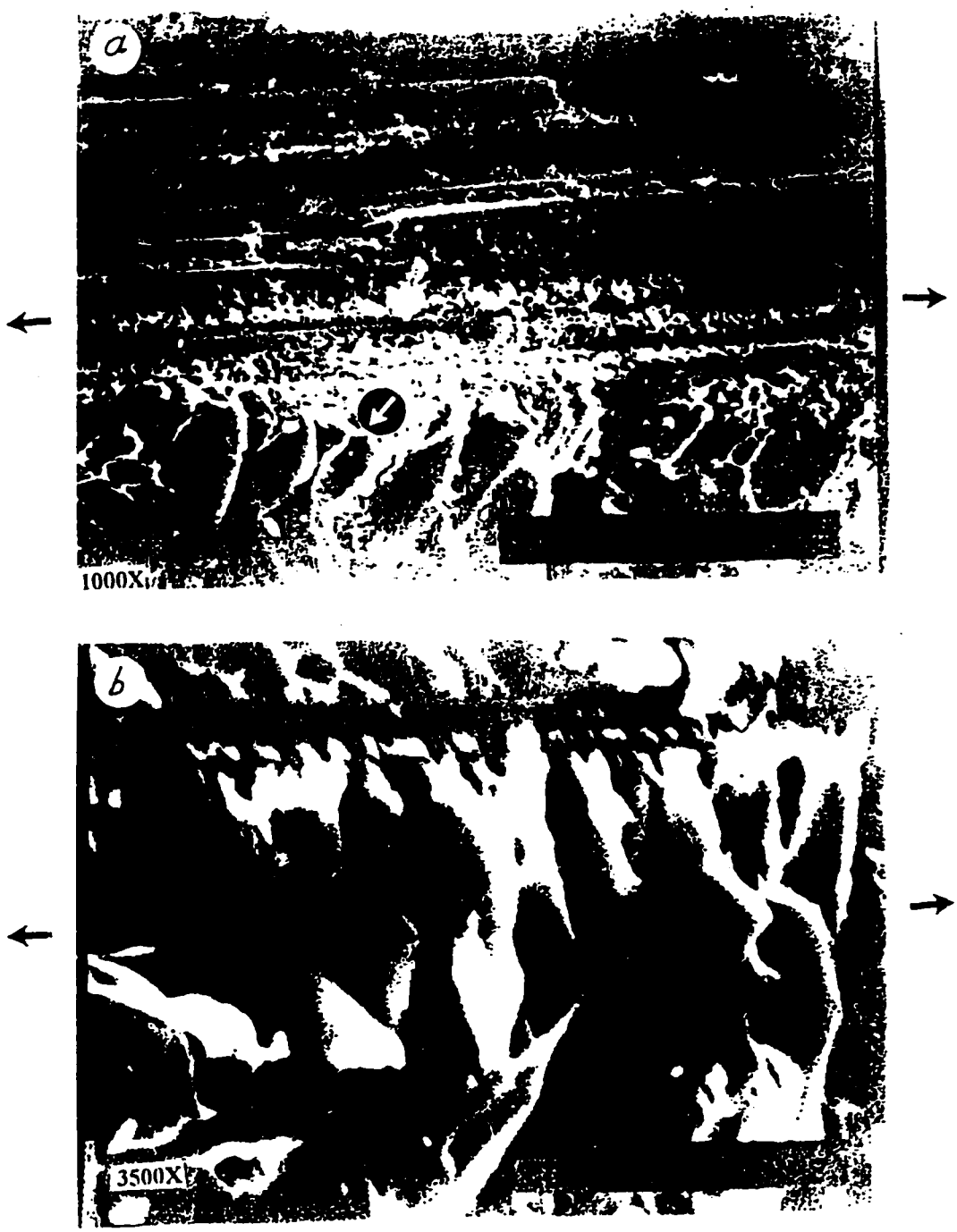

Figure 27: SEM micrograph showing debris and hackles (arrow) in the matrix material (a). Hackles at higher magnification in class 3 $(45_2\text{-}45_2,0,0)_{2s}$ CFRP (b)

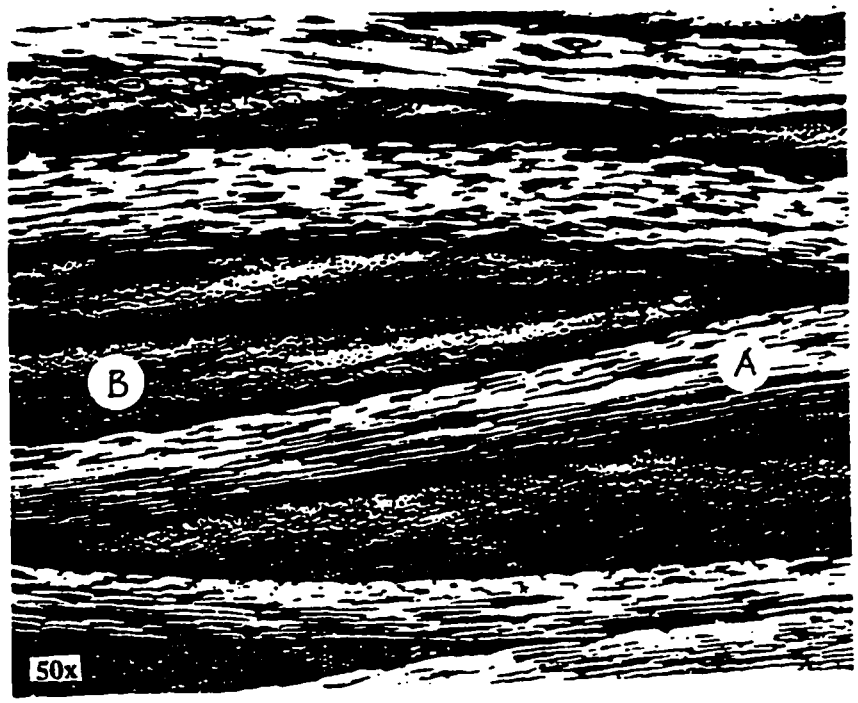

Figure 28: Photomicrograph of complex edge structure of the woven fabric with 0° fiber (A) and the weft fiber bundles (B)

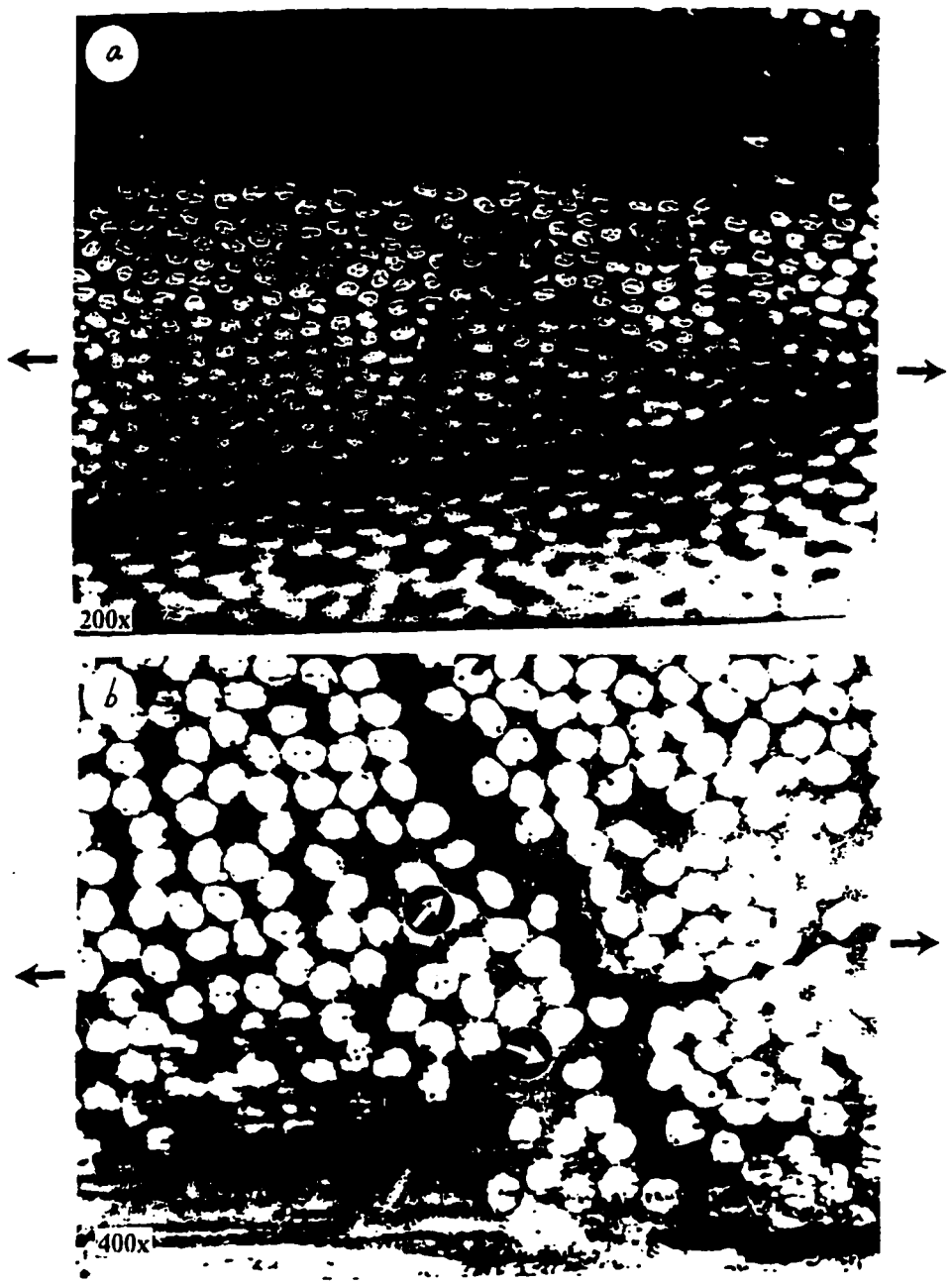

Figure 29: Photomicrograph of delamination front moving along and through 45° fiber bundle (arrow) in a class 3 $(45,-45,0,0)_{2s}$ CFRP specimen (a), Matrix crack through fiber bundle and fiber-matrix debonding shown (arrows) in class 3 $(45,-45,0,0)_{2s}$ CFRP (b)

Figure 30: Photomicrograph of totally splitted and delaminated plies shown by arrows in class 3 $(45,-45,0,0)_{2s}$ CFRP

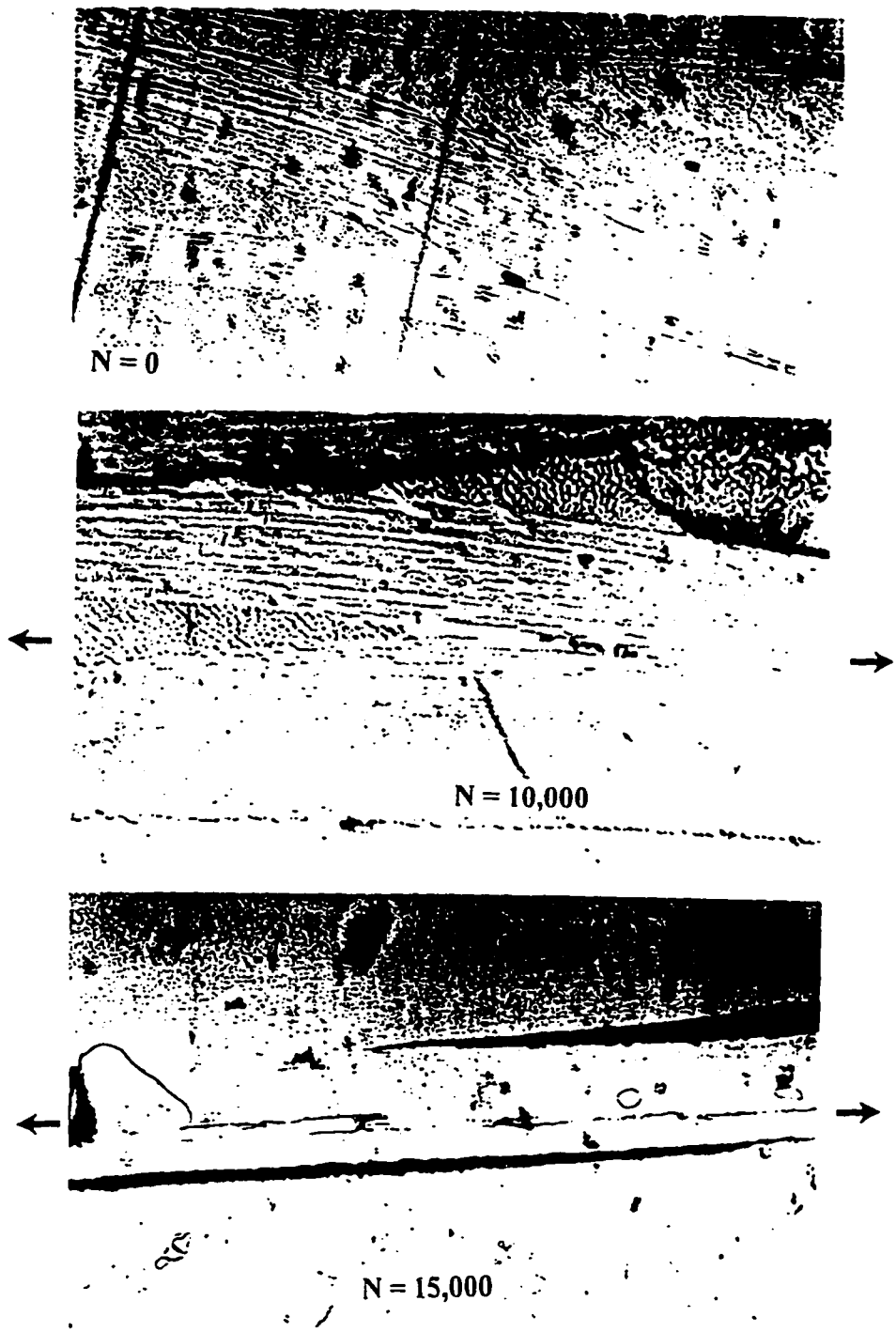

Figure 31a: Edge replicas showing progressing damage in class 3 $(45,-45,0,0)_{2s}$ CFRP, σ_{max} = 62% σ_{TS}. N_f = 80,000 cycles

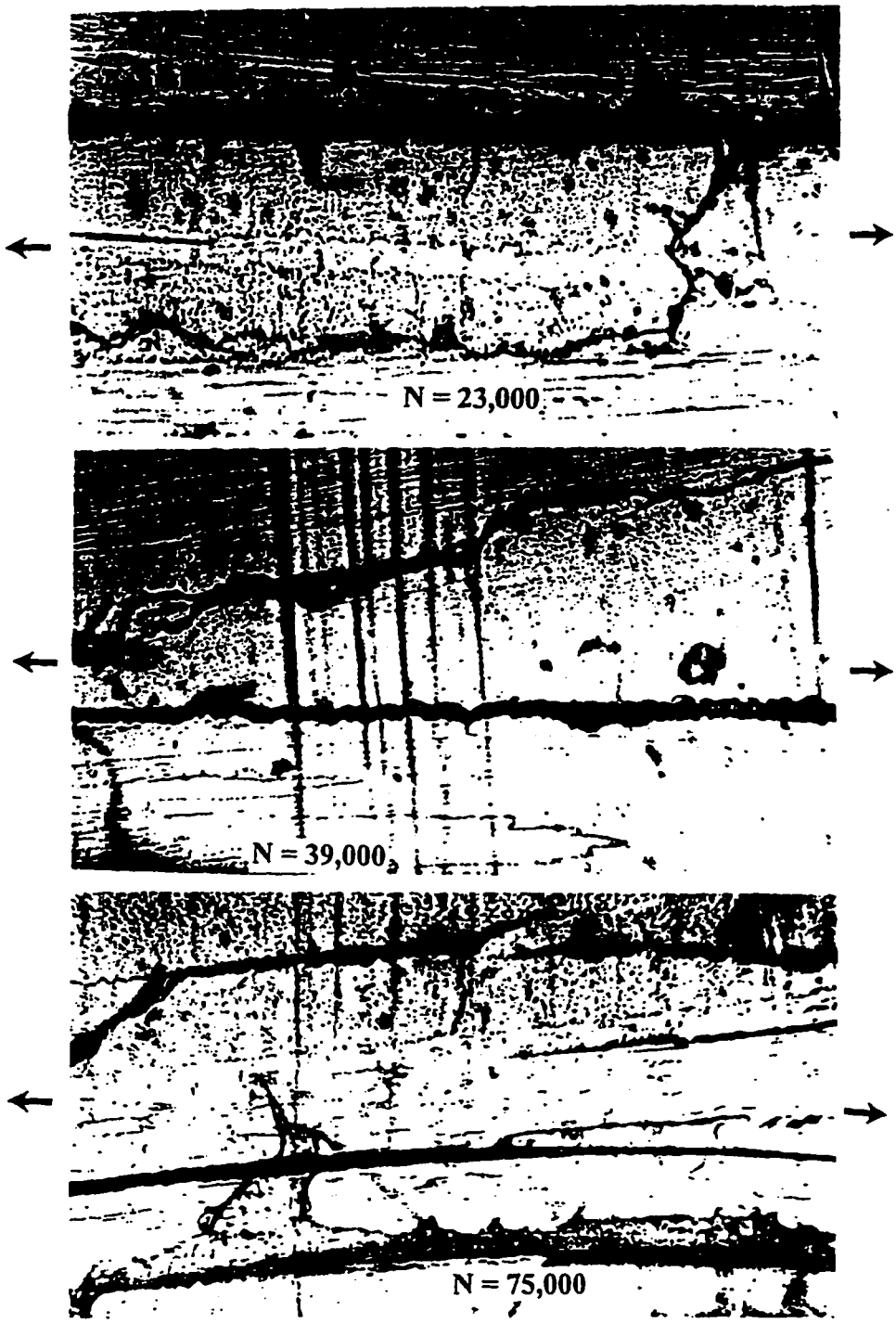

Figure 31b: Edge replicas showing progressing damage in class 3 $(45,-45,0,0)_{2s}$ CFRP, σ_{max} = 62% σ_{TS}. N_f = 80,000 cycles

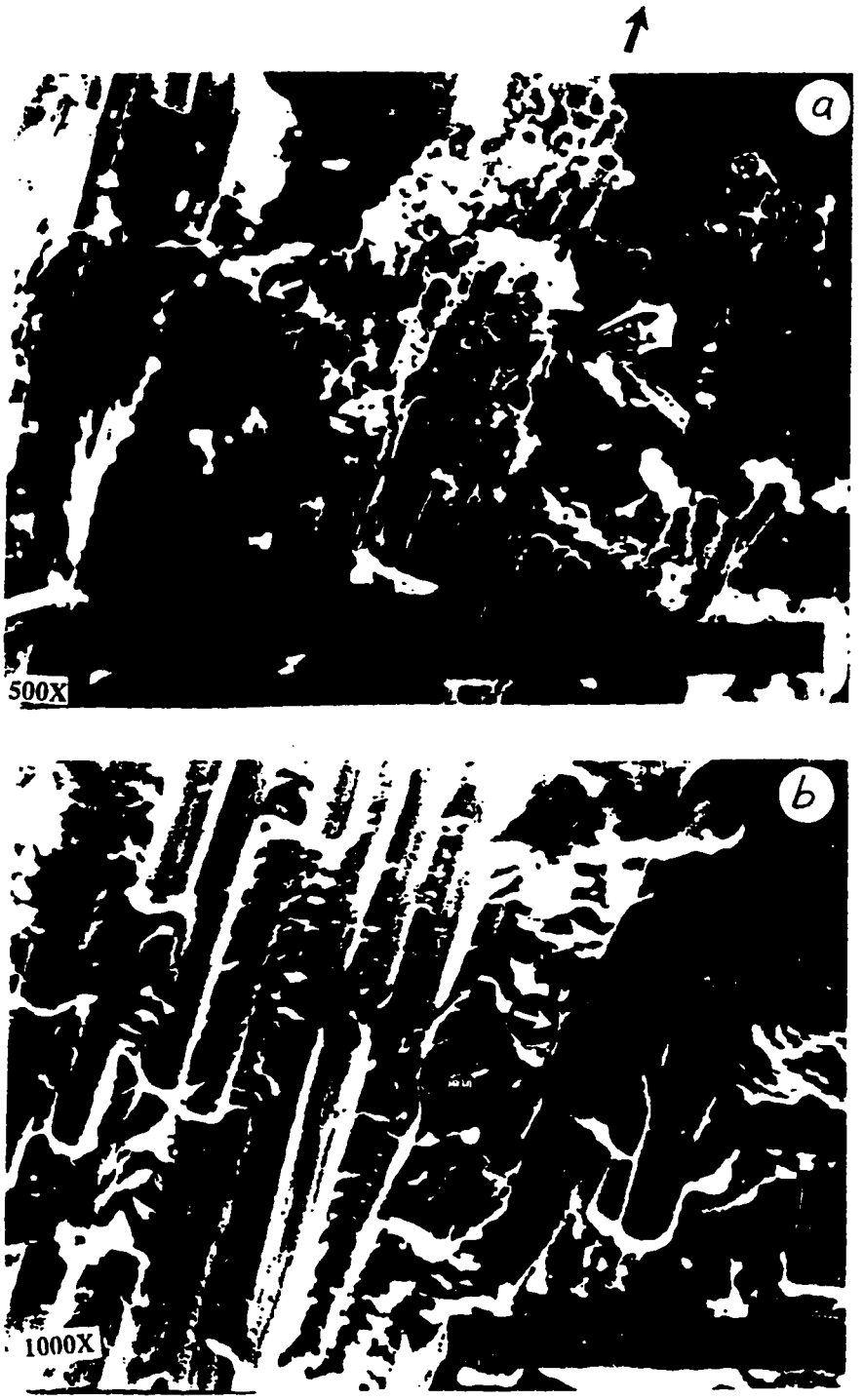

Figure 32: SEM micrographs show fiber-matrix debonding (arrow) and fiber fracture in class 3 $(45,-45.0,0)_{2s}$ CFRP (a.b)

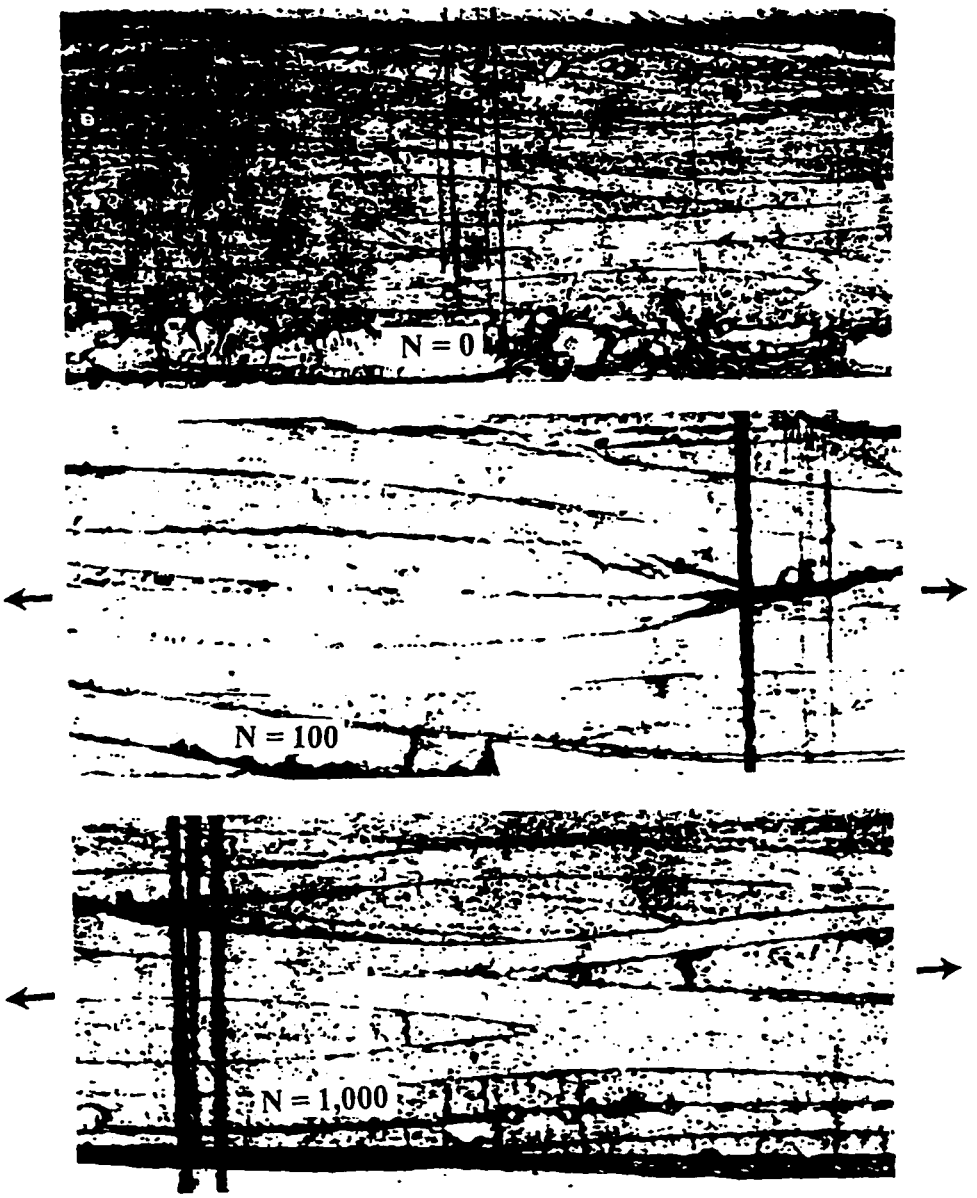

Figure 33: Edge replicas showing progressing damage in class 1 $(0^{\circ})_8$ CFRP. σ_{max} = 75% σ_{TS}. N_f = 1,100 cycles

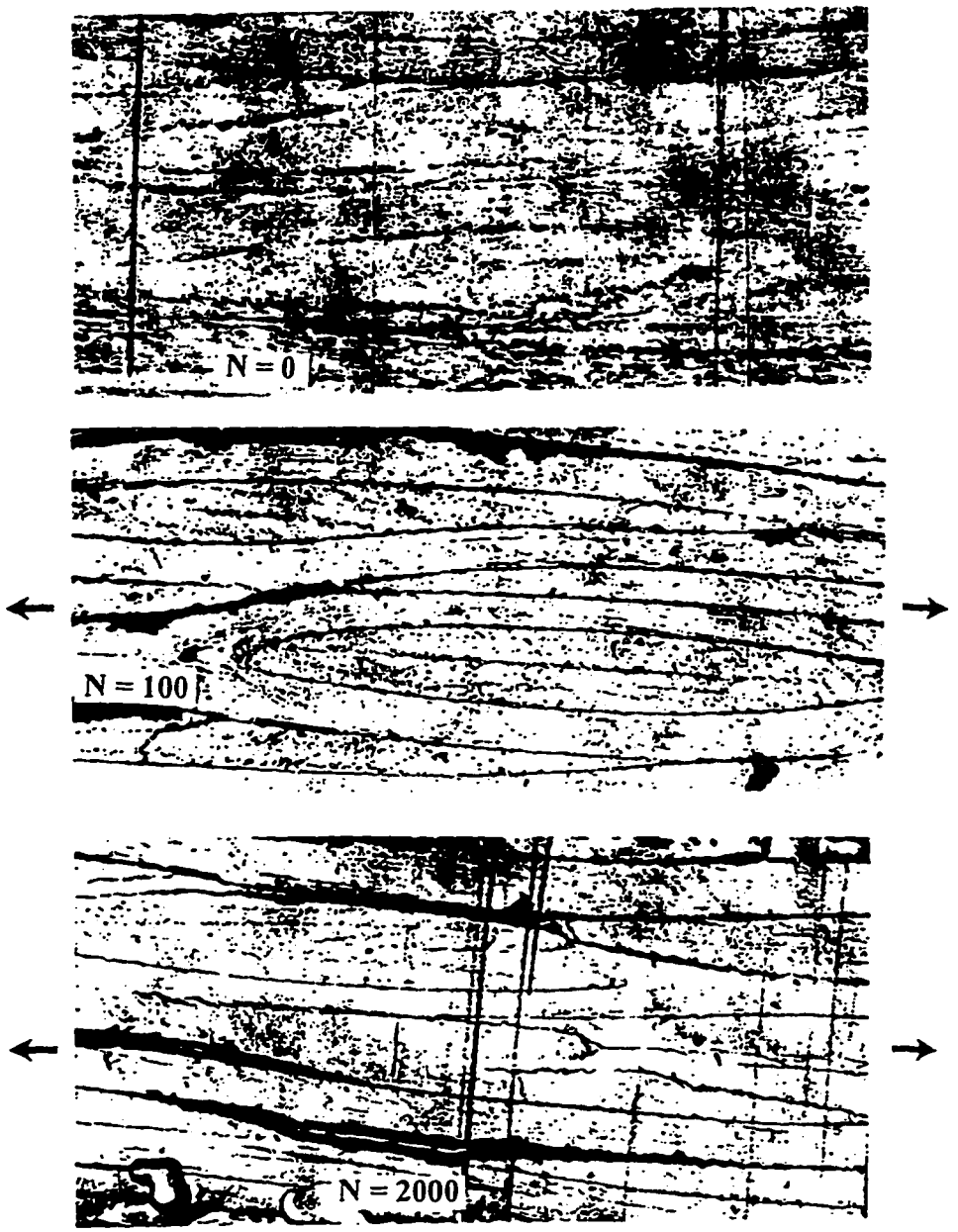

Figure 34a: Edge replicas showing progressing damage in class 1 $(0°)_8$ CFRP, σ_{max} = 70% σ_{TS}. N_f = 40,000 cycles

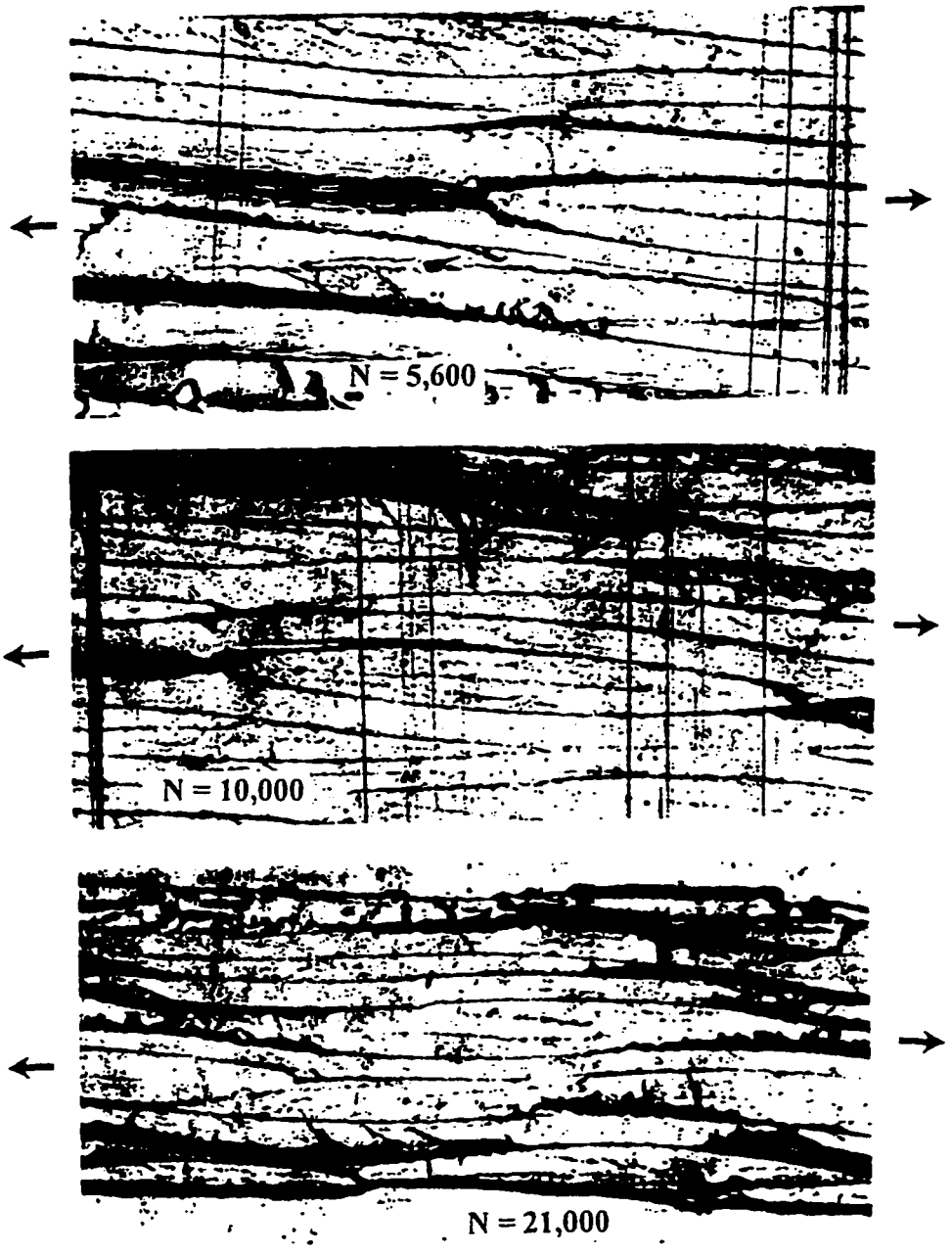

Figure 34b: Edge replicas showing progressing damage in class 1 $(0°)_8$ CFRP. σ_{max} = 70% σ_{TS}. N_f = 40,000 cycles

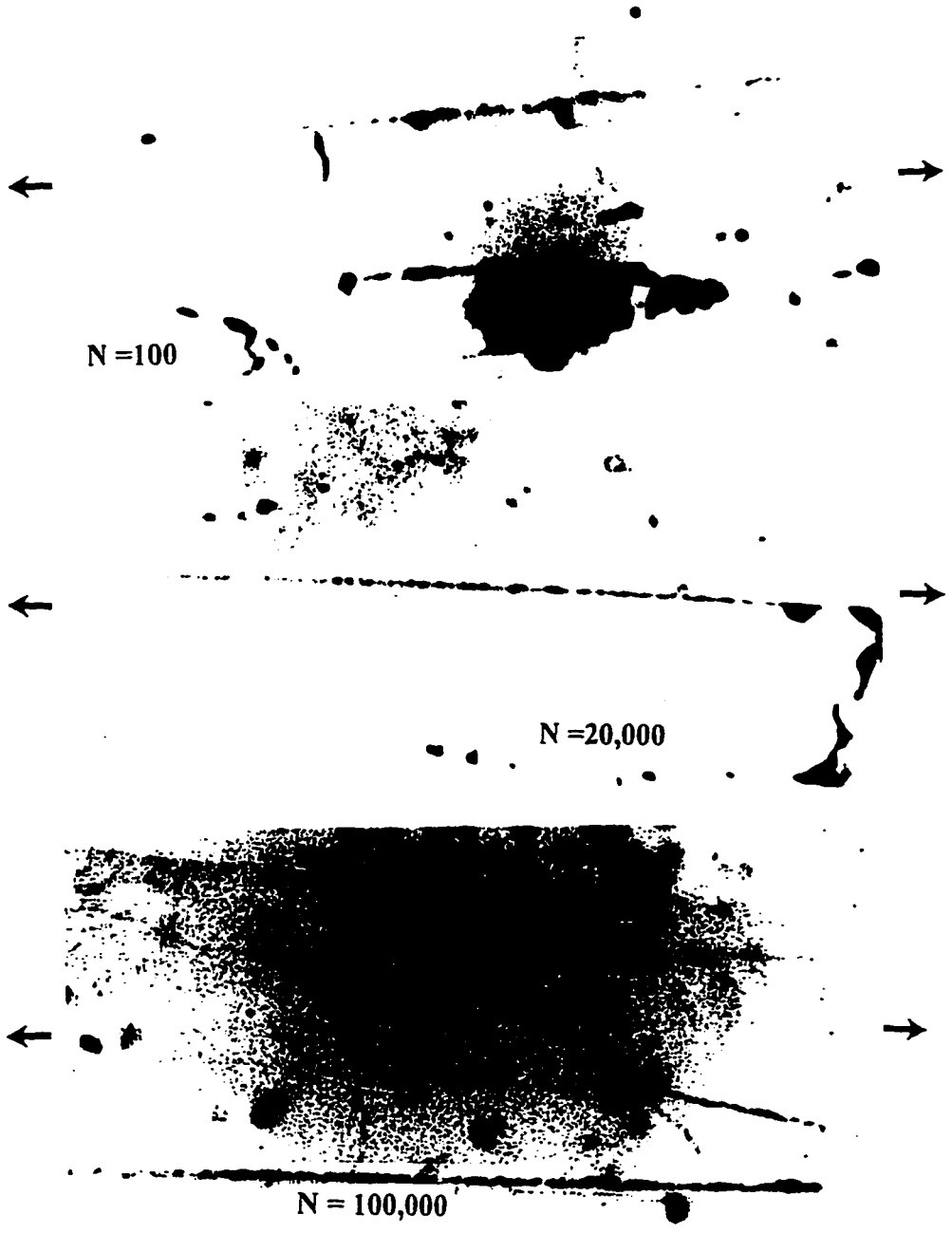

Figure 35a: Edge replicas showing progressing damage in class 2 $(0,0.45,-45)_{2s}$ CFRP, σ_{max} = 60% σ_{TS}. N_f = 440,500 cycles

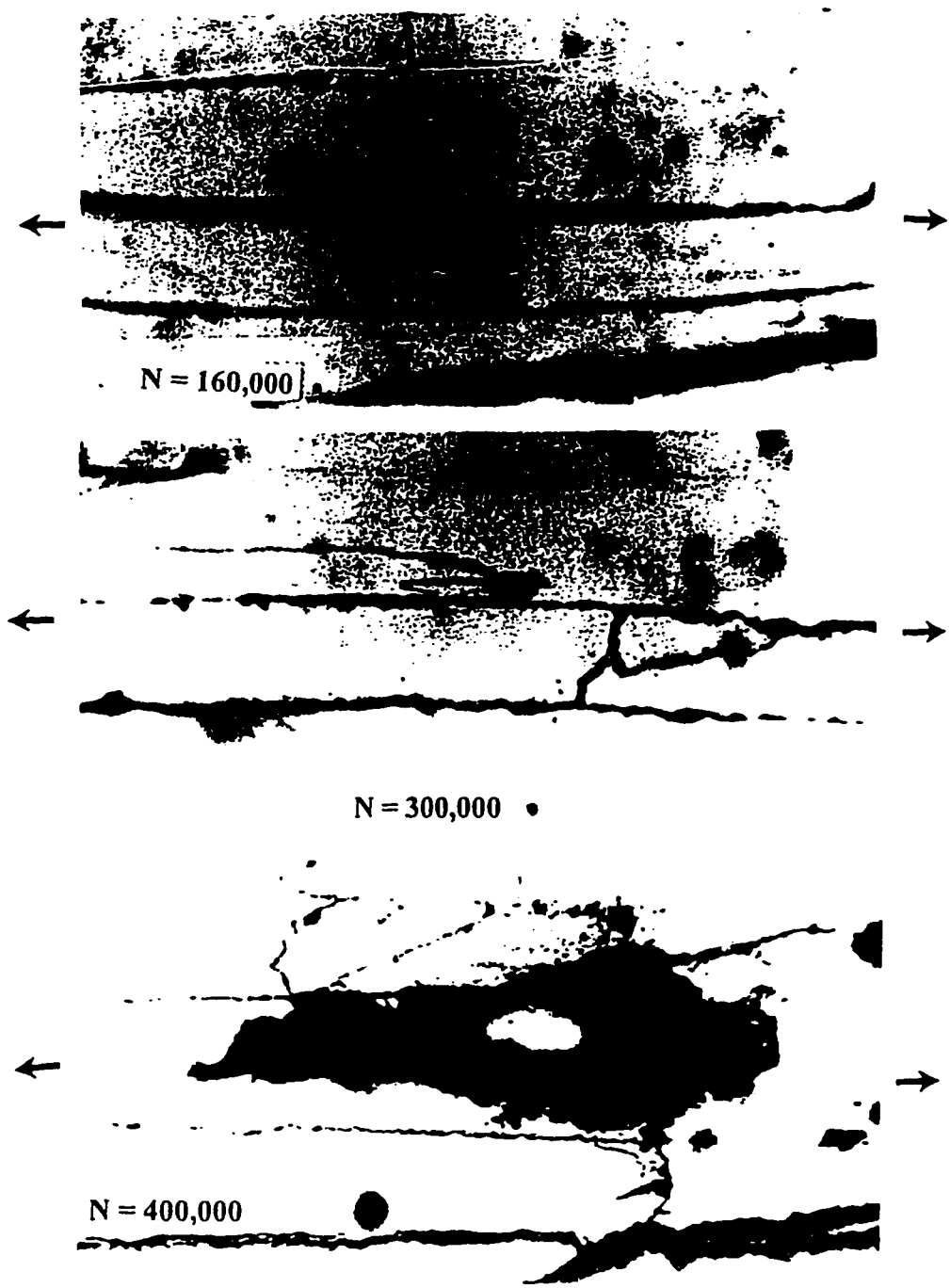

Figure 35b: Edge replicas showing progressing damage in class 2 $(0,0,45,-45)_{2s}$ CFRP, σ_{max} = 60% σ_{TS}. N_f = 440,500 cycles

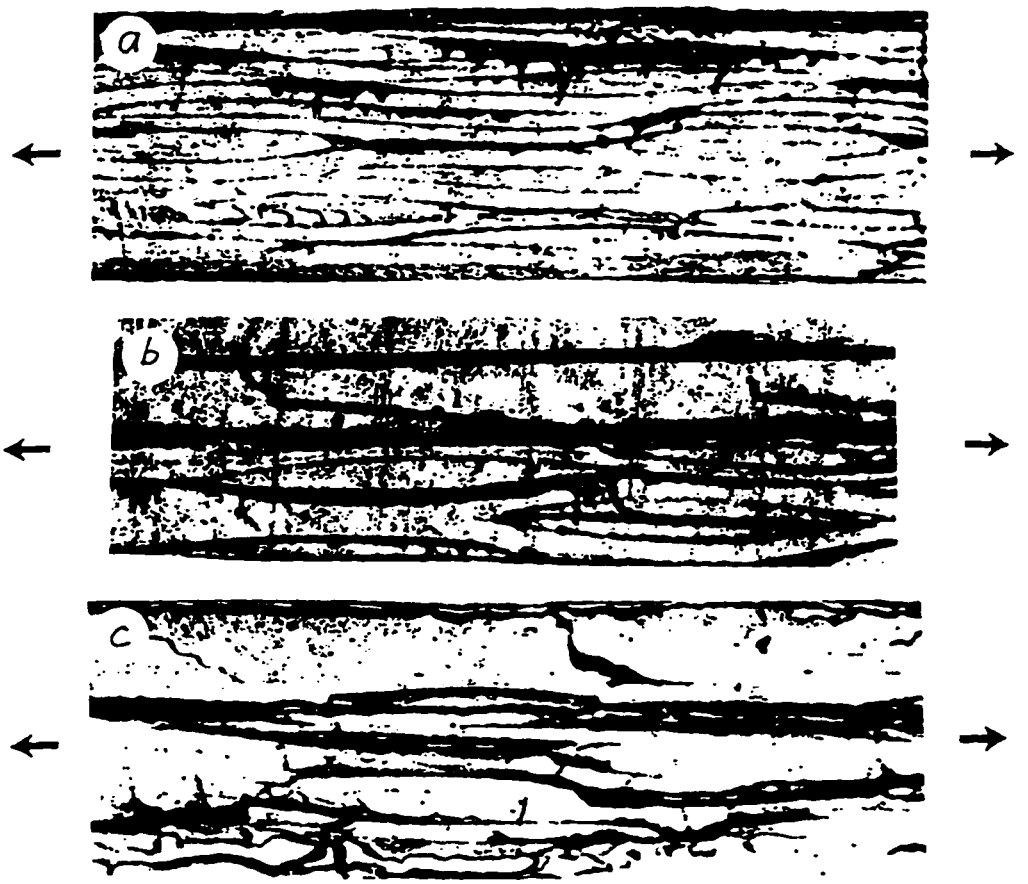

Figure 36: Edge Replicas showing a comparison of Fatigue damage in class 1 $(0°)_8$ (a) class 2 $(0,0,45\text{-}45)_{2s}$ (b) and class 3 $(45,\text{-}45,0,0)_{2s}$ (c) CFRP specimens with typical damage mode dominance in each at 60% life and $\sigma_{max} = 65\%\ \sigma_{TS}$

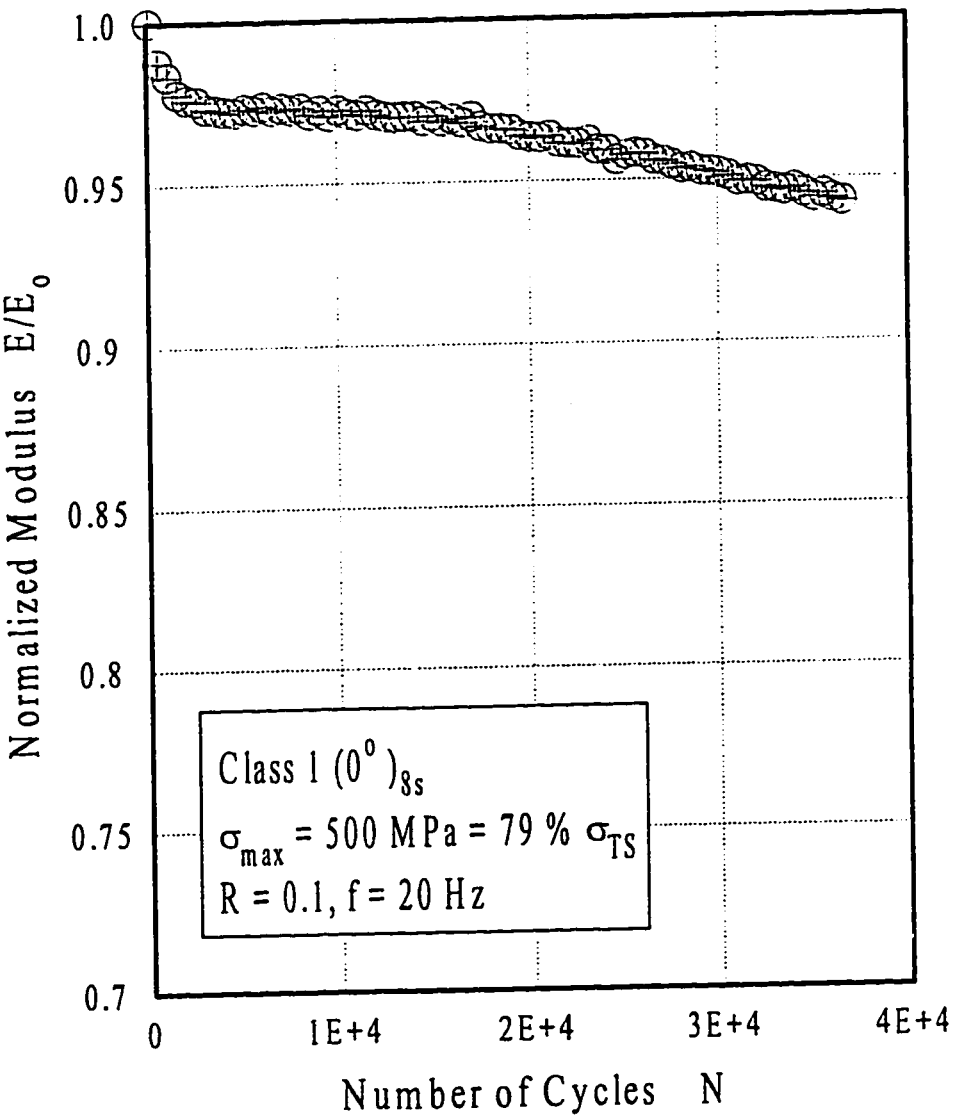

Figure 37: Elastic Modulus Degradation with the number of fatigue cycles for class 1 $(0°)_8$ CFRP

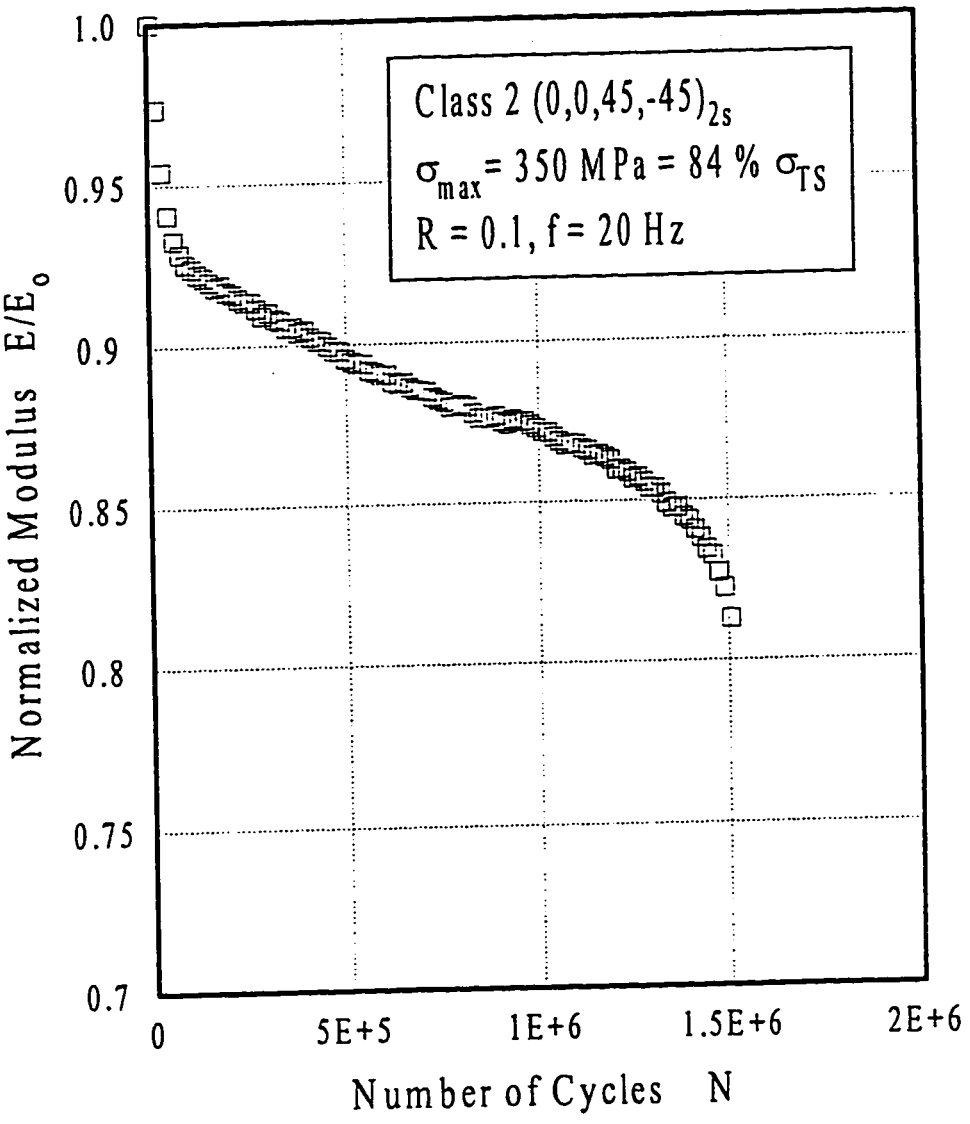

Figure 38: Elastic Modulus Degradation with the number of fatigue cycles for class 2 $(0,0,45,-45)_{2s}$ CFRP

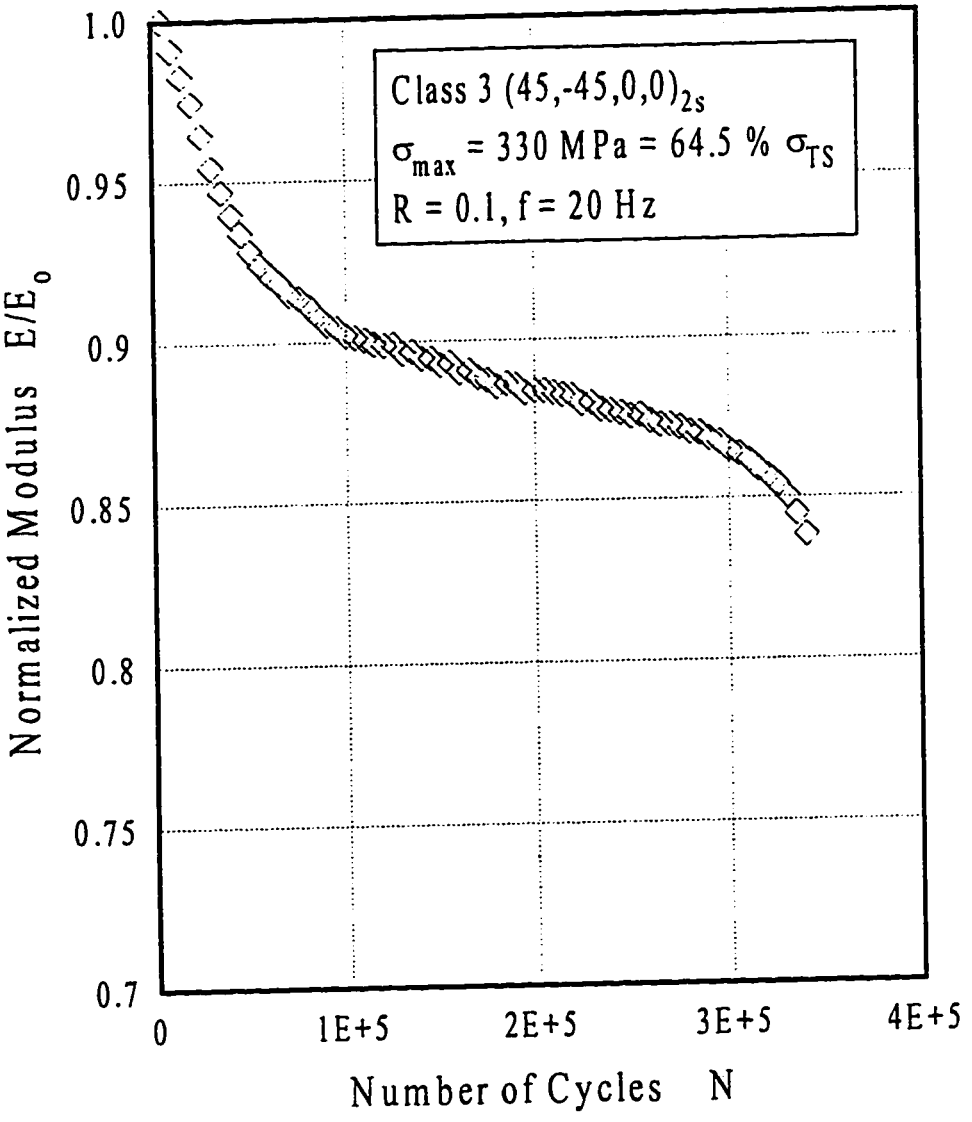

Figure 39: Elastic Modulus Degradation with the number of fatigue cycles for class 3 $(45,-45,0,0)_{2s}$ CFRP

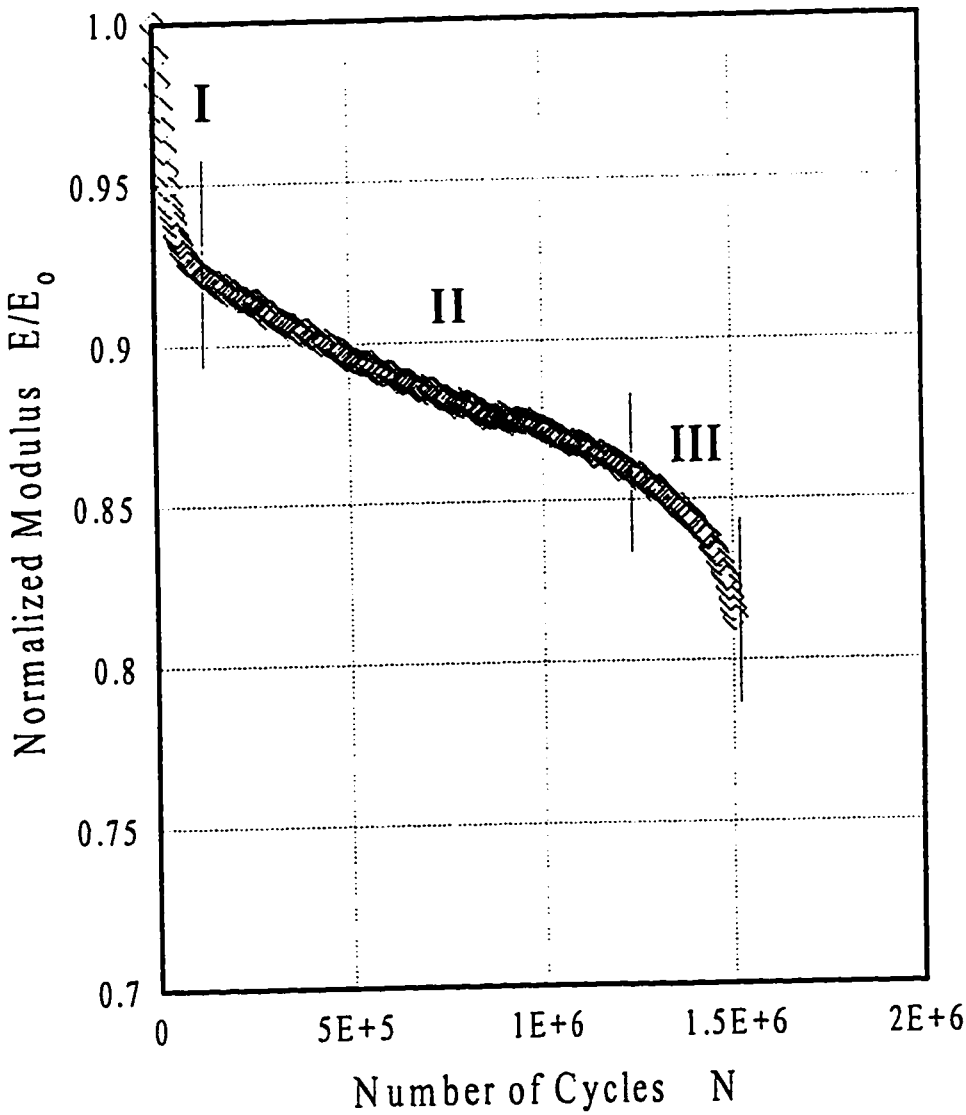

Figure 40: Modulus reduction along with load cycling showing three typical damage stages of Elastic Modulus reduction

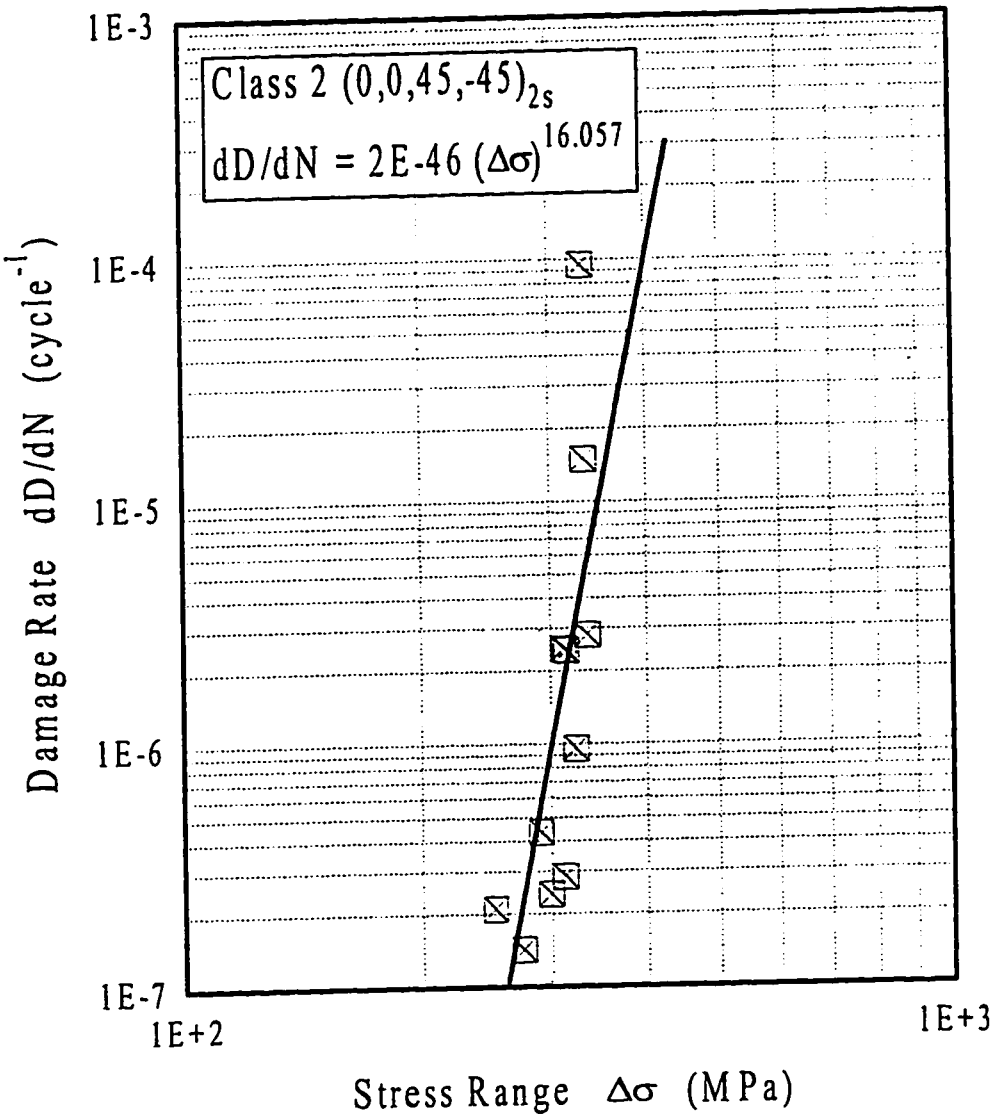

Figure 41: Damage Rate as a function of the applied stress range, $\Delta\sigma$, for class 2 $(0,0,45,-45)_{2s}$ CFRP composite.

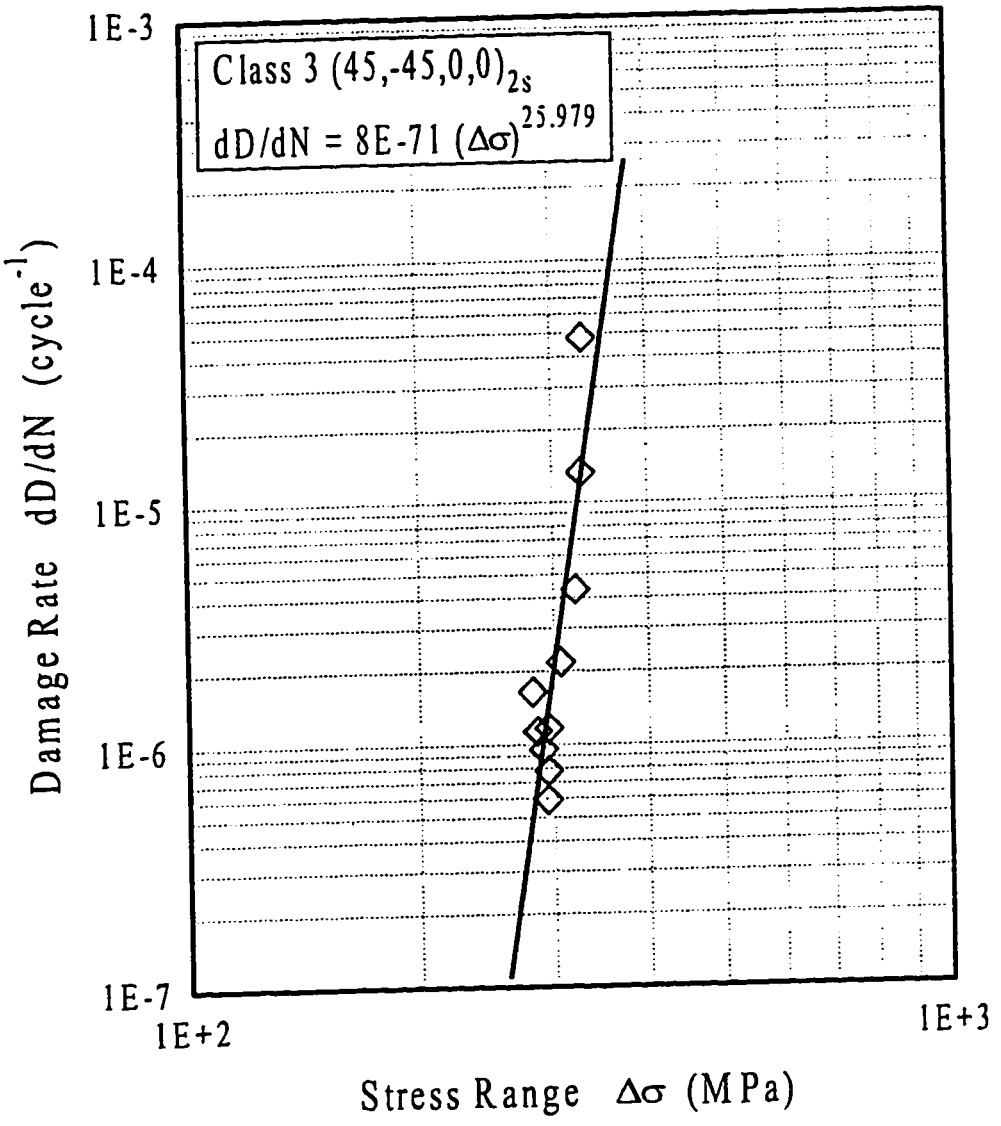

Figure 42: Damage Rate as a function of the applied stress range, $\Delta\sigma$, for class 3 $(45,-45,0,0)_{2s}$ CFRP composite.

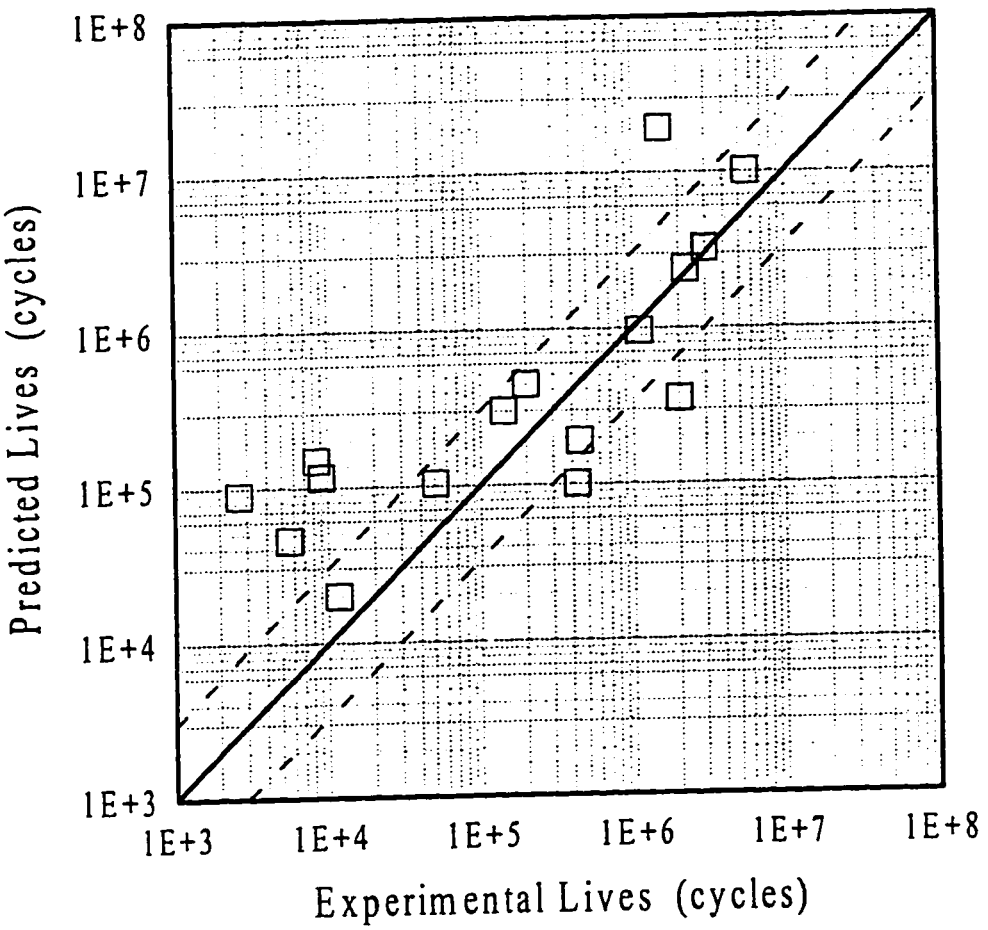

Figure 43: Experimental Lives vs Predicted Lives (using stiffness reduction model) for class 2 $(0,0,45,-45)_{2s}$ CFRP

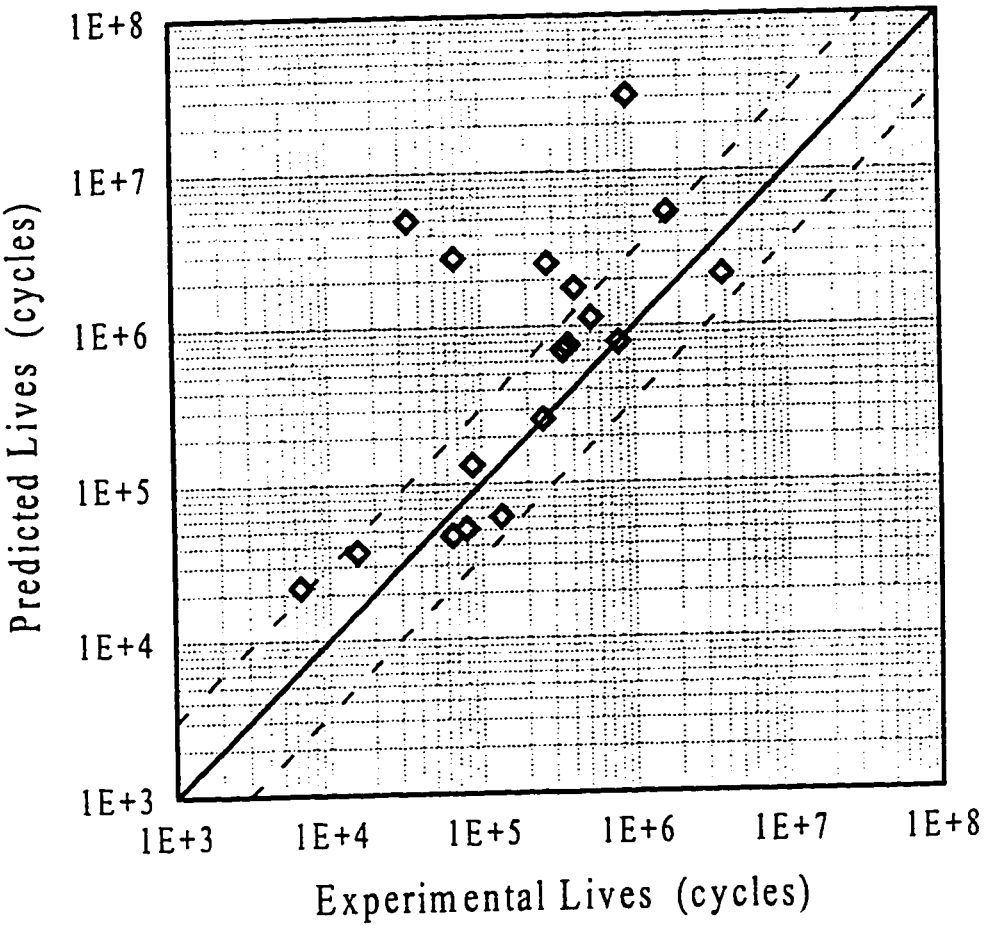

Figure 44: Experimental Lives vs Predicted Lives (using stiffness reduction model) for class 3 $(45,-45,0,0)_{2s}$ CFRP

Figure 45: Photomicrograph showing a large void inside a class 3 $(45_2/-45_2/0_2)_{2s}$ CFRP specimen

Table 1: Constant 'c' evaluated from the mechanical properties of class 1 $(0°)_8$, class 2 $(0,0,45,-45)_{2s}$, and class 3 $(45,-45,0,0)_{2s}$ CFRP

Mechanical Properties	*Symbol*	*Class 1 Composite*	*Class 2 Composite*	*Class 3 Composite*
Elastic Modulus - Longitudinal (GPa)	E_A	41,270	29,398	29,398
Elastic Modulus - Transverse (GPa)	E_T	41,270	29,398	29,398
Shear Modulus (MPa)	G_A	3,773	9,684	9,684
Poisson's Ratio	ν_A	0.3233	0.51795	0.51795
Model Constant	C	11.0142	6.2831	6.2831

Table 2: Monotonic mechanical properties of the three classes of composites

Mechanical Properties	*Symbol*	*Woven Carbon Fabric (66.66%)*	*Polyester Matrix (33.33%)*	*Single Laminate Properties*	*Class 1 Composite*	*Class 2 Composite*	*Class 3 Composite*
Elastic Modulus (Longitudinal)	E_A *(MPa)*	59,990	3,842	41,275	41,275	29,398	29,398
Elastic Modulus (Transverse)	E_T *(MPa)*	59,990	3,842	41,275	41,275	29,398	29,398
Shear Strength	G_A *(MPa)*	5,057	1,215	3,773	560	9,684	9,684
Poisson's Ratio	ν_T	0.31	0.35	0.3233	0.3233	0.51795	0.51795
Tensile Strength (Longitudinal)	$\sigma_{TS,A}$ *(MPa)*	805	69	560	560	392.84	392.84
Tensile Strength (Transverse)	$\sigma_{TS,T}$ *(MPa)*	805	69	560	560	486.24	486.24

Table 3a: Class 1 $(0°)_8$ CFRP Fatigue Test Data

Sample Name	P_{max} (kN)	σ_{max} (MPa)	*Number of Cycles to Failure,* N_f	*Type of Failure* *
1BF7	25	625	347	LAT+LIB
1BF4	24	600	2,194	LIT
1CF2	24	594	1,117	LGT+LGB
1DF3	24	592	5,621	LGT+LGB
1DF2	23	575	428,794	LGM
1BF3	24	564.71	3,347	LIT
1BF5	22	551.11	3,375	LGT+LIB
1BF2	22	550	1,342,656	LIT+LGM
1BF8	22	550	9,901	LAT
1CF1	22	550	1,357	LIB+LAT
1DF1	22	550	>1,000,000	Runout
1EF3	22	528.2	23,501	LIT
1EF9	22	527.14	2,608,265	Runout
1BF9	22	519.73	3,698	LIB
1BF6	20	500	>2,000,000	Runout
1EF8	20	497.38	2,320,324	Runout
1EF7	21	496.1	36,727	Runout
1EF6	20	482.75	1,535,482	Tabs Failed
1BF1	18	450	>2,000,000	Runout
1EF2	18	428.67	>2,360,000	Runout
1EF1	16	382.98	>1,152,431	Runout

* *Types of Failure are given in Figure (11) in detail*

Table 3b: Class 2 $(0,0,45,-45)_{2s}$ CFRP Fatigue Test Data

Sample Name	P_{max} (kN)	σ_{max} (MPa)	*Number of Cycles to Failure,* N_f	*Type of Failure*
2CF3	16	411.86	11,592	AGM+LGB
2DF2	16	391.34	5,621	MGB
2DF3	15.5	388.98	26,060	LGB
2DF1	15	386.12	448,419	SGM+AGM
2AF2	15	375	2,691	AGM
2CF1	14.5	372.18	431,113	LGT+AGM
2CF4	15	371.51	50,446	LGT
2BF7	15	368.65	9,092	LGT
2BF5	15	363.64	8,443	LGT
2BF2	14	347.45	142,863	Removed
2CF2	14	346.75	1,508,576	AGM
2CF5	13.5	344.39	>2,000,000	Runout
2BF1	14	339.34	200,000	Runout
2BF6	13	323.54	1,101,819	AGT or SGT
2BF3	12	305.50	2,212,155	AGT
2AF1	12	300	>3,000,000	Runout
2BF4	11	279.47	>5,600,000	Runout

Table 3c: Class 3 $(45,-45,0,0)_{2s}$ CFRP Fatigue Test Data

Sample Name	P_{max} (kN)	σ_{max} (MPa)	*Number of Cycles to Failure,* N_f	*Type of Failure*
3AF1	15	375	6,451	LGM+AGM
3CF3	15	367.98	64,931	AGM
3DF3	15	367.65	15,318	LGM
3CF5	15	363.11	79,774	LGM+LGT
3DF5	14.5	357.23	133,368	LGT
3AF2	14	350	87,401	LGM+AGM
3CF1	14.2	340.97	253,878	LGM or LGB
3DF4	13.5	328.15	344,047	AGM
3DF1	13.8	327.32	369,704	AGM+LGM
3CF4	13.5	326.79	793,554	MGM
3BF2	13	322.66	527,122	AGT
3BF6	13	316.8	410,949	AGT
3BF1	13	315.15	3,811,335	AGM
3BF3	13	312.5	274,414	AGT
3BF4	13	312.12	68,861	AGT
3DF6	12.5	307.96	2,958,656	AGM
3BF5	13	304.7	34,408	AGM
3CF2	12.5	302.96	>1,659,951	Runout
3DF2	12	283.82	>920,040	No Failure

Table 4: Stiffness reduction and Damage rate data for class 2 $(0,0,45,-45)_{2s}$ CFRP (a), class 3 $(45,-45,0,0)_{2s}$ CFRP (b)

Sr. #	*Specimen Name*	σ_{max} *(MPa)*	*Modulus Reduction* E_f / E_o	$\Delta\sigma$ *(MPa)*	*Damage Rate dD/dN*
1	2BF7	369	0.91383	332	9.52E-5
2	2CF1	372	0.90926	324	9.56E-7
3	2CF4	383	0.89845	333	1.50E-5
4	2DF1	386	0.89951	336	2.81E-6
5	2BF1	350	0.93027	315	2.43E-6
6	2BF2	347	0.89793	313	2.46E-6
7	2CF2	347	0.81525	313	2.86E-7
8	2CF5	344	0.88973	300	2.41E-7
9	2BF6	324	0.88448	291	4.35E-7
10	2BF3	305	0.82406	275	1.42E-7
11	2BF4	279	0.89888	251	2.10E-7

(a)

Sr. #	*Specimen Name*	σ_{max} *(MPa)*	*Modulus Reduction* E_f / E_o	$\Delta\sigma$ *(MPa)*	*Damage Rate dD/dN*
1	3DF3	368	0.93154	331	4.78E-5
2	3CF3	365	0.88163	328	1.33E-5
3	3CF4	327	0.84279	294	5.91E-7
4	3DF5	357	0.85495	322	4.33E-6
5	3CF1	341	0.88450	307	2.16E-6
6	3DF4	328	0.83812	295	1.17E-6
7	3DF1	327	0.82818	295	7.79E-7
8	3BF2	323	0.86220	290	9.52E-7
9	3BF6	317	0.83468	285	1.13E-6
10	3BF3	313	0.85253	281	1.64E-6

(b)

Table 5: Experimentally observed and Predicted life data against applied maximum stress for class 2 $(0,0,45,-45)_{2s}$ (a), class 3 $(45,-45,0,0)_{2s}$ (b)

(a)

Max. Stress MPa	Experimental Lives	Predicted Lives
371	11,592	19,950
352	5,621	45,606
338	2,691	89,613
335	431,113	100,976
334	50,446	103,924
332	9,092	116,667
327	8,443	148,856
322	448,419	190,642
313	142,863	300,542
310	2,000,000	352,627
306	200,000	443,645
291	1,101,819	968,570
275	2,212,155	2,401,572
270	3,000,000	3,224,429
252	5,600,000	10,079,111
242	1,508,576	19,335,718

(b)

Max. Stress MPa	Experimental Lives	Predicted Lives
338	6,451	21,928
331	15,318	36,685
328	64,931	46,039
327	79,774	51,043
325	133,368	60,643
315	87,401	131,645
307	253,878	256,831
295	344,047	702,901
295	369,704	756,219
294	793,554	790,350
290	527,122	1,128,176
285	410,949	1,772,556
283	3,811,335	2,128,407
281	274,414	2,559,016
280	68,861	2,807,347
274	34,408	4,928,249
273	1,659,951	5,419,324
255	920,040	30,482,885

Table 6: Tension Test Data

Monotonic Properties	S#	1A	1B	1C	1D	1E	2A	2B	2C	2D	3A	3B	3C	3D
σ_{uts} (GPa)	T1	0.74	0.66	0.60	0.65	*No Failure*	0.46	0.48	0.43	0.56	0.48	0.46	0.54	0.51
	T2	0.75	0.78	0.68	0.67	*No Failure*	0.45		0.40	0.52	0.49		0.51	0.50
	T3	0.66	0.79			*No Failure*				0.53				
	T4	0.82	0.68			*No Failure*								
	T5	0.70	0.75			0.59								
	T6	0.65				0.59								
	T7					0.70								
	T8					0.63								
Average		0.72	0.73	0.64	0.66	0.63	0.46	0.48	0.41	0.54	0.48	0.46	0.53	0.51
E (GPa)	T1	41.75	56.99	55.79	55.53	41.73	35.03	35.03	41.78	35.03	41.45	41.87	32.11	30.82
	T2	52.46	58.89	58.62	54.59	44.55	40.48		41.18	35.55	40.57		31.58	31.10
	T3	51.18	56.53			44.52				33.90				
	T4	53.50	57.31			43.33								
	T5	51.72	57.32			46.09								
	T6	49.47				44.53								
	T7					43.86								
	T8					41.58								
Average		50.01	57.41	57.20	55.06	43.77	37.75	35.03	41.48	34.82	41.01	41.87	31.85	30.96
ε_f	T1	0.017	0.013	0.013	0.012	*No Failure*	0.012	0.013	0.010	0.019	0.013	0.011	0.020	0.018
	T2	0.014	0.015	0.013	0.013	*No Failure*	0.012		0.011	0.014	0.013		0.018	0.019
	T3	0.013	0.015			*No Failure*				0.018				
	T4	0.016	0.013			*No Failure*								
	T5	0.014	0.014			0.017								
	T6	0.013				0.016								
	T7					0.022								
	T8					0.018								
Average		0.015	0.014	0.013	0.013	0.018	0.012	0.013	0.011	0.017	0.013	0.011	0.019	0.019

Bibliography

[1] Schwartz, M.; *"Composite Materials Handbook"*, (2nd ed.), 1992

[2] Pagano, N. J., Pipes, R. B.; The influence of Stacking Sequence on the Laminate Strength; *Journal of Composite Materials*; Vol. 5, January 1971, pp. 50-57

[3] Harris, B.; Fatigue and Accumulation of Damage in Reinforced Plastics; *Composites*; Vol. 8, no. 2, October 1977, pp. 214-220

[4] Salkind, M. J.; Fatigue of Composites; *Composite Materials: Testing and Design (Second Conference). ASTM STP 497*; 1972, pp. 143-169

[5] Fong, J. T.; What is Fatigue Damage; *"Damage in Composite Materials", ASTM STP 775, (K. L. Reifsnider ed.)*; 1982, pp. 243-266

[6] Schutz, D., Gerharz, J. J.; Fatigue of a Fiber Reinforced Material, *Composites*; Vol. 8, no. 2, October 1977, pp. 245-250

[7] Sturgeon, J. B.; Fatigue of multidirectional Carbon Fiber Reinforced Plastics, *Composites*; Vol. 8, no. 2, October 1977, pp. 221-226

[8] Peters, P. W. M.; Constrained 90-Deg Ply Cracking in 0/90/0 and $\pm 45/90/\mp 45$ CFRP Laminates; *Composite Materials: Fatigue and Fracture ASTM STP 907. (H. T. Hahn ed.)*, 1986, pp. 84-99

[9] Hahn, H. T., Kim, R. Y.; Fatigue Behavior of Composite Laminate; *Journal of Composite Materials* ;Vol. 10, April 1976, pp. 156-180

[10] Hojo, M., Tanaka, K., Gustafson, C. G., Hayashi, R.; Effect of Stress Ratio on Near-Threshold Propagation of Delamination Fatigue Cracks in Unidirectional CFRP; *Composite Science and Technology*; Vol. 29, no. 4, 1987, pp. 273-292

[11] Reifsnider, K. L., Jamison, R.; Fracture of Fatigue-loaded Composite Laminates; *Int. Journal of Fatigue*; Vol. 4, October 1982, pp. 187-197

[12] Ishikawa, T., Chou, T. W.; Nonlinear Behavior of Woven Fabric Composites; *Journal of Composites Materials*; Vol. 17, no. 5, September 1983, pp. 399-413

[13] Hahn, H. T., Tsai, S. W.; Nonlinear Elastic Behavior of Unidirectional Composite Laminac; *Journal of Composite Materials*; Vol. 7, January 1973, pp. 102-118

[14] Schulte, K.; Fatigue Damage Development in Carbon Fiber Reinforced Composites; *IMechE* 1986, C252/86, *International Conference on Fatigue of Engineering Materials and Structures, Sheffield, England*; Vol. 2, Part 15-19, September 1986, pp. 321-327

[15] Rotem, A.; Fatigue and Residual Strength of Composite Laminates; *Engineering Fracture Mechanics*; Vol. 25, no. 5-6, 1986, pp. 819-827

[16] Bader, G., Pickering, K. L., Buxton, A., Rezaifard, A., Smith, P. A.; Failure Micromechanisms in Continuous Carbon-Fiber/Epoxy-Resin Composites, *Composite Science & Technology*; Vol. 48, 1993, pp. 135-142

[17] Talreja, R.; Estimation of Weibull Parameters for Composite Material Strength and Fatigue Life Data; *"Fatigue of Fibrous Composite Materials", ASTM STP 723, (K. N. Lauraitis ed.)*; 1981, pp. 291-311

[18] Beetz Jr., C. P.; The Analysis of Carbon Fiber Strength Distributions exhibiting Multiple Modes of Failure; *Fibre Science and Technology*; Vol. 16, no. 1, 1982, pp. 45-59

[19] Whitney, J. M.; Fatigue Characterization of Composite Materials; *"Fatigue of Fibrous Composite Materials", (K. N. Lauraitis ed.), ASTM STP 723*; 1981, pp. 133-151

[20] Ginty, C. A., Chamis, C. C.; Fracture Characteristics of Angleplied Laminates Fabricated from overaged Graphite/Epoxy Prepreg; *"Fractography of Modern*

Engineering Materials: Composites and Metals", (J. E. Masters. J. J. Au ed.). ASTM STP 948; 1987, pp. 101-130

[21] Harrison, R. P., Bader, M. G.; Damage Development in CFRP Laminates under Monotonic and Cyclic Stressing; *Fibre Science and Technology*; Vol. 18, no. 3, 1983, pp. 163-180

[22] Curtis, P. T.; Tensile Fatigue Mechanisms in Unidirectional Polymer Matrix Composite Materials; *Int. Journal of Fatigue*; Vol. 13, no. 5, 1991, pp. 377-382

[23] Ratwani, M. W., Kan, H. P.; Effect of Stacking Sequence on Damage Propagation and Failure Modes in Composite Laminates; *"Damage in Composite Materials". ASTM STP 775, (K.L.Reifsnider ed.)*; 1982, pp. 211-228

[24] O'Brien, T. K.; Characterization of Delamination Onset and Growth in a Composite Laminate; *"Damage in Composite Materials". ASTM STP 775, (K.L.Reifsnider ed.)*; 1982, pp. 140-167

[25] Jamison, R. D., Schulte, K., Reifsnider, K. L., Stinchcomb, W. W.; Characterization and Analysis of Damage Mechanisms in Tension-Tension Fatigue of Graphite/Epoxy Laminates; *"Effects of Defects in Composite Materials". ASTM STP 836*, 1984, pp. 21-55

[26] Masters, J. E., Reifsnider, K. L.,; An Investigation of Cumulative Damage Development in Quasi-Isotropic Graphite/Epoxy Laminates; *"Damage in Composite Materials", ASTM STP 775, (K. L. Reifsnider ed.)*; 1982, pp. 40-62

[27] Xian, X. J., Li, H., Yan, K. H.; Failure of Specimen of Carbon Fiber-Reinforced Epoxy plastics in Static and Fatigue Loading, *Mechanics of Composite Materials*; Vol. 21, no. 6, DEC 1985-May 1986, pp. 686-693

[28] Wevers, M., Verpoest, I., DeMeester, P., Aernoudt, E.; Identification of Fatigue Failure modes in Carbon Fiber Reinforced Composites with the Energy Discriminating Acoustics Emission Method; *ASTM STP 1077*, 1991, pp. 416-423

[29] Bhat, M. R., Murthy, C. R. L.; Fatigue Damage Stages in Unidirectional Glass Fiber/Epoxy Composites: Identification through Acoustic Emission Technique; *Int. Journal of Fatigue*; Vol. 15, no. 5, 1993, pp. 401-405

[30] Gellert, E. P., Bandyopadhyay, S.; Interlaminar Fracture Energy of Fiber Reinforced Composites; *Polymer 85; International Symposium on Characterization and Analysis of Polymers*; Part V, February 1985, pp. 143-145

[31] Gathercole, N., Reiter, H., Adam, T., Harris, B.; Life Prediction for Fatigue of T800/5245 Carbon-Fiber Composites: I - Constant Amplitude Loading; *Int. Journal of Fatigue*; Vol. 16, no. 8, November 1994, pp. 523-532

[32] Prakash, R.; A Fractographic Study of Fatigue in CFRP; *Composites*; Vol. 10, no. 3, July 1979, pp. 174-178

[33] Cruse, T. A., Stout, M. G.; Fractographic Study of Graphite-Epoxy Laminated Fracture Specimens; *"Carbon Reinforced Epoxy Systems* - Vol. 1, Materials Technology Series*" (Carlos J. Hilado ed.)*, 1974, pp. 200-204

[34] Chou, C. T., Gaur, U., Miller, B.; Fracture mechanisms during fiber Pull-out for Carbon-Fiber-Reinforced thermosetting Composites; *Composite Science and Technology*; Vol. 48, 1993, pp. 307-316

[35] Xian, X. J., Li, H.; Fatigue Behavior of Carbon Fiber Reinforced Epoxy Composite Material with Edge Notch; *"Progress in Science and Engineering of Composite* - Vol. 1 *(T. Hayashi, K. Kawata, S. Umekawa ed.)"*; ICCM-IV, Tokyo, 1982, pp. 725-732

[36] Seldén, R. B.; Fractography of Carbon/Epoxy Angle-Ply Laminates; *"Progress in Science and Engineering of Composites* - Vol. 2 *(T. Hayashi, K. Kawata, S. Umekawa ed.)"*; ICCM-IV, Tokyo, 1982, pp. 1525-1533

[37] Frandsen, R. R., Naerheim, Y.; Fracture Morphology of Graphic/Epoxy Composites; *"Carbon Reinforced Epoxy Systems* - Vol. 13, Materials Technology Series - Part 5*" (Carlos J. Hilado ed.)*, 1984, pp. 220-231

[38] O'Brien. T. K. et al.; Fatigue Damage Evaluation through Stiffness Measurement in Boron Epoxy Laminates; *Journal of Composite Materials*, Vol. 15, 1981, pp. 55-70

[39] Morris, G. E., Hetter, C. M.; Fractographic Studies of Graphite/Epoxy Fatigue Specimens; *"Damage in Composite Materials". ASTM STP 775. (K. L. Reifsnider ed.)*; 1982, pp. 27-39

[40] Razvan, A., Bakis, C. E., Reifsnider, K. L.; SEM Investigation in Fiber Fracture in Composite Materials; *Materials Characterization*, Vol. 24, no. 2, March 1980, pp. 179-190

[41] Theocaris, P. S., Stassinakis, C. A.; Crack Propagation in Fibrous Composite Materials studied by SEM; *Journal of Composite Materials*, Vol. 15, March 1981, pp. 133-141

[42] Purslow, D.; Some Fundamental Aspects of Composites Fractography; *Composites*, Vol. 12, no. 4, October 1981, pp. 241-247

[43] Ramakumar, R. L.; Compression Fatigue Behavior of Composites in the presence of Delaminations; *"Damage in Composite Materials". ASTM STP 775. (K.L.Reifsnider ed.)*; 1982, pp. 184-210

[44] Crossman, F. W. and Wang, A. S. D.; The Dependence of Transverse Cracking and Delamination on Ply Thickness in Graphite/Epoxy Laminates; *"Damage in Composite Materials", ASTM STP 775, (K.L.Reifsnider ed.)*; 1982, pp. 118-139

[45] Shulte, K., Stinchcomb, W. W.; Damage Development near the Edges of a Composites specimen during quasi-static and fatigue loading; *Composite Technology Review*, Vol. 6, no. 1, Spring 1984, pp. 3-9

[46] Stalnaker, D. O., Stinchcomb, W. W.; Load History-Edge Damage Studies in two Quasi-Isotropic Graphite Epoxy Laminates; *"Composite Materials: Testing and Design (Fifth Conference)", ASTM STP 674, (S. W. Tsai ed.)*; 1979, pp. 620-641

[47] Strelyaev, V. S., Sachkovskaya, L. L., Baikov, V. M., Rumyantsev, A. F.; Relationship Governing Fatigue Failure of Carbon Reinforced Plastics; *Mechanics of Composite Materials*; Vol. 20, no. 5, September-October 1984, pp. 600-605

[48] Yang, J. N., Liu, M. D.; Residual Strength Degradation Model and Theory of Periodic Proof Tests for Graphite/Epoxy Laminates; *Journal of Composite Materials*, Vol. 11, April 1977, pp. 176-203

[49] Yang, J. N., Jones, D. L., Yang, S. H., Mesinski, A.; A Stiffness Degradation Model for Graphite/Epoxy Laminates; *Journal of Composite Materials*, Vol. 24, July 1990, pp. 753-769

[50] Radhakrishnan, K.; Fatigue and Reliability Evaluation of Unnotched Carbon Epoxy Laminates; *Journal of Composite Materials*; Vol. 18, no. 1, January 1984, pp. 21-31

[51] Lee, L. J., Yang, J. N., Sheu, D. Y.; Prediction of Fatigue life for Matrix-Dominated Composite Laminates; *Composite Science and Technology*; Vol. 45, 1993, pp. 21-28

[52] Hwang, W., Han, K. S.; Fatigue of Composites - Fatigue Modulus Concept and Life Prediction; *Journal of Composite Materials*; Vol. 20, March 1986, pp. 154-165

[53] Hahn, H. T.; Fatigue Behavior and Life Prediction of Composite Laminates; *"Composite Materials: Testing and Design (Fifth Conference)". ASTM STP 674. (S. W. Tsai ed.)*; 1979, pp. 383-417

[54] Highsmith, A. L., Reifsnider, K. L.; Stiffness Reduction Mechanism in Composite Laminates; *"Damage in Composite Materials". ASTM STP 775. (K. L. Reifsnider ed.)*; 1982, pp. 103-117

[55] Poursartip, A., Ashby, M. F., Beaumont, P. W. R.; The Fatigue Damage Mechanics of a Carbon Fibre Composite Laminate: I - Development of the Model; *Composite Science and Technology*; Vol. 25, no. 3, 1986, pp. 193-218

[56] Poursartip, A., Beaumont, P. W. R.; The Fatigue Damage Mechanics of a Carbon Fibre Composite Laminate: II - Life Prediction; *Composite Science and Technology*; Vol. 25, no. 4, 1986, pp. 283-299

[57] Spearing, S. M., Beaumont, P. W. R.; Fatigue Damage Mechanics of Composite Materials. I: Experimental measurement of Damage and Post-Fatigue properties; *Composite Science and Technology*; Vol. 44, 1992, pp. 159-168

[58] Petitpas, E., Renaults, M., Valentin, D.; Fatigue Behavior of Cross-ply CFRP laminates made of T 300 or T 400 fibers; *Int. Journal of Fatigue*; Vol. 12, no. 4, 1990, pp. 245-251

[59] Kobelev, V. V.; Fracture of Fibers by a Crack Propagation in a Composite; *Mechanics of Composite Materials*; Vol. 24, no. 2, March-April 1988-September 1988, pp. 180-188

[60] Spearing, S. M., Beaumont, P. W. R., Ashby, M. F.; Fatigue Damage Mechanics of Composite Materials. II: A Damage Growth Model; *Composite Science and Technology*; Vol. 44, no. 2, 1992, pp. 169-177

[61] Bathias, C., Esnault, R., Pellas, J.; Application of Fracture Mechanics to Graphite Fiber Reinforced Composites; *Composites*, Vol. 12, no. 3, July 1981, pp. 195-200

[62] Wright, M. A., Iannuzzi, F. A.; The Application of the Principles of Linear Elastic Fracture Mechanics (LEFM) to Unidirectional Fibre Reinforced Composite Materials; *"Carbon Reinforced Epoxy Systems* - Vol. 1, Materials Technology Series*" (Carlos J. Hilado ed.)*, 1974, pp. 205-222

[63] Kortschot, M. T., Beaumont, P. W. R.; Damage Mechanics of Composite Materials: I - Measurement of Damage and Strength; *Composite Science and Technology*; Vol. 39, 1990, pp. 289-301

[64] Kortschot, M. T., Beaumont, P. W. R.; Damage Mechanics of Composite Materials: II - A Damage based Notched Strength Model; *Composite Science and Technology*; Vol. 39, 1990, pp. 303-326

[65] Shimokawa, T., Hamaguchi, Y.; Distribution of Fatigue Life and Fatigue Strength in Notched Specimens of a Carbon Eight-Harness-Satin Laminate; *"Carbon Reinforced Epoxy System - Part 5"* Material Technology Series - Vol. 13. *(Carlos J. Halido ed.)*, 1984, pp. 155-167

[66] Prakash, R.; Significance of Defects in the Fatigue Failure of Carbon Fiber Reinforced Plastics; *Fibre Science and Technology*; Vol. 14, 1981, pp. 171-181

[67] Adam, T., Gathercole, N., Reiter, H., Harris, B.; Life Prediction for Fatigue of T800/5245 Carbon Fibre Composites: II - Variable Amplitude Loading; *Int. Journal of Fatigue*; Vol. 16, no. 8, November 1994, pp. 533-547

[68] Stinchcomb, W. W., Reifsnider, K. L.; Fatigue Damage Mechanisms in Composite Materials: A Review; "Fatigue Mechanisms", *Proceedings of an ASTM-NBS-NSF Symposium. Kansas City, Mo., May 1978. ASTM STP 675. (J. T. Fong ed.)*, 1979, pp. 762-787

[69] Kedward, K. T., Beaumont, P. W. R.; The treatment of Fatigue and Damage Accumulation in Composite Design; *Int. Journal of Fatigue*; Vol. 14, no. 5, September 1992, pp. 283-294

[70] Vol'mir, A. S.; Trends in the Use of Composite Materials in Aircrafts and Engines; *Mechanics of Composite Materials*; Vol. 21, no. 6, Nov-Dec 85 - May 86, pp. 720-726

[71] Green, A. K., Pratt, P. L.; The Axial Fatigue Behavior of Unidirectional type IIIs Carbon Fibre-Epoxy Resin Composite; Composites; Vol. 5, no. 2, 1974, pp. 63-66

[72] Poursartip, A., Beaumont, P. W. R.; A Damage Approach to the Fatigue of Composites; *"Mechanics of Composite Materials: Recent Advances", (Z. Hashin, C. T. Herakovich eds.)*, 1982, pp. 449-456

[73] Eshelby, J. D.; The Determination of the Elastic Field of an Ellipsoidal Inclusion, and related problems; *Proceedings of Royal Society*, A-214, 1957, pp. 314-396

[74] Bristow, J. R.; Microcracks, and the Static and Dynamic Elastic Constants of Annealed and Heavily Cold-Worked metals; *British Journal of Applied Physics*, Vol. 11, 1960, pp. 81-85

[75] Budiansky, B., O'Connell, R. J.; Elastic Moduli of a cracked solid; *International Journal of Solids and Structures*, Vol. 12, 1960, pp. 81-97

[76] Gottesman, T., Hashin, Z., Brull, M. A.; *"Advances in Composite Materials", A. R. Bunsell (ed.);* Vol. I, Pergamon Press, Oxford, 1980

[77] Berlin, A. A., Volfson, S. A., Enikolopian, N. S., Negmatov, S. S.; *"Principles of Polymer Composites"*, Springer-Verlag, Berlin, 1985, pp. 48

[78] American Society of Testing and Materials, Vol. 03.01; *ASTM Designation* #D-3039/D-3039M-93: Standard Test Method for Tensile Properties of Polymer Matrix Composite Materials, 1993

[79] Reifsnider, K. L.; Damage and Damage Mechanics; (Reifsnider, K. L. ed.),*"Fatigue Of Composite Materials"*, Composite Material Series Vol. 4, Elsevier, 1991, pp. 11-77

Vitae

- **Johar Khurshid Ahmed Farooqi**
- Born at Alkhobar, Saudi Arabia in 17th June, 1970
- Completed Higher Secondary School from Alkhobar in 1987
- Received Bachelor of Science (B.Sc.) degree in Mechanical Engineering from University of Engineering & Technology, Lahore, Pakistan in 1993
- Joined KFUPM as Research Assistant in September 1994
- Received Master of Science (MS) degree in Mechanical Engineering from KFUPM, Dhahran, Saudi Arabia in December 1996